An Investigation of the Aryl and Methyl CH Stretching Overtones of Substituted Benzenes and Aromatic Heterocycles Using Absorption and Photoacoustic Spectroscopy

A thesis presented to the University of Manitoba

in partial fulfillment of the requirements for the

degree of Ph. D.

by

Michael G. Sowa

Department of Chemistry

University of Manitoba

Winnipeg, Manitoba

AN INVESTIGATION OF THE ARYL AND METHYL CH STRETCHING OVERTONES OF SUBSTITUTED BENZENES AND AROMATIC HETEROCYCLES USING ABSORPTION AND PHOTOACOUSTIC SPECTROSCOPY

BY

MICHAEL G. SOWA

A thesis submitted to the Faculty of Graduate Studies of the University of Manitoba in partial fulfillment of the requirements of the degree of

DOCTOR OF PHILOSOPHY

PART D

AN INVESTIGATION OF THE EFFECTS OF METHYL INTERNAL ROTATION ON THE VIBRATIONAL OVERTONE SPECTRA OF METHYL CONTAINING MOLECULES

- Introduction

Most descriptions of molecular vibration start by singling out a particular molecular geometry and assuming that the relative displacements of the nuclei from this reference geometry are infinitesimal. In fact this rigid picture of the molecule is virtually ubiquitous throughout chemistry. However, there are many situtations where models based on rigid molecular systems fail. This section is concerned with a particular situation in which infinitesimal amplitude descriptions of molecular vibration might be expected to fail.

As discussed in the introductory paragraphs of this manuscript, descriptions of the internal motion of nuclei are usually formulated within the framework of the Born-Oppenheimer (BO) approximation. The electronic and nuclear motions are considered as being separable in the BO approximation. The fast electronic motion contributes an effective internuclear potential field. A rigid molecule is a consequence of a localization of the system wavefunction at the bottom of a deep well in the potential energy field or hypersurface. The localization leads to the definition of an

equilibrium structure. The potential energy surface of a completely nonrigid system is flat and admits no bound-states. Since a collection of isolated nuclei is typically less stable than bound systems, a totally nonrigid description of assemblies of nuclei is not realistic. In the same vein, a completely rigid picture of the molecule is not completely realistic. The potential well which describes the equilibrium configuration of the molecule is neither infinitely sharp nor infinitely deep. The quality of a rigid or nonrigid description of a molecular system depends on the degree of localization of the wavefunction in a particular well in the potential energy surface. Each description represents a limiting picture of assemblies of nuclei. Since the bound states of molecular systems are usually probed well below the dissociation energy, it's not surprising that rigid descriptions represent a better zero order description of the internal motion of molecules. However, breakdowns of the rigid molecule description must be acknowledged to understand some of the most central chemical concepts. A chemical reaction, the breaking and subsequent formation of bonds, is by its very nature a highly nonrigid process. A more restrictive breakdown of the rigid molecule concept is the class of phenomena

which can be catagorized as the interconversion between molecular conformations. A classic example of such a process is the chair-boat interconversion in cyclohexane molecules.

The quality of a rigid or non-rigid description of a collection of nuclei depends both on the potential energy surface which is related to the electronic structure of the system and the internal energy of the system. The rigid limit begins breaking down once the internal energy of the system is sufficient to permit the nuclei to have wide access to the potential well describing the minimum energy conformation. The term, conformational interconversion, applies to systems which have access to a number of wells in the potential energy surface. Even with modest amounts of internal energy, the properties of many molecules can only be understood if conformational interconversion is considered. One specific class of conformational interconversion, methyl top internal rotation, is studied in this section.

The rotation of sections of the molecule relative to each other, internal rotation, is an important and widely studied phenomenon. Due to the simplicity of the motion, its common occurrence and its varying degree of nonrigidity, the internal rotation of methyl groups

has been the subject of intense studies over a number of years which have used a number of experimental and theoretical methods. The fundamental and overtone vibrational spectra of methyl containing molecules have been exhaustively studied. In most cases and as will be done in Chapter 11, the spectra are analysed assuming that the torsional angle of the methyl group is fixed and the vibrations of the atoms that make up the methyl group are of infinitesimal displacements. Since most of the methyl vibrational spectral features can be understood by representing it as a rigid group, it may be argued that the infinitesimal vibrational amplitude approximation is valid. However, nonrigid effects, in particular the torsional motion of the group clearly manifest themselves in other spectroscopic regions. On the NMR timescale, methyl torsional motions are rarely frozen-out and the group is most often treated as freely rotating. The torsional motion of the group must be taken into account in the analysis of the rotational spectral features in the microwave and far infrared regions. From these spectroscopic data, the barrier to internal rotation can often be inferred. Methyl group torsions as compared to the torsions of other bound groups typically have low barriers. Many methyl rotor systems have zero or very

close to zero torsional barriers. Much of the vibrational spectrum and in particular the methyl CH stretching features of these "low-barrier" systems are not readily assignable based on a rigid methyl group treatment. Chapter 12 attempts to provide a systematic study of the highly vibrationally excited methyl CH stretching states of low-barrier methyl rotor systems.

CHAPTER 11

THE RIGID METHYL ROTOR LOCAL MODE INTERPRETATION

i.) LM Analysis of Some Methyl Substituted Aromatic Heterocycles.

The CH stretching overtone spectra of a number of methyl containing molecules have been reported[33-35,124,134,178-182]. At higher overtones, two peaks generally dominate the methyl region. Analogous to the situation with the aryl CH stretching overtones, these peaks have been assigned as the overtone transitions associated with the chemically nonequivalent oscillators of the methyl group. This description essentially relies on the vastly differing timescales between internal rotation and methyl CH stretching. The description also assumes the presence of a significant barrier to internal rotation for the methyl group. Under these conditions, the methyl rotor is predominantly localized at the bottom of the well in the torsional potential. The stretching transitions essentially arise from oscillators at their equilibrium torsional conformation.

The liquid phase high overtone regions of methyl substituted furans and thiophenes are consistent with other methyl containing

molecules. Figures 9.15, 10.7 and 10.8 show the two peak structure in the higher methyl overtone regions of both methyl substituted furans and thiophenes. *Ab initio* calculations predict a substantial barrier to methyl group internal rotation in the aromatic heterocycles. Table 11.1 reports the theoretical and experimental[183-185] torsional barrier heights for some of the methyl substituted aromatic heterocycles. Figure 11.1 plots the torsional potential of 2 methylfuran. On the basis of the high methyl overtone features and the predicted torsional barrier heights, the methyl regions will be analysed assuming that the rotor is fixed at its equilibrium conformation. Optimized *ab initio* geometries and microwave[183-185] studies predict a "planar" equilibrium conformation for the methyl group in the furan and thiophene systems. This conformation has one methyl CH oscillator in the plane of the heterocyclic ring with the remaining oscillators staggering the ring. Figure 11.2 depicts the predicted minimum energy conformations for the various methyl substituted thiophenes and furans. The *ab initio* calculations also predict a structural asymmetry between the in-plane (ip) and out-of-plane (op) oscillators. The predicted methyl CH bondlengths are presented in table 11.2.

TABLE 11.1

The Experimental† and *Ab initio* STO-3G and 3-21G Predicted Methyl Torsional Barrier Heights

		$V(3)_{STO-3G}$	$V(3)_{3-21G}$	$V(3)_{exp}$
		(kJ mol^{-1})		
2	methylthiophene	3.52	4.07	2.32
3	methylthiophene	3.41	4.75	3.10
2	methylfuran	2.40	4.46	4.98

† see references 183-185.

FIGURE 11.1

Predicted 3-21G *Ab initio* methyl torsional potential of 2 methylfuran.

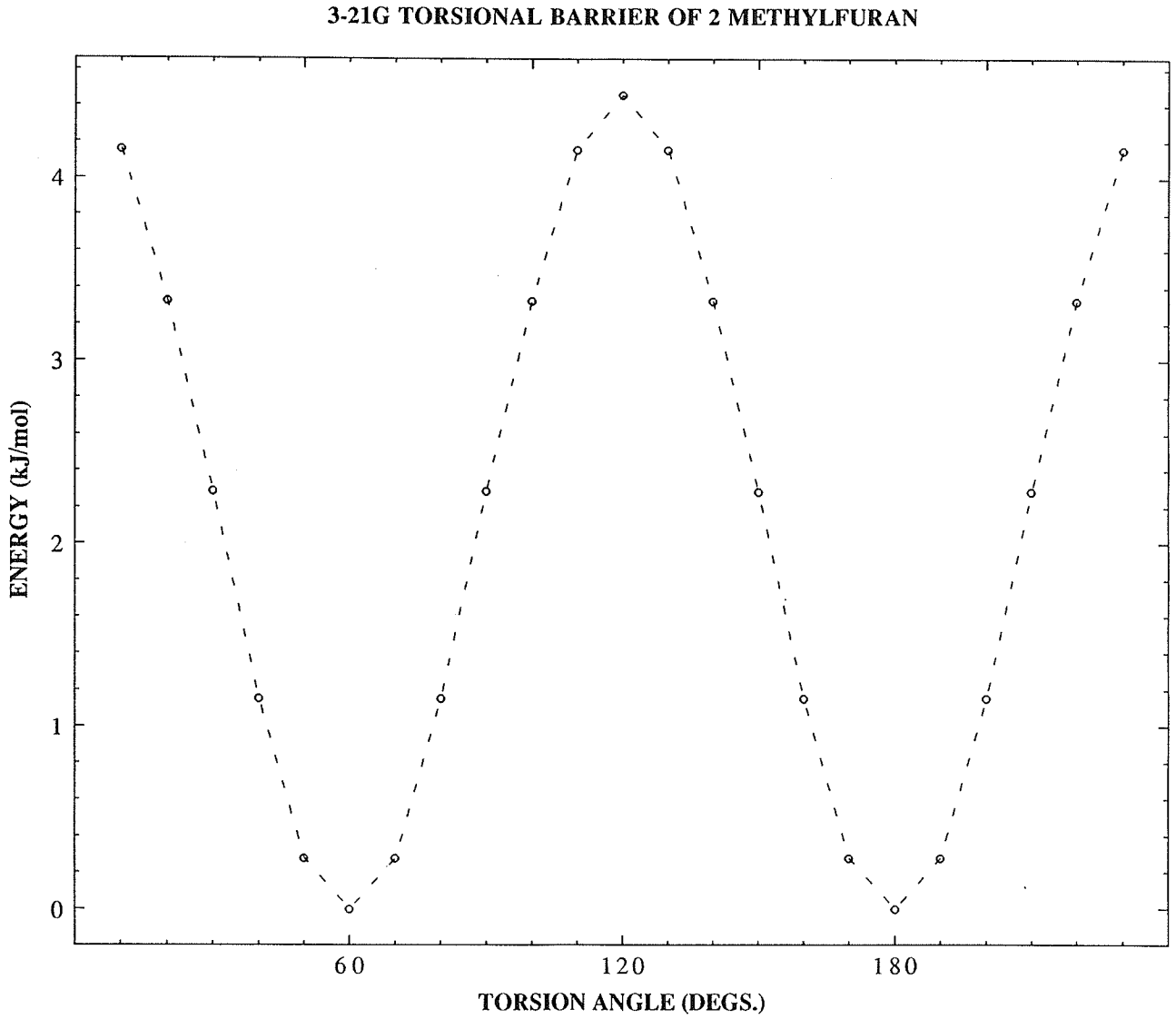
3-21G TORSIONAL BARRIER OF 2 METHYLFURAN
ENERGY (kJ/mol)
0
1
2
3
4
60
120
180
TORSION ANGLE (DEGS.)

FIGURE 11.2

Schematic representation of the minimum energy, planar conformations of 2 and 3 methyl substituted furans and thiophenes.

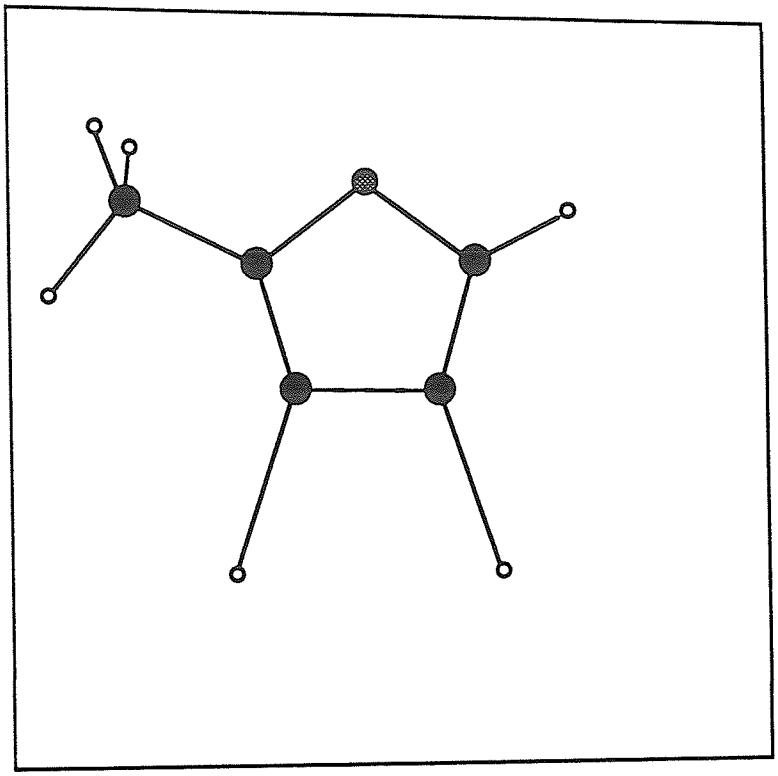

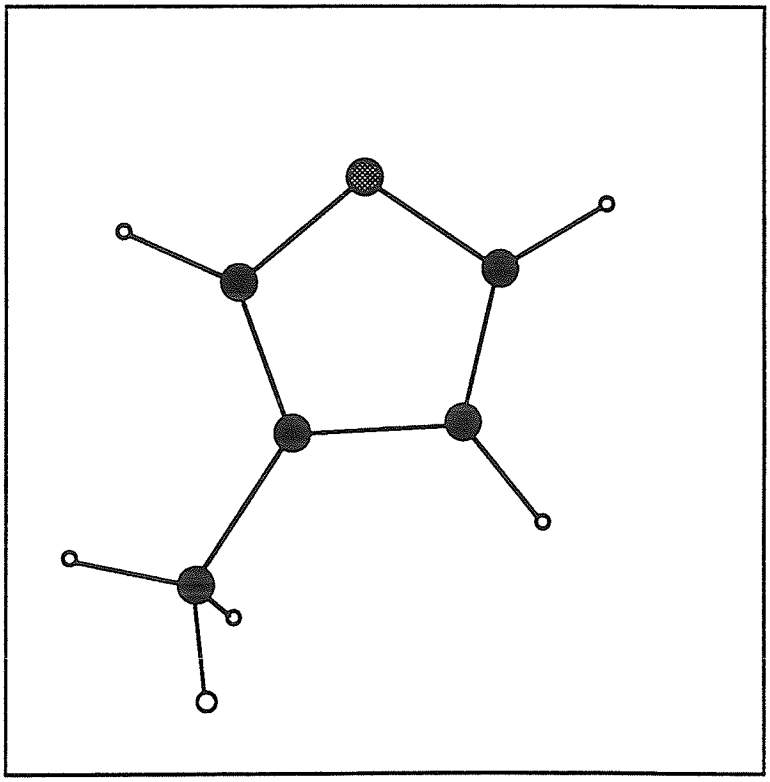

TABLE 11.2

The *Ab initio* Methyl CH In-Plane and Out-of-Plane Bondlengths of Methyl Thiophenes and Furans.

	STO-3G		3-21G		6-31G	
(Å)	r_{ip}	r_{op}	r_{ip}	r_{op}	r_{ip}	r_{op}
THIOPHENES						
2 methyl	1.086	1.088	1.083	1.085	1.083	1.084
3 methyl	1.086	1.088	1.082	1.085	1.082	1.085
2,5 dimethyl	1.086	1.088	1.083	1.085	1.083	1.084
FURANS						
2 methyl	1.085	1.088	1.082	1.084	1.082	1.084
2,5 dimethyl	1.085	1.088	1.082	1.084	1.082	1.084

Distinguishing between the ip and op oscillators reduces the local symmetry of the methyl group from C_{3v} to C_s. The zero order LM model predicts two unique methyl CH stretching fundamental - overtone progressions. At this order the symmetric and antisymmetric out-of-plane CH stretching fundamental-overtone states are degenerate. Isolated oscillator harmonic frequencies derived from *ab initio* force field calculations are higher for the ip oscillator than the op oscillators (see Table 11.3). At a given level of methyl CH stretch excitation, the lower frequency, higher intensity transition is associated with the op oscillators, the higher frequency transition with the ip oscillator. This is consistent with the LM assignments of methyl benzenes[134]. The assignment of the stretching features of the fundamental-overtone progressions affords a zero order parameterization of the LM Hamiltonian. The high quality of the fit of the fundamental-overtone progressions to the anharmonic oscillator equation corroborates the assignment. The zero order LM methyl CH stretching parameters are given in table 11.4.

Although the higher methyl overtone regions can be understood in terms of the zero order local mode model, the fundamental and

TABLE 11.3

The *Ab initio* 3-21G Isolated Oscillator In-Plane and Out-of-Plane Methyl CH Stretching Frequencies of Methyl Thiophenes and Furans.

(cm-1)	ω_{ip}	ω_{op}
2 methylthiophene	3268	3247
3 methylthiophene	3273	3241
2,5 dimethylthiophene	3265	3245
2 methylfuran	3287	3252
2,5 dimethylfuran	3285	3250

TABLE 11.4

The Liquid Phase Zero Order Local Mode In-Plane and Out-of-Plane Methyl CH Stretching Parameters of Methyl Thiophenes and Furans.

(cm^{-1})	ω_{ip}	χ_{ip}	ω_{op}	χ_{op}
THIOPHENES				
2 methyl	3087 ± 1	64.0 ± 0.6	3065 ± 8	64.7 ± 2.2
3 methyl	3069 ± 3	60.6 ± 0.7	3050 ± 1	63.3 ± 0.2
FURANS				
2 methyl	3091 ± 10	61.0 ± 2.8	3058 ± 1	63.1 ± 0.3
2,5 dimethyl	3075 ± 1	58.7 ± 0.8	3051 ± 2	62.9 ± 0.6

$\Delta v_{CH}=2$ regions deviate considerably from the predicted pattern. The $\Delta v_{CH}=2$ regions of the 2,5 dimethyl substituted thiophene and furan are presented in Figures 11.3 and 11.4. Similar deviations are present in the lower energy regions of other methyl containing molecules. The one-bond harmonic coupling extension and similar coupling models were introduced to explain such deviations. Unlike aryl oscillators, the methyl hydrogens share a common central carbon atom. In local coordinates the CH stretching modes are kinetically coupled and coupled through quadratic and higher order terms in the potential. The deviations in the spectroscopic features at the lower vibrational manifolds have largely been attributed to the harmonic CH stretch-stretch couplings. Many of the coupled oscillator treatments have involved equivalent oscillators[29-33,36-38]. In this case, the conformational nonequivalence of the ip and op CH oscillators is considered from the outset of the analysis.

The methyl stretching Hamiltonian has four diagonal oscillator parameters; ω_i, χ_i, ω_o and χ_o. The one-bond coupling operator also has four unique interaction parameters: two kinetic energy terms; γ_{oo} γ_{io} and two potential terms ϕ_{oo} ϕ_{io}. The kinetic and potential

FIGURE 11.3

Gas phase overtone spectrum of 2,5 dimethylthiophene in the $\Delta v_{CH} = 2$ region. The 2,5 dimethylthiophene spectrum was measured with a 3.25 m pathlength cell and at 80°C.

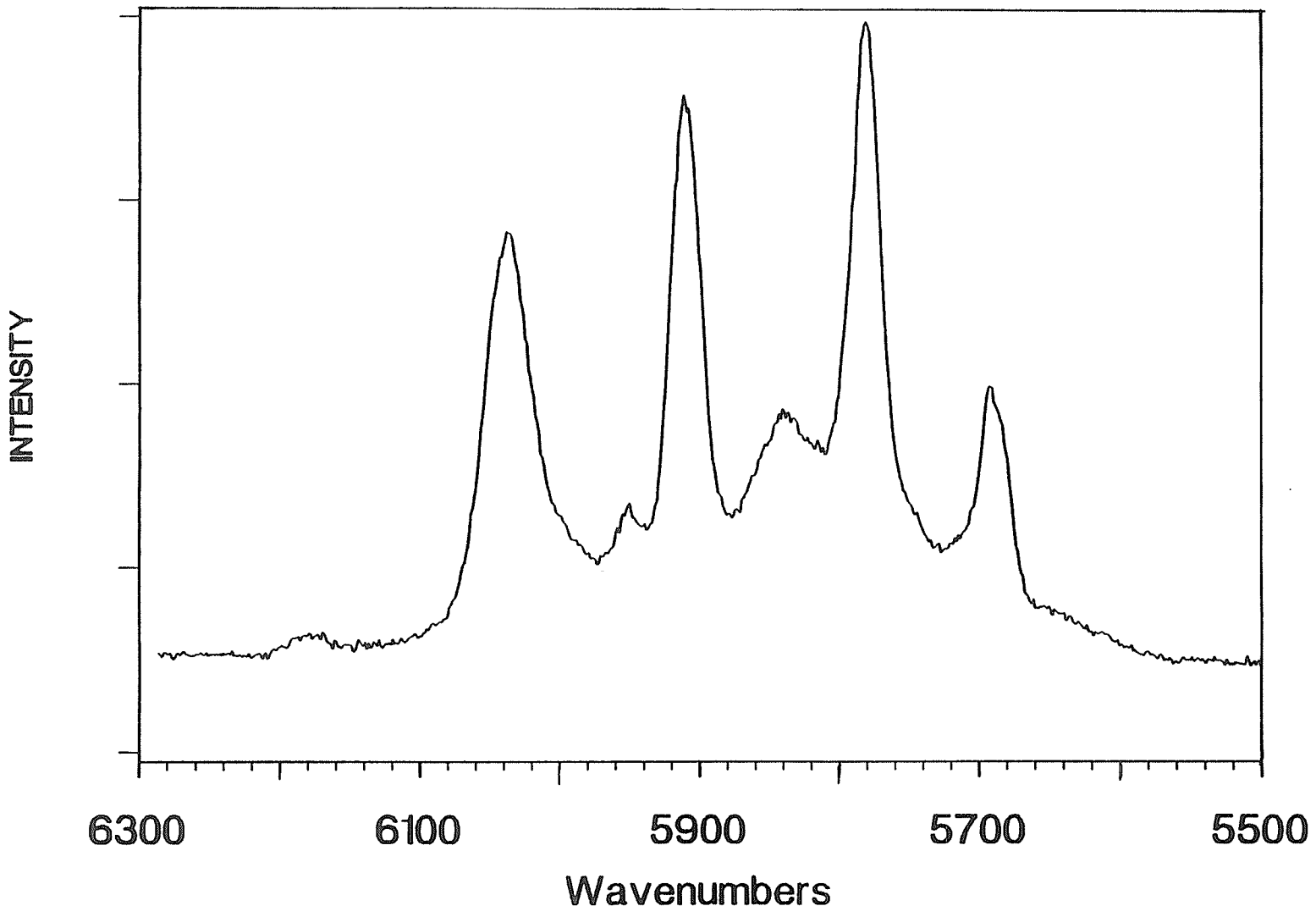
INTENSITY
6300
6100
5900
5700
5500
Wavenumbers

FIGURE 11.4

Gas phase overtone spectrum of 2,5 dimethylfuran in the $\Delta v_{CH} = 2$ region. The 2,5 dimethylfuran spectrum was measured at a pressure of 44 Torr with a 0.75 m pathlength cell.

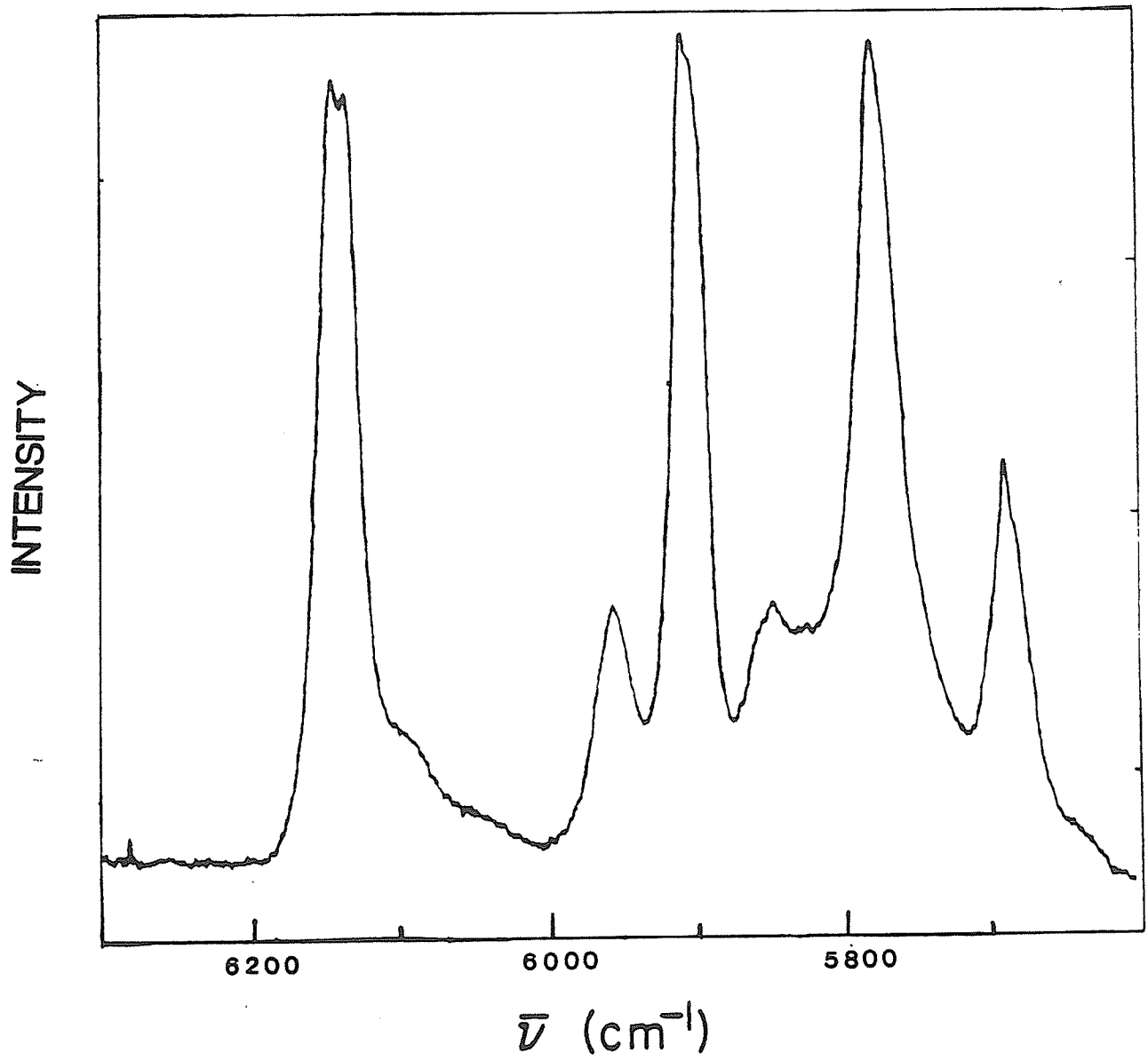
INTENSITY
6200
6000
5800
$\bar{\nu}$ (cm^{-1})

coupling terms are defined in equation (1.19). By ignoring the long range CH stretch-stretch couplings, methyl CH stretching is considered to be isolated from the other vibrational degrees of freedom. In dimethyl species, each methyl group is treated independently. The analysis thus predicts the methyl CH stretching states of symmetrical dimethyl systems to simply have twice the degeneracy of those of an equivalent single methyl system. The stretch-stretch combination states ignored by this analysis are expected to be of little importance in the overtone spectra of these molecules. The strength of the one-bond coupling approximation is discussed in the next paragraph. Zero order eigenstates are labelled as being either symmetric or antisymmetric with respect to the interchange of equivalent op oscillators. We write these symmetrized states [$|i(1)j(2)\rangle\ |k(3)\rangle \pm |j(1)i(2)\rangle\ |k(3)\rangle$] in a shortened form $|ij\rangle_{\pm}\ |k\rangle$ where the equivalent out-of-plane methyl oscillators are numbered as "1" and "2". Introducing effective out-of-plane and in-plane - out-of-plane coupling parameters,

$$c_{oo} = \gamma_{oo} + \phi_{oo} \quad , \quad c_{io} = \gamma_{io} + \phi_{io} \tag{11.1}$$

the one-bond intramanifold methyl CH stretching coupling operator can be written as

$$H'_{ij} = c_{oo}\left(a_1^+ a_2 + a_1 a_2^+\right) + c_{io}\left(a_1^+ a_3 + a_1 a_3^+ + a_2^+ a_3 + a_2 a_3^+\right) \qquad (11.2)$$

Equation (11.2) is used to investigate the effects of interoscillator coupling.

A glance at the methyl CH stretching regions of the various methyl substituted furans and thiophenes confirms many of the aspects predicted by the one-bond, intramanifold coupling model. At given levels of methyl CH stretching excitation, the spectra of the mono and symmetrically disubstituted molecules are virtually identical with the exception of the expected differences in transition intensities (see Figures 11.7,11.8,11.9). The identical appearance of the spectra supports the one-bond coupling approximation. Spectroscopically, interactions between methyl groups or between the methyl and aryl CH stretching states are not resolved. In addition, combinations with vibrational excitation

distributed between methyl groups or between methyl and aryl CH oscillators are not observed. The absence of such combinations suggests that these type of methyl CH stretching states do not effectively interact with the LM and combination methyl CH stretching states where the excitation is localized in a particular methyl group. Therefore combination states which have vibrational energy distributed between methyl groups or between methyl and aryl oscillators can be considered separately in the analysis. The absence of these additional combination transitions and the unresolved long-range coupling splittings supports the one-bond coupling analysis.

The similarity between the spectral features of the furans and thiophenes (see Figure 11.8) supports the model in a different way. Differences in the CH and CC stretching as well as CH bending frequencies between furans and thiophenes would seem to make it unlikely for the methyl CH stretching regions of the molecules to have the identical Fermi resonance structure at each overtone. The difference in the Fermi resonance structure of the aryl overtone regions of the furans and thiophenes was pointed out in Chapter 10. The similarity between the features in the methyl regions of furan

and thiophene suggests that they are predominantly CH stretching features as opposed to combinations involving other vibrational modes. Again this is in accord with the model.

The general pattern along the fundamental-overtone progression is predicted by the one-bond, intramanifold, harmonic coupling extension of the LM model. The single most striking feature of the interoscillator coupling in the fundamental stretching region is the lifting of the degeneracies of the out-of-plane methyl CH stretching fundamentals. The effects of interoscillator coupling on the overtone states is less dramatic. In the harmonic coupling model, the overtone CH stretching states are not directly coupled. The degeneracy of the symmetric-antisymmetric out-of-plane overtone states is broken through the coupling with the stretch-stretch combination states. Due to the anharmonicity defect, the energy mismatch between the overtone and combination states increases with increasing CH stretch excitation. The degeneracy splitting between the out-of-plane states is therefore expected to decrease for the higher overtone levels. Perturbations in the in-plane overtone state from its zero order position should be less marked at the higher overtone regions for the same reason. These

predictions of the coupling model are in general accord with the observations. As one proceeds to the higher overtone regions, the spectra take on an increasingly zero order LM appearance.

Applying the intramanifold one-bond quadratic coupling model, it is hoped that the detailed features of the methyl stretching manifolds can be understood. The symmetric fundamental states are directly coupled by the intramanifold component of the quadratic coupling. This coupling breaks the zero order degeneracy of the symmetric and antisymmetric out-of-plane methyl CH stretch. In some studies[35,186] the degeneracy splitting was assumed to arise solely from the coupling between the two equivalent oscillators of the methyl group. Assuming weak interoscillator coupling, the observed spectral splitting in the fundamental region was used in the parameterization of this coupling. Phenomenologically the equivalent oscillator coupling assumption seemed successful. Physically however, the basis for the assumption is not at all obvious. For typical methyl geometries, the kinetic energy coupling constants, G_{ij}, are nearly of equal value for both types of interactions. The potential energy interactions are also predicted to be of the same order of magnitude for both interactions. These

assumptions are tested in the course of this analysis.

Interoscillator couplings obtained from *ab initio* optimized geometries and harmonic force fields suggest that the ip - op coupling (coupling between nonequivalent oscillators) is significant and should not be overlooked. In fact, for methyl substituted furans and thiophenes, the absolute value of the effective CH_{ip} - CH_{op} intramanifold coupling is predicted to be greater than intramanifold CH_{op} - CH_{op} coupling. The kinetic and potential energy coupling parameters obtain at the 3-21G basis set level for selected methyl substituted furans and thiophenes are listed in table 11.5. To examine the effects of the interoscillator couplings in more detail, the coupling operator (Equation 11.2) is diagonalized within the symmetrized basis at various coupling limits. Figure 11.5 illustrates the effects of the interoscillator coupling on the fundamental states. The point to note from Figure 11.5 is that the $|10\rangle_{\pm}|0\rangle$ degeneracy is broken by any of the coupling schemes. The fundamental splitting is not solely indicative of the coupling between the equivalent op oscillators. The practise of using the fundamental splitting of the $|10\rangle_{\pm}|0\rangle$ states to parameterize the equivalent oscillator coupling, is valid only if the coupling between

TABLE 11.5

The Internal Coordinate Quadratic Kinetic and Potential Energy Methyl Inter-Oscillator Coupling Constants Obtained From Analytical *Ab initio* 3-21G Force Field Calculations.

		γ_{io}	φ_{io}	γ_{oo}	φ_{oo}
		(cm^{-1})			
2	methylthiophene	-39.71	16.06	-39.05	20.49
3	methylthiophene	-39.65	16.49	-38.93	20.11
2,5	dimethylthiophene	-39.65	16.15	-38.96	20.79
2	methylfuran	-41.05	15.37	-38.75	19.99
2,5	dimethylfuran	-40.94	15.50	-38.68	20.36

FIGURE 11.5

Energy level diagram of the effects of various intramanifold interoscillator coupling limits. The extreme left and right columns of the diagram show the uncoupled energy level spacings using the zero order in-plane methyl parameters $\omega_i = 3008$ cm^{-1} $\chi_i = 60.6$ cm^{-1} and the out-of-plane methyl parameters $\omega_o = 2988$ cm^{-1} $\chi_o = 63.3$ cm^{-1}. The central column considers the coupling between all the methyl oscillators ($c_{io} = 20$ cm^{-1} and $c_{oo} = 20$ cm^{-1}) while only the coupling between out-of-plane oscillators is depicted to the left of the central column and only the in-plane to out-of-plane coupling is treated to the right of the central column.

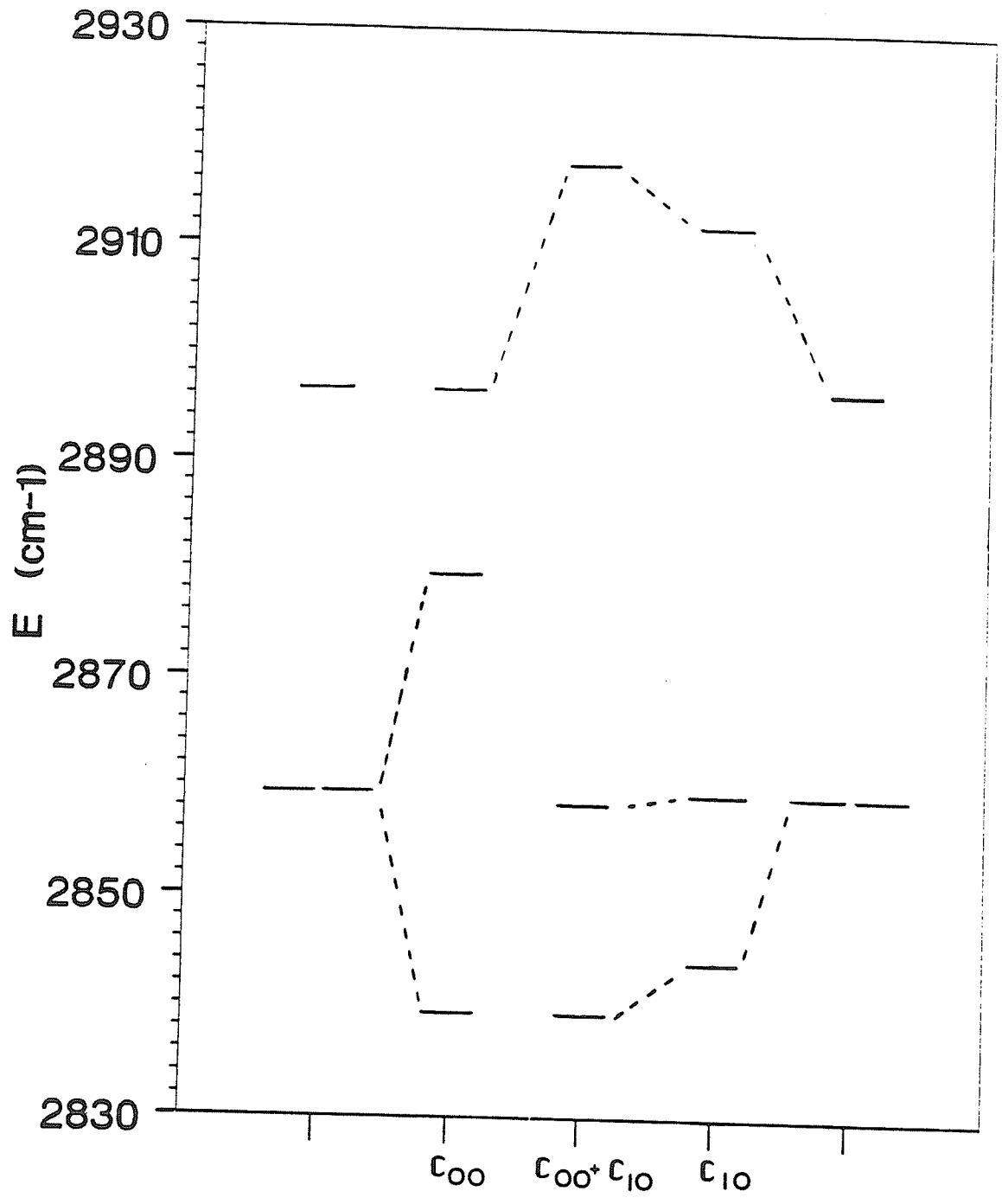
2930
2910
2890
2870
2850
2830
E (cm-1)
C00
C00+C10
C10

the ip and op oscillators is identically zero. The theoretical calculations however do not support this coupling assumption.

If the interoscillator coupling is weak, then in principle, the three fundamental transitions are sufficient to parameterize the complete coupling operator. The weak coupling condition is necessary in order that the zero order oscillator parameters can be retained in the coupled oscillator extension of the model without a reparameterization. The three fundamental methyl transition frequencies cannot be fit to provide a consistent set of effective op-op and ip-op coupling parameters in either the methylfuran or the methylthiophene molecules. This inability to consistently fit the methyl fundamentals can be rationalized within the model as arising from the breakdown of the weak coupling assumption. This breakdown is supported by the *ab initio* calculations. The interoscillator couplings obtained from *ab initio* calculations are not much smaller than the zero order oscillator anharmonicities. An additional complication plaguing the fundamental states is the Fermi resonances between the symmetric out-of-plane methyl stretch and a nearby combination[117,118]. This interaction may shift the level and alter intensities sufficiently to make the set of fundamental

transitions of relatively little use in the parameterization of the Hamiltonian. Alone, the fundamental transitions offer little help in understanding the interoscillator couplings in these systems. Investigation of the methyl CH stretching overtone regions can supply additional information on the coupling pathways and further test the coupling model.

In the lower overtone regions of the methyl furans and thiophenes, the most noticeable feature which can be attributed to interoscillator coupling is the presence of methyl CH stretch - stretch combinations. At zero order these combinations are forbidden within the linear dipole approximation. Only the local mode overtone states carry any oscillator strength. Interoscillator coupling however mixes the zero order states. The effect of zero order state mixing on the linear dipole transition intensity originating from the ground state to a final XH stretching state within the intramanifold coupling approximation can be expressed as,

$$I^{f0} \propto \left| \sum_{i}^{XH} \left(\frac{\partial \mu}{\partial q_i} \right)_0 \sum_{j} c_j^f \left\langle \psi_j^f \left| q_i \right| \psi^0 \right\rangle \right|^2 \qquad (11.3)$$

where c^f_j are the coefficients of the final wavefunction in the zero order intramanifold LM basis. The summation i runs over the set of XH oscillators and j over the intramanifold basis. The only nonvanishing integrals involving the LM ground state are with the LM fundamental-overtone states. Through the intramanifold interoscillator coupling terms, combination states which mix with local mode states can acquire intensity even within the linear dipole approximation.

Using the zero order LM oscillator parameters, the interoscillator methyl couplings obtained from *ab initio* optimized geometries and harmonic force fields and CH stretching dipole moment derivatives, a preliminary estimate of the transition frequencies and intensities of the methyl stretching features can be calculated. The observed and predicted methyl CH stretching features of 2,5 dimethylfuran and 2,5 dimethylthiophene are reported in tables 11.6 - 11.13. Linear dipole transition intensities were calculated using the 3-21G numerical CH stretching dipole moment derivatives. Interoscillator coupling parameters were obtained from the *ab initio* analytical harmonic force field again using the 3-21G basis set. The intramanifold Hamiltonians were

diagonalized using the harmonic coupling as well as the exact Morse quadratic coupling matrix elements. The required harmonic matrix elements are easily obtained if the position and momentum operators are expressed in terms of raising and lowering operators. The analytical Morse oscillator matrix elements required for the evaluation of the Morse quadratic couplings and the linear dipole transition intensities have been reported[26,27].

Before explicitly considering the individual vibrational manifolds, some of the general aspects of the model deserve comment. Overall, the predicted transition intensities are grossly unaffected by the choice of harmonic or Morse oscillator coupling matrix elements. The rule of thumb in measuring a CH stretching fundamental-overtone progression is to expect a large decrease in the transition intensity between the fundamental and first overtone region. The intensity of each succeeding overtone region drops an order of magnitude in intensity. The model predicts such a general fall-off in overtone intensities. In addition, the intensities of the combinations decrease relative to the overtone transitions as one proceeds to higher levels of excitation. Again this is consistent with experiment. The model calculations also consistently predict

the antisymmetric methyl transitions to be less intense than a corresponding symmetric methyl transition. In 2,5 dimethylfuran the symmetric out-of-plane methyl CH stretching overtone is predicted to be about a factor of seven more intense than the antisymmetric out-of-plane methyl CH stretching overtone of the corresponding vibrational manifold. For 2,5 dimethylthiophene the difference in overtone intensities is predicted to be about a factor of three. The difference between symmetric and antisymmetric combination intensities is predicted to be even greater by the model.

The predicted transition energies are affected by the choice of harmonic or Morse oscillator matrix elements. At the lower manifolds, the transition frequencies predicted by the harmonic coupling model are lower than the observed transitions. Using the Morse matrix elements considerably improves the agreement at the low manifolds. Proceeding to the higher manifolds, the transition frequencies are overestimated when the Morse matrix elements are used. These systematic deviations in the model can, for the most part, be simultaneously corrected. By decreasing the effective coupling and slightly increasing the oscillator frequency and anharmonicity the overall fit of the model to the observed spectral

features is improved. This improvement occurs regardless of which matrix elements are used. A reparameterization of the Hamiltonian is perhaps not too surprising since neither the oscillator parameters nor the couplings were optimized to fit the spectral features within the coupling model. Split valence *ab initio* basis sets appear to slightly overestimate the interoscillator coupling. The zero order methyl oscillator parameters also seem to require a small reparameterization consistent with a break-down of the weak coupling assumption.

In the model description, the large energy mismatch between methyl overtone and combination states at the high levels of CH stretch excitation decreases the spectral manifestations of the interoscillator coupling. These spectral regions usually have a "zero order" LM appearance. At $\Delta v_{CH} = 3$ (Figures 11.6,11.7) weak features not predicted by the zero order LM model appear. The highest intensity peak in that region and the peak immediately to its high energy side were assigned as the zero order out-of-plane and in-plane methyl CH stretching overtones respectively. Unlike in the fundamental region, the out-of-plane degeneracy splitting isn't observed at this overtone. The splitting is only predicted to be on

FIGURE 11.6

Gas phase overtone spectrum of 2,5 dimethylthiophene in the $\Delta v_{CH} = 3$ region. The 2,5 dimethylthiophene spectrum was measured at 80°C with a 9.75 m gas cell pathlength.

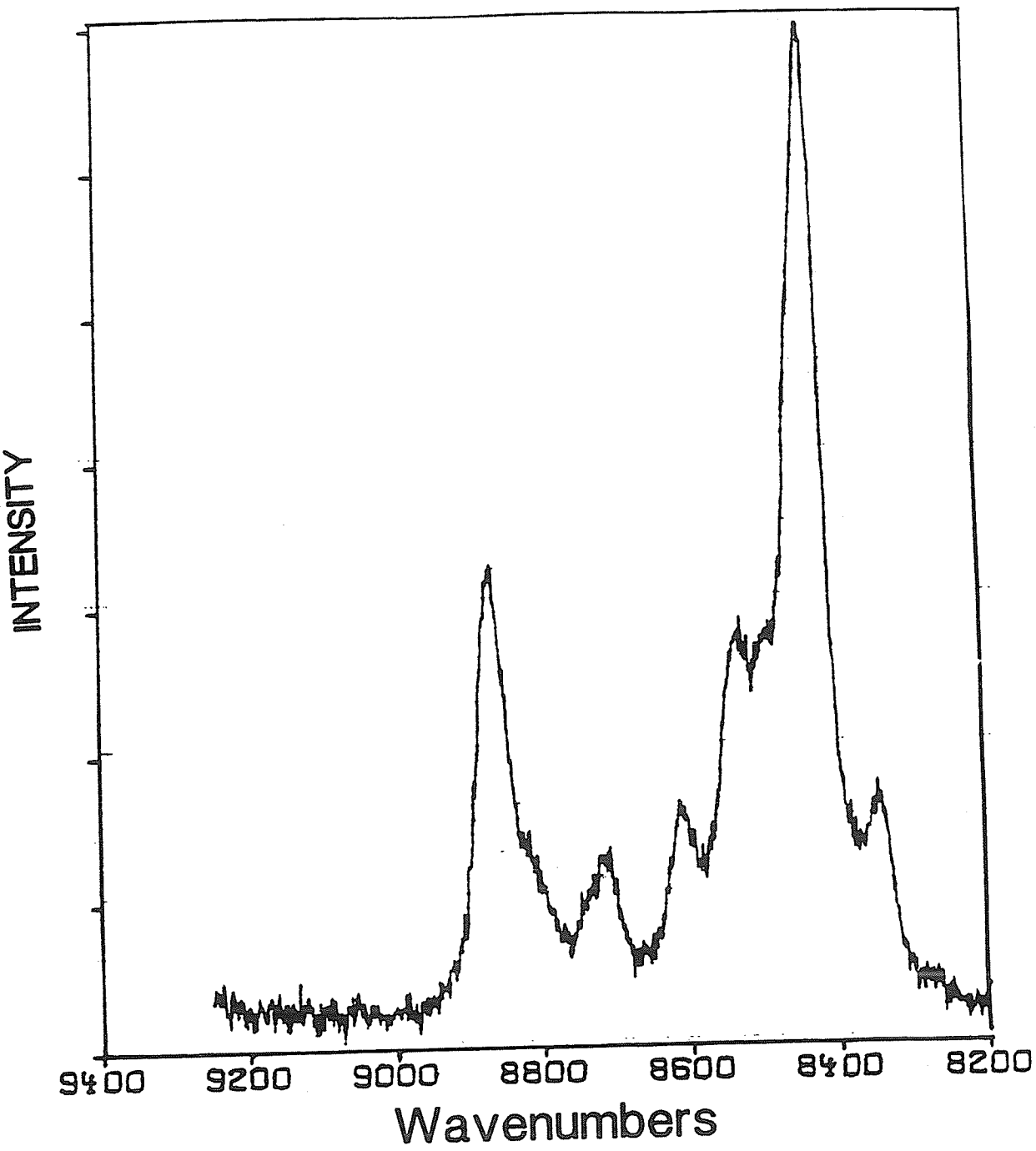
INTENSITY
9400
9200
9000
8800
8600
8400
8200
Wavenumbers

FIGURE 11.7

Gas phase overtone spectrum of 2 methyl (upper trace) and 2,5 dimethyl (lower trace) furan in the $\Delta v_{CH} = 3$ region. The 2 methylfuran sample pressure was 75 Torr and a gas cell pathlength of 11.25 m was used. The 2,5 dimethylfuran spectrum was measured with a sample pressure of 44 Torr with a gas cell pathlength of 8.25 m.

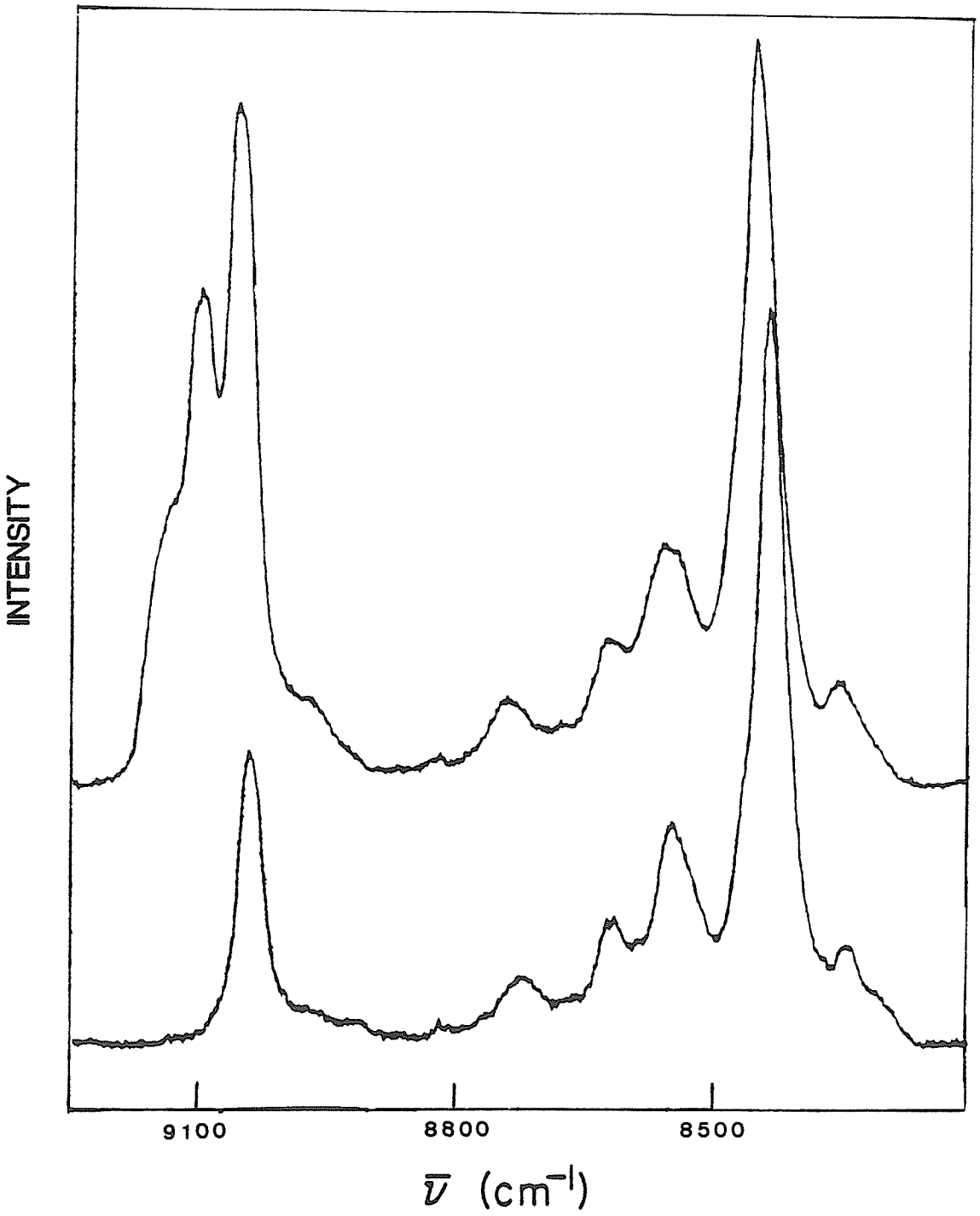
INTENSITY
9100
8800
8500
$\bar{\nu}$ (cm^{-1})

the order of 1 cm^{-1} for these methyl systems at $\Delta v_{CH} = 3$ (see Tables 11.6 and 11.8). Weaker peaks within the methyl stretching region appear at higher energy. These weak peaks roughly correspond to the predicted positions of the methyl CH stretch - stretch combinations. In the intramanifold coupling model, their intensity arises from the small but finite mixing of zero order local mode states and combinations. Predicted combination intensities (see Tables 11.7 and 11.9) vary as to whether harmonic or Morse oscillator matrix elements are used in the analysis. Lower combination intensities are predicted when the Morse oscillator matrix elements are used. Regardless of the choice of matrix elements, the general relative ordering of combination intensities are reproduced. The combination with the zero order label, $|21\rangle_+ |0\rangle$, is predicted to be the most intense combination. The intensity of the combination ranges from somewhat less than 2% to nearly 4% of the intensity of the $|30\rangle_+ |0\rangle$ overtone. The $|20\rangle_+ |1\rangle$ combination, is predicted to be a third the intensity of the $|21\rangle_+ |0\rangle$ labelled state. The only other combination with significant intensity when Morse matrix elements are used is the state labelled as the $|10\rangle_+ |2\rangle$ combination. This transition is predicted to be less than 0.5% of the intensity of the highest

TABLE 11.6

OBSERVED AND PREDICTED METHYL CH STRETCHING OVERTONE AND COMBINATION POSITIONS OF 2,5 DIMETHYLTHIOPHENE IN THE $\Delta v_{CH} = 3$ REGION.

Assignment	Observed		Local Mode	
	gas	Zero Order	Harmonic	Morse
V = 3				
$30\rangle_+ 0\rangle$	8432	8392	8384	8421
$30\rangle_- 0\rangle$			8385	8422
$00\rangle 3\rangle$	8534	8480	8469	8507
$21\rangle_+ 0\rangle$	8611	8645	8601	8661
$21\rangle_- 0\rangle$			8654	8708
$20\rangle_+ 1\rangle$	8720	8669	8704	8687
$20\rangle_- 1\rangle$			8686	8740
$10\rangle_+ 2\rangle$	-	8699	8660	8737
$10\rangle_- 2\rangle$	-		8722	8791
$11\rangle 1\rangle$	-	8796	8819	8859

TABLE 11.7

PREDICTED METHYL CH STRETCHING OVERTONE AND COMBINATION INTENSITIES OF 2,5 DIMETHYLTHIOPHENE IN THE $\Delta v = 3$ REGION.

Assignment	Local Mode		
	Zero Order	Harmonic	Morse
$30>_+ 0>$	1.13E-23	1.09E-23	1.11E-23
$30>_- 0>$	2.75E-24	2.68E-24	2.71E-24
00> 3>	5.35E-24	5.07E-24	5.23E-24
$21>_+ 0>$	0	3.06E-25	2.18E-25
$21>_- 0>$	0	6.69E-26	2.22E-26
$20>_+ 1>$	0	1.39E-25	7.29E-26
$20>_- 1>$	0	3.27E-28	1.77E-26
$10>_+ 2>$	0	1.99E-25	5.78E-26
$10>_- 2>$	0	2.81E-27	5.05E-28
11> 1>	0	1.25E-26	2.19E-27

TABLE 11.8

OBSERVED AND PREDICTED METHYL CH STRETCHING OVERTONE AND COMBINATION POSITIONS OF 2,5 DIMETHYLFURAN IN THE $\Delta v_{CH} = 3$ REGION.

Assignment	Observed		Local Mode		
	liquid	gas	Zero Order	Harmonic	Morse
$30\rangle_+ 0\rangle$				8390	8426
	8398	8437	8399		
$30\rangle_- 0\rangle$				8391	8427
$00\rangle 3\rangle$	8522	8553	8523	8508	8547
$21\rangle_+ 0\rangle$				8605	8680
	8598	8625	8650		
$21\rangle_- 0\rangle$				8664	8720
$20\rangle_+ 1\rangle$				8677	8716
	8698	8729	8683		
$20\rangle_- 1\rangle$				8698	8752
$10\rangle_+ 2\rangle$	-	-		8728	8769
			8724		
$10\rangle_- 2\rangle$	-	-		8748	8792
$11\rangle 1\rangle$	-	-	8809	8836	8867

TABLE 11.9

PREDICTED METHYL CH STRETCHING OVERTONE AND COMBINATION INTENSITIES OF 2,5 DIMETHYLFURAN IN THE $\Delta v = 3$ REGION

Assignment	Local Mode		
	Zero Order	Harmonic	Morse
$30>_+ 0>$	1.16E-23	1.12E-23	1.14E-23
$30>_- 0>$	1.64E-24	1.60E-24	1.62E-24
$00> 3>$	4.62E-24	4.17E-24	4.54E-24
$21>_+ 0>$	0	4.25E-25	1.97E-25
$21>_- 0>$	0	4.36E-26	1.05E-26
$20>_+ 1>$	0	2.30E-25	4.33E-26
$20>_- 1>$	0	5.55E-28	9.93E-27
$10>_+ 2>$	0	1.60E-25	4.18E-26
$10>_- 2>$	0	1.07E-27	3.03E-28
$11> 1>$	0	2.48E-26	2.57E-27

intensity overtone transition of that manifold. The intensities of the combinations fall off less rapidly when the harmonic matrix elements are used.

The fitting of stretching features in the $\Delta v_{CH} = 3$ region to a set of Lorentzian lines enables comparison of the relative intensities of the transitions. The intensities (full-width at half maximium times the amplitude) of the transitions assigned as the $|21\rangle_+ |0\rangle$ and $|20\rangle_+ |1\rangle$ combinations in the gas phase spectrum of 2,5 dimethylfuran are about 1.8% and 1.4% of the $|30\rangle_\pm |0\rangle$ overtone. Higher energy combinations are not readily apparent in the spectra. These observed combination intensities are consistent with the predicted mixing intensities of these transitions.

Considering the crude dipole moment function used, the quality of the predicted relative overtone intensities between the in-plane and out-of-plane oscillators is perhaps surprising. For the $\Delta v_{CH} = 3$ region, from the fit of the spectral features, the $|00\rangle |3\rangle$ transition is about 35% of the intensity of the $|30\rangle_\pm |0\rangle$ transitions in both the methyl furans and thiophenes. This is also the relative predicted $|00\rangle |3\rangle$ transition intensity for 2,5 dimethylfuran. The situation for 2,5 dimethylthiophene is not much worse. The $|00\rangle |3\rangle$ transition is

predicted to be about 38% of the intensity of the $|30\rangle_{\pm}|0\rangle$ transitions.

The relative overtone intensities and the combination intensities for the $\Delta v_{CH} = 3$ region can be reasonably well understood using the intramanifold coupling model, the linear dipole approximation and a low level dipole moment function. Since in our model combinations derive intensity by LM state mixing through the intramanifold interoscillator couplings, combination intensities offer some information on the operative model couplings. In the absence of coupling between ip and op oscillators only the $|21\rangle_{+}|0\rangle$ combination should have significant intensity. Alternatively, in the limit of the op oscillators being decoupled, $|20\rangle_{+}|1\rangle$ should be the most intense combination. The presence of both combinations with similar intensities suggests that both couplings are operative.

At $\Delta v_{CH} = 2$ (see Figures 11.3,11.4, 11.8 and 11.9) the combination features are much more intense than at $\Delta v_{CH} = 3$. This is partially predicted by the model. The improved energy match between the combination and local mode states, make the spectral manifestations of the coupling greater at the lower overtone. Aside from differences in relative intensities and small shifts in band

FIGURE 11.8

Gas phase overtone spectrum of 2 methylfuran (lower trace) and 2,5 dimethylthiophene (upper trace) in the methyl $\Delta v_{CH} = 2$ region. The room temperature 2 methylfuran spectrum was measured at a pressure of 75 Torr and with a gas cell pathlength of 0.75 m. The 2,5 dimethylthiophene spectrum was measured at 80°C with a 3.25 m gas cell pathlength.

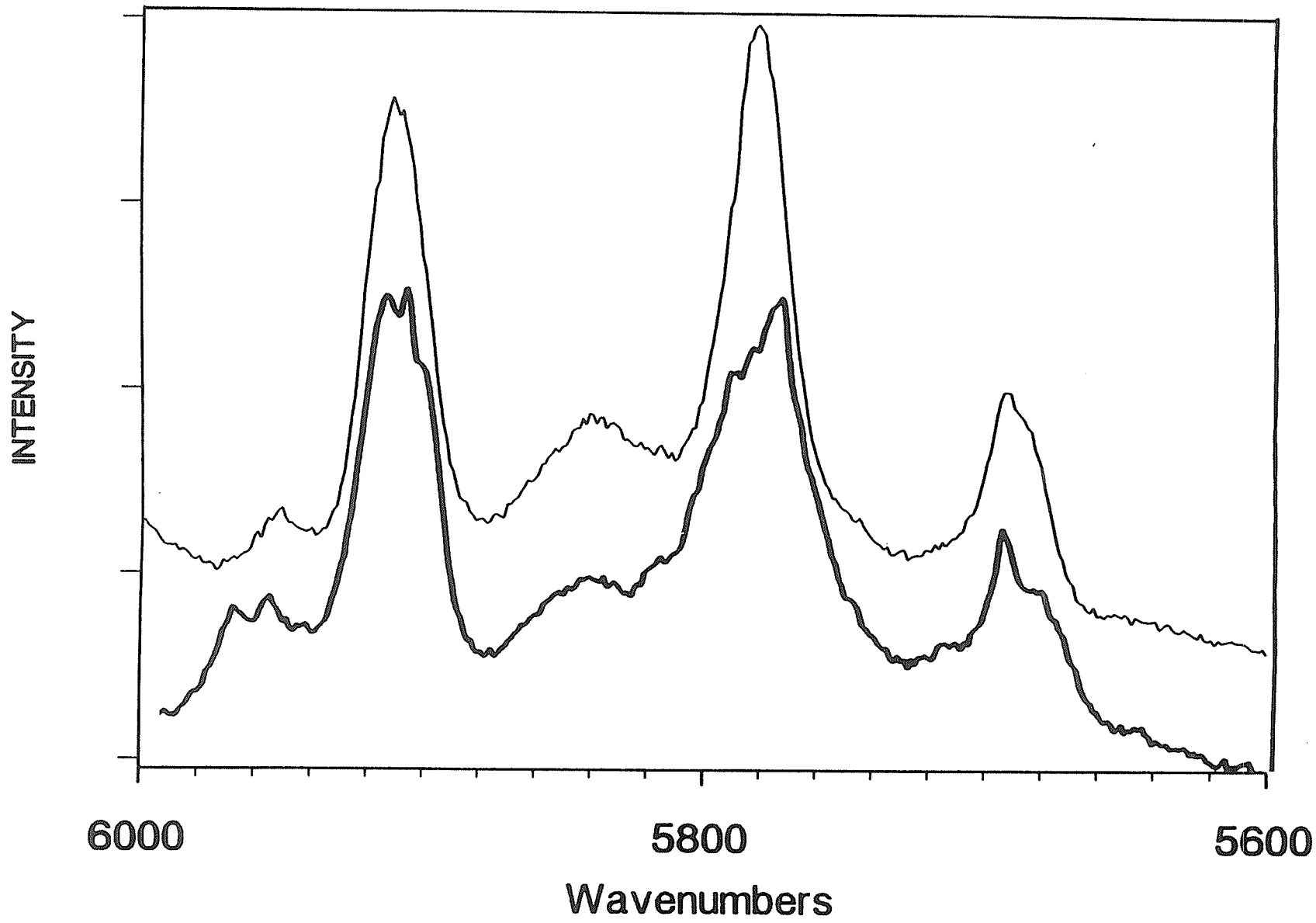
INTENSITY
6000
5800
5600
Wavenumbers

FIGURE 11.9

Gas phase overtone spectrum of the methyl $\Delta v_{CH} = 2$ stretching region of 3 methyl (lower trace), 2 methyl (middle trace), and 2,5 dimethyl (upper trace) thiophene. The sample pressures of 2 and 3 methyl thiophene were 18 Torr and the gas cell pathlength was 2.25m. The 2,5 dimethylthiophene spectrum was measured at 80°C with a 3.25 m gas cell pathlength.

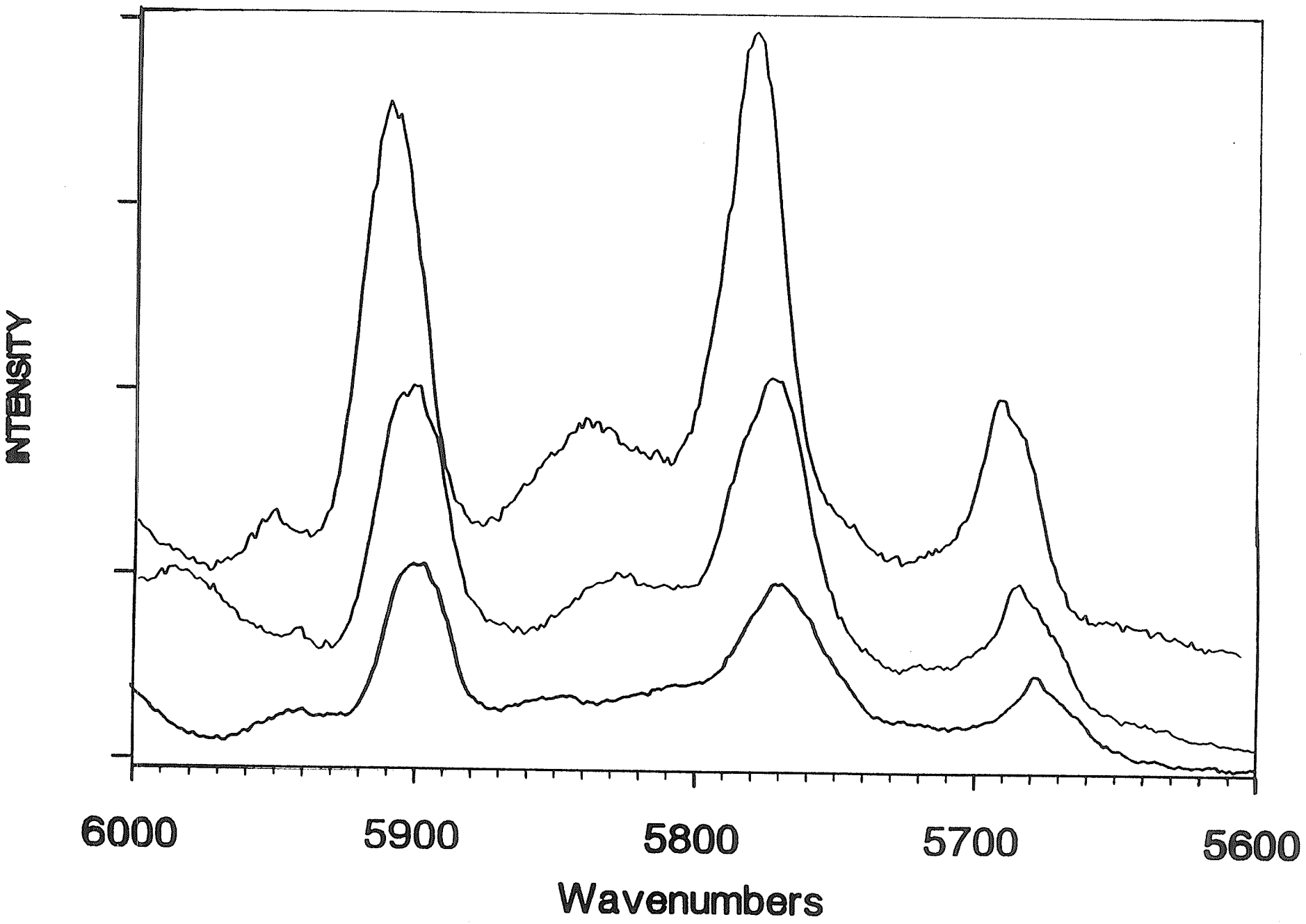
INTENSITY
6000
5900
5800
5700
5600
Wavenumbers

maxima, the methyl regions of all the furans and thiophenes have the same overall appearance. In the $\Delta v_{CH} = 2$ region, there are five major bands which the spectra have in common. Although these bands appear to have substructure, splittings are not clearly resolved. The highest intensity peak and the peak immediately to its high energy side are again assigned as the overtone transitions to the $|20\rangle_{\pm}\ |0\rangle$ and $|00\rangle\ |2\rangle$ states. At this manifold, as at $\Delta v_{CH} = 3$, the predicted relative intensies of the overtone transitions are in agreement with the spectroscopic data (see table 11.10-11.13). The higher energy peaks coincide with the predicted energies of the stretch-stretch combinations. All three combinations seem to appear in the spectra. The $|11\rangle\ |0\rangle$ and $|10\rangle_{+}|1\rangle$ transitions are predicted to be separated by between 16 and 56 cm^{-1}. The highest intensity combination, which is in the correct frequency range to be these transitions, appears as an unresolved doublet consistent with these predictions. The highest energy methyl transition is assigned as the $|10\rangle_{-}\ |1\rangle$ combination. Consistent with model predictions, the antisymmetric $|10\rangle_{-}\ |1\rangle$ combination transition has a much lower intensity than the assigned symmetric combinations. The peak to the low energy side of the $|20\rangle_{-}\ |0\rangle$ overtones is not accounted for in the

model assignment.

The presence of all three combinations at $\Delta v_{CH} = 2$ cannot be explained by the intramanifold coupling model if only the equivalent op oscillators couple to each other. In the limit of strictly out-of-plane coupling, the symmetric out-of-plane overtone $|20\rangle_+ |0\rangle$ is only coupled to the out-of-plane combination $|11\rangle |0\rangle$. Thus in this limit, only the out-of-plane combination, $|11\rangle |0\rangle$, can acquire significant intensity. In addition, the degeneracy of the symmetric and antisymmetric combinations, $|10\rangle_\pm |1\rangle$ is only weakly broken in this coupling limit. In the absence of out-of-plane coupling, but allowing coupling between the in-plane and out-of-plane oscillators, the degeneracy of the symmetric - antisymmetric combination states $|10\rangle_\pm |1\rangle$ is significantly broken. In the ip-op coupling limit, the out-of-plane combination $|11\rangle |0\rangle$ mixes only indirectly with the overtone states. Transitions to all combination states become allowed in this limit but the $|11\rangle |0\rangle$ combination is expected to be weak. Like the observations at $\Delta v_{CH} = 3$, the analysis suggests that neither coupling limit applies. In fact if the $|11\rangle |0\rangle$ and $|10\rangle_+ |1\rangle$ transitions could be well enough resolved to get the relative

TABLE 11.10

OBSERVED AND PREDICTED METHYL CH STRETCHING OVERTONE AND COMBINATION POSITIONS OF 2,5 DIMETHYLTHIOPHENE IN THE $\Delta v_{CH} = 1$ AND 2 REGIONS.

Assignment	Observed			Local Mode
	gas	Zero Order	Harmonic	Morse
V = 1		(cm^{-1})		
$10>_+ 0>$	—	2924	2894	2912
$10>_- 0>$			2938	2959
$00> 1>$	—	2948	2963	2958
V = 2				
$20>_+ 0>$	5782	5721	5706	5734
$20>_- 0>$			5716	5743
$00> 2>$	5841	5775	5761	5791
$11> 0>$	5911	5848	5844	5881
$10>_+ 1>$	5954	5872	5891	5900
$10>_- 1>$			5891	5918

TABLE 11.11

PREDICTED METHYL CH STRETCHING OVERTONE AND COMBINATION INTENSITIES OF 2,5 DIMETHYLTHIOPHENE IN THE $\Delta v = 2$ REGION.

Assignment		Local Mode	
	Zero Order	Harmonic	Morse
$20\rangle_+ 0\rangle$	3.85E-22	2.92E-22	3.56E-22
$20\rangle_- 0\rangle$	9.63E-23	9.10E-23	9.29E-23
$00\rangle 2\rangle$	1.92E-22	1.91E-22	1.86E-22
$11\rangle 0\rangle$	0	4.13E-23	2.76E-23
$10\rangle_+ 1\rangle$	0	1.58E-23	6.75E-24
$10\rangle_- 1\rangle$	0	2.54E-24	7.00E-25

TABLE 11.12

OBSERVED AND PREDICTED METHYL CH STRETCHING OVERTONE AND COMBINATION POSITIONS OF 2,5 DIMETHYLFURAN IN THE Δv_{CH} = 1 AND 2 REGIONS.

Assignment	Observed		Local Mode		
	liquid	gas	Zero Order	Harmonic	Morse
V = 1					
$\|10\rangle_+ \|0\rangle$	2926		2925	2895	2907
$\|10\rangle_- \|0\rangle$				2940	2938
$\|00\rangle \|1\rangle$	2952		2958	2974	2973
V = 2					
$\|20\rangle_+ \|0\rangle$	5753	5775	5725	5708	5734
$\|20\rangle_- \|0\rangle$				5720	5747
$\|00\rangle \|2\rangle$	5824	5847	5799	5781	5814
$\|11\rangle \|0\rangle$	5884	5903	5850	5849	5881
$\|10\rangle_+ \|1\rangle$	5937	5955	5884	5906	5896
$\|10\rangle_- \|1\rangle$				5903	5943

TABLE 11.13

PREDICTED METHYL CH STRETCHING OVERTONE AND COMBINATION INTENSITIES OF 2,5 DIMETHYLFURAN IN THE $\Delta v = 2$ REGION

Assignment		Local Mode	
	Zero Order	Harmonic	Morse
$20>_+ 0>$	3.98E-22	3.98E-22	3.75E-22
$20>_- 0>$	5.63E-23	5.48E-23	5.58E-23
$00> 2>$	1.72E-22	1.16E-22	1.47E-22
$11> 0>$	0	5.95E-23	4.28E-23
$10>_+ 1>$	0	2.72E-23	4.49E-24
$10>_- 1>$	0	1.57E-24	5.59E-25

intensities of the combinations and the $|10\rangle_{\pm}|1\rangle$ splitting could be resolved, the magnitudes of the couplings within the model description could be ascertained. Although these values cannot be obtained from the unresolved spectral features, the lower overtone regions do not support the equivalent oscillator assumption for these methyl systems.

One disturbing problem in the analysis of relative overtone - combination intensities is the anomalous symmetric combination intensities at $\Delta v_{CH} = 2$. Since in our model the combinations acquire intensity from mixing with the local mode states of the same manifold, the combination intensity cannot exceed the intensities of the overtone transitions. In the $\Delta v_{CH} = 2$ region, it is not uncommon to observe combinations with higher intensities than the overtones. In the case of the methylfurans and methylthiophenes the unresolved $|11\rangle|0\rangle$, $|10\rangle_{+}|1\rangle$ combination is roughly the same intensity as the $|20\rangle_{\pm}|0\rangle$ overtone and much more intense than the $|00\rangle|2\rangle$ overtone. The antisymmetric combination, $|10\rangle_{-}|1\rangle$, is considerably less intense than its symmetric counterpart, yet in the furan systems it has roughly the same intensity as the weak $|00\rangle|2\rangle$ overtone. The

next section addresses the issue of the $\Delta v_{CH} = 2$ combination intensities. Qualitatively the combination intensities can be understood retaining the simple linear dipole approximation but using improved LM wavefunctions.

In addition, the intramanifold coupling model cannot account for all the observed transitions in the CH stretching regions of the molecules. For the methyl systems we have examined in this section, peaks to the low energy side of the out-of-plane overtone transition standout. The low energy peak is especially intense in the $\Delta v_{CH} = 2$ region. This problem will be discussed in greater depth in Chapter 12.

The predictions of this simplistic description of relative overtone - combination intensities in the $\Delta v_{CH} = 2$ and 3 regions are quite remarkable. This suggests that even at the lowest level of theoretical sophistication, predicted intensities are sufficiently accurate to aid in the assignment of the vibrational overtone spectra. The intensity data are particularly valuable in the lower overtone regions where combinations added to the complexity of the overtone spectra. Existing discrepancies between the predicted and observed relative overtone intensities may in fact be due to crude

dipole moment function used in the calculations. In infrared intensity studies of smaller molecules, larger basis sets with diffuse functions were crucial in obtaining good dipole moment functions[105,115,187,188]. The small 3-21G basis employed is unlikely to give a highly accurate dipole picture of the molecule. To obtain accurate absolute overtone - combination intensities a high quality dipole moment function expanded beyond the first derivative term in its Taylor expansion is essential. We have not been concerned with absolute transition intensities and hence such steps were not taken to improve our intensity analysis.

ii.) Ground State Mixing: An Additional Intensity Source

The success of the intramanifold, harmonic coupling extension of the LM model in describing the methyl CH stretching features of substituted furans and thiophenes is quite remarkable. Most of the general features can be explained with relatively few model parameters. Indeed what may be more impressive is that many of the model parameters were obtained independently from the spectra to which they were applied. Although the experimental - model agreement can be improved by fine-tuning these parameters, even without any optimization the model predictions are quite good. However, as noted at the end of the last section, the model has some inadequacies regarding the relative predicted methyl overtone - combination intensities at $\Delta v_{CH} = 2$. As discussed in the last section, the inadequacies of the intensity predictions are not surprising considering the crude model employed. However, a simple extension of this model markedly improves intensity predictions in the $\Delta v_{CH} = 2$ manifold.

In the methyl substituted furans and thiophenes the total intensity of the $|11\rangle |0\rangle$ and $|10\rangle_+ |1\rangle$ combination transitions is predicted to range from around 15% to 30% of the intensity of the

$|20\rangle_{\pm}$ $|0\rangle$ overtone. The antisymmetric combination is predicted to be less than 1% of the overtone intensity. The observed intensity of the antisymmetric combination is in reasonable agreement with prediction but the symmetric combinations have almost the same intensity as the $|20\rangle_{\pm}$ $|0\rangle$ overtone. At the higher methyl stretching manifolds both the symmetric and antisymmetric combination intensities relative to the overtone transition intensities are well predicted. These observations suggest that there is an additional intensity source for the dipole allowed transitions to the symmetric $v = 2$ combination states not considered in our model.

The intensities of single photon, multiquanta XH stretching transitions have been the subject of a number of studies[106-108,176]. Typically these investigations have attempted to accurately model the absolute transition intensities by employing improved dipole moment functions. In practise, higher order terms in the dipole expansion are retained. To achieve even moderate success at predicting absolute transition intensities along a fundamental-overtone progression these high order terms are important. For up to the n^{th} overtone level, it is generally considered that the n^{th} diagonal dipole derivative term is required. In this section, we are primarily

concerned with the one-photon transitions to the v = 2 XH stretching states. Of particular interest are the relative intensities of the methyl combinations and overtones at this manifold. Following the above scheme, the quadratic terms in the dipole expansion should be retained if accurate absolute fundamental and $\Delta v = 2$ overtone methyl stretching intensities are required. If the quadratic terms are retained, transitions between the LM ground state and zero order combination states of the general form $|0_1 0_2 .. n_j 0_k .. m_l .. 0_z\rangle$ become directly allowed through the cross terms in the expansion. Transitions to the $|11\rangle |0\rangle$ and $|10\rangle_{\pm} |1\rangle$ states acquire intrinsic intensity through the quadratic cross terms in the dipole expansion. If the cross quadratic dipole terms are cited as the sole additional source of $\Delta v = 2$ methyl combination transition intensity, two questions arise. The first problem is that it isn't readily apparent why the cross quadratic dipole terms should be a more effective intensity source for the symmetric combinations and not contribute substantially to the antisymmetric $\Delta v = 2$ combinations. Second, if the intensities of the combinations at $\Delta v_{CH} = 2$ are solely accounted for by parameterizing the quadratic terms, then the agreement between observed and predicted combination intensities

at the higher vibrational manifolds is poor. Thus although higher order dipole terms are important in understanding the absolute intensities along a fundamental-overtone progression, alone, they do not satisfactorily account for the relative methyl $\Delta v = 2$ overtone-combination intensities.

An intensity source not considered in the intramanifold coupling scheme but readily apparent in the full harmonic coupling model, plays an important role in contributing to the intensity of the symmetric $\Delta v_{CH} = 2$ combinations. We call the additional intensity source arising from the full harmonic coupling model, the ground state mixing contribution. Even within the linear dipole approximation the importance of ground state mixing on symmetric $\Delta v = 2$ combination intensities is evident. Rather than attempting to further improve model intensity calculations by employing higher order dipole terms, intensities will be calculated within the linear dipole approximation but with an improved methyl CH stretching wavefunction which results from considering ground state mixing. This approach was taken for a number of reasons. Retaining only linear dipole terms considerably simplifies the calculation of intensities. Since only relative intensities are being considered and

the desired effect of ground state mixing is evident at the linear dipole level, a more sophisticated dipole moment function for our purposes seems unneccessary. There were some practical reasons for considering only the linear dipole intensities. Modest split valence basis sets were used in the calculation of the dipole moment derivatives. Several extensive theoretical investigations[105,110,115,187,188] of calculated vibrational intensities suggest that rather high level basis sets which incorporate diffuse functions are important for the calculation of good dipole moment functions. The quality of the dipole function employed in our calculations, particularly for the sulphur containing thiophenes, is probably insufficient to warrant an extensive treatment. Also, since the available *ab initio* programs calculate dipole moment derivatives numerically, high order derivatives are subject to the propagation of round-off and step-size errors. For all these reasons, intensities were calculated at the linear dipole level of approximation.

If ground state mixing is an important intensity source, it suggests the breakdown of the intramanifold coupling approximation. The contribution of ground state mixing to the intensities of transitions to the symmetric v = 2 combination states can be readily

understood within the simple harmonic oscillator algebra. In terms of this algebra the quadratic coupling operator for a system of harmonic oscillators contains terms which couple states within a vibrational manifold, $a_i^\dagger a_j$, and states which differ by two in total vibrational quantum number, $a_i^\dagger a_j^\dagger$ and $a_i a_j$. On the basis of the large energy mismatch between manifolds, these latter couplings were ignored in the previous section. Indeed, due to the decreasing manifold separation with increasing energy, this approximation is expected to the strongest in the lower energy realm. Since we have been primarily concerned with the lower energy overtone regions, the intramanifold coupling restriction seemed reasonable. Consistent with this approximation, the XH stretching transition energies and intensities in general are grossly unaffected if intermanifold coupling is considered. The one potential exception is the symmetric $\Delta v = 2$ combinations.

If intermanifold terms are considered in the harmonic coupling extension of the LM Hamiltonian, the only states directly coupled to the ground state are the symmetric $v = 2$ combination states. The $v = 4, 6, \ldots$ symmetric combination states are coupled indirectly to the zero order ground state through these terms. The question is, how

important is the intermanifold state mixing in determining the methyl CH stretching intensities? Theoretical calcualtions on 2,5 dimethylfuran and 2,5 dimethylthiophene molecules predict rather large kinetic and potential energy contributions to the interoscillator coupling. Due to the sign difference between the predicted kinetic and potential energy components of the coupling, the effective intramanifold coupling constant suffers from a substantial cancellation effect. However, in the expression for the effective intermanifold coupling constant the kinetic and potential energy contributions are additive. Thus despite the energy mismatch between the vibrational manifolds, the intermanifold coupling may be more important than it is commonly thought to be.

The intensity of a transition between a final state and initial state (the initial state is considered to be the ground state in this case) within the linear dipole approximation is proportional to,

$$I^{f0} \propto \left| \frac{1}{2} \left(\sum_{i}^{XH} \left(\frac{\partial \mu}{\partial q_i} \right)_0 \sum_{j,k} c_j^f c_k^0 \left\langle \phi_j^f \middle| q_i \middle| \phi_k^0 \right\rangle \right) \right|^2 \qquad (11.4)$$

where c^f_j and c^0_k are the expansion coefficients of the final state and the ground state in terms of the zero order LM basis. Since the states are orthogonal, the static term makes no contribution to the transition intensity and is not included in equation 11.4. The expression for the linear dipole intensity can be partitioned into two sets of terms.

$$\text{let } d_i = \left(\frac{\partial \mu}{\partial q_i}\right)_0 \tag{11.5}$$

$$I^{f0} \propto \left| \sum_i^{XH} \left\{ \frac{d_i}{2} \sum_j c^f_j c^0_j \left\langle \phi^f_j \middle| q_i \middle| \phi^0_j \right\rangle + \frac{d_i}{2} \sum_{j \neq k} c^f_j c^0_k \left\langle \phi^f_j \middle| q_i \middle| \phi^0_k \right\rangle \right\} \right|^2 \tag{11.6}$$

The first term is denoted as the self-mixing term. The second term is called the cross-mixing component. In the intramanifold coupling restriction, the zero order ground state remains unmixed with other states. No self-mixing contribution to the transition intensity can arise. In addition, the only cross mixing contribution is between the zero order ground state and zero order local mode overtone states.

Lifting the intramanifold coupling assumption, no longer ensures such simplifications in the transition dipole expression. The mixing of the zero order ground state with other states manifests itself in nonvanishing self and cross mixing terms in the transition moment operator. The symmetric ground state cannot mix with antisymmetric states and hence antisymmetric transitions have no self-mixing contribution. In addition, many of the cross-mixing terms vanish for transitions to antisymmetric states. Therefore including the intermanifold coupling increases the relative difference in intensity between a corresponding symmetric - symmetric and symmetric - antisymmetric transition.

Of all the zero order methyl CH stretching overtone and combination states, the symmetric v = 2 combinations suffer from the greatest ground state mixing. Hence the intensities of these states are most affected by the lifting of the intramanifold coupling restriction. This is true if the Morse oscillator or harmonic oscillator algebra is used. Using the harmonic oscillator algebra however simplifies the treatment. If the quadratic coupling is treated in a harmonic oscillator basis, the dimensionality of the intensity problem is reduced. The even vibrational manifolds (v =

0,2,4,...) are completely separable from the odd manifolds. This separation does not occur if the coupling is considered within a Morse oscillator basis. The ground state mixing contribution to methyl CH stretching intensities will be investigated using the simpler harmonic oscillator algebra.

Diagonalizing the full harmonic coupling operator in a truncated harmonic oscillator basis of even and odd vibrational manifolds yields the expansion coefficients. Using the oscillator parameters reported in the previous section for 2,5 dimethylfuran and 2,5 dimethylthiophene, the energies and linear dipole transition intensities are calculated considering the ground state mixing contribution. The even manifold basis was truncated at $v = 4$ while only the $v = 1$ and $v = 3$ manifolds were used in the odd basis for the calculation. The stretching positions are quite insensitive to the basis set expansion. Small shifts to higher energy for the highest even and odd manifold are a basis set truncation effect. The small shifts to lower energy for the lower manifolds are in accordance with variational principles. Lifting the intramanifold coupling approximation therefore has little effect on the predicted transition energies. In general, the transition intensities are also relatively

unaffected by the introduction of intermanifold coupling. The major exception are the transitions to the symmetric v = 2 states. Tables 11.14 and 11.15 compare the predicted methyl CH stretching positions and intensities of the symmetric v=2 states of 2,5 dimethylfuran and 2,5 dimethylthiophene with and without the intramanifold coupling restriction. In both molecules, ground state mixing reduces the intensities of the symmetric overtone transtions while the symmetric combination intensities increase. For both molecules, the intensity of the |11> |0> combination relative to the |20>± |0> overtone is predicted to be about 1.6 times greater if ground state mixing is included. In 2,5 dimethylfuran the |11> |0> combination is predicted to be more intense than the |00> |2> overtone, consistent with observation. In addition, the predicted decrease in overtone intensities is greater for the in-plane overtone than the out-of-plane overtone. Thus ground state mixing in part can account for the discrepancy in relative overtone intensities predicted within the intramanifold coupling approximation.

The splittings and small shifts in band maxima observed in the lower energy CH stetching overtone - combination regions can be readily understood in terms of a one-bond, intramanifold coupling

TABLE 11.14

PREDICTED GROUND STATE MIXING CONTRIBUTION TO THE SYMMETRIC METHYL CH STRETCHING OVERTONE AND COMBINATION INTENSITIES OF 2,5 DIMETHYLTHIOPHENE IN THE $\Delta v = 2$ REGION.

Assignment	Intramanifold Coupling		Intermanifold Coupling	
	cm^{-1}	rel Int	cm^{-1}	rel Int
$20\rangle_+ 0\rangle$	5706	0.540	5702	0.491
$00\rangle 2\rangle$	5761	0.355	5758	0.336
$11\rangle 0\rangle$	5844	0.076	5842	0.123
$10\rangle_+ 1\rangle$	5891	0.029	5890	0.050

TABLE 11.15

PREDICTED GROUND STATE MIXING CONTRIBUTION TO THE SYMMETRIC METHYL CH STRETCHING OVERTONE AND COMBINATION INTENSITIES OF 2,5 DIMETHYLFURAN IN THE $\Delta v = 2$ REGION.

Assignment	Intramanifold Coupling		Intermanifold Coupling	
	cm^{-1}	rel Int	cm^{-1}	rel Int
$20\rangle_+ 0\rangle$	5708	0.663	5705	0.600
$00\rangle 2\rangle$	5781	0.193	5778	0.162
$11\rangle 0\rangle$	5849	0.099	5847	0.174
$10\rangle_+ 1\rangle$	5906	0.045	5905	0.064

extension of the LM model. However, such a model extension inadequately describes the relative intensities of the $\Delta v_{CH} = 2$ overtones and combinations. Dipole transition intensities appear to be much more sensitive to the form of the CH stretching wavefunction. The subtle intermanifold couplings which give rise to ground state mixing is an important intensity source for the $\Delta v_{CH} = 2$ combination transitions. It is preferentially an intensity source for the symmetric combination transitions. This in part explains the apparent anomalous symmetric combination intensities at $\Delta v_{CH} = 2$. Therefore, as a first step towards fully accounting for CH stretching intensities the intermanifold one-bond couplings must be retained in the coupling model. This increases the dimensionality of the coupled oscillator problem particularly if Morse oscillator matrix elements are used throughout the problem. Considering intermanifold coupling using harmonic oscillator algebra helps keep the treatment of the problem simple. Expressing the quadratic couplings in terms of harmonic creation and annihilation operators readily identifies the dominant terms in the transition moment operator. Only the symmetric v = 2 combination states directly mix with the ground state in the harmonic oscillator algebra. The other

higher even manifold combinations mix only indirectly. The dimensionality of the problem is relatively small within this algebra since the even manifolds can be considered separately from odd manifolds. Using harmonic oscillator intermanifold coupling leads to a tractable method of investigating the importance of ground state mixing on the relative overtone - combination transition intensities.

CHAPTER 12

BREAKDOWN OF THE RIGID METHYL ROTOR INTERPRETATION

i.) Previous Work On Low-Barrier Methyl Rotor Systems

Internal rotation and specifically the internal rotation involving methyl groups has been extensively studied over the last sixty years[100,189,190]. Despite the vast array of literature on the subject, the interpretation of the vibrational spectra of molecules which have low barriers to methyl group internal rotation is not completely clear. In particularly, the fundamental and higher energy CH stretching features of methyl rotor systems are not understood.

There have been a number of investigations specifically aimed at understanding the effect of internal rotation on the methyl CH stretching fundamentals. In a series of papers[191-193], Sheppard and coworkers analysed the infrared spectra of nitromethane, methyl boron difluoride, as well as toluene and some of its deuterated derivatives. The methyl fundamental vibrations and in particular the perpendicularly polarized bands displayed complex bandshapes.

These complicated bandshapes were considered to be made up of internal rotational fine structure. Reed and Lovejoy's[194] re-examination of the fundamental spectrum of methyl boron difluoride and methyl-d_3 boron difluoride suggested that Jones and Sheppard's assignment of the methyl CH stretching fundamentals was not completely correct. More recent studies by McKean and coworkers[195,196] as well as Cavagnat and Lascombe[197,198] have attempted to resolve the assignment and probe more deeply the effects of internal rotation on the methyl CH stretching fundamental transitions.

McKean's group has used the method of selective deuteration to solve many problems associated with the understanding of the fundamental XH stretching regions of a wide range of molecules[125]. Molecules in which all but one selected hydrogen are replaced by deuterium have a simplified methyl CH stretching fundamental spectrum. The spectral simplification arises from the large mass difference between the isotopes which results in a substantial difference between the XH and XD stretching frequencies. The single XH stretching mode in the selectively deuterated molecule is effectively isolated from the remaining vibrational degrees of

freedom due to this large frequency mismatch. McKean and coworkers re-examined the fundamental stretching regions of nitromethane[195] and methyl boron difluoride[196] and the selectively deuterated species. The assignment of the CH_3 and CD_3 fundamentals is complicated by a number of strong interactions which perturb the methyl CH stretching features. The CH stretching region of the CHD_2 group of the selectively deuterated molecules is easier to assign. In the nitromethane case, a single, broad but weak band is observed in the gas phase. The single methyl CH stretching band was interpreted as that due to the average CH stretching frequency during internal rotation.

The methyl CH stretching features of methyl boron difluoride were expected to be similiar to those of nitromethane. This is particularly true in terms of the effects of internal rotation. Microwave studies[199,200] have determined that both molecules have very low, six-fold torsional barriers. Surprisingly, the fundamental CH stretching region of methyl boron difluoride is very different from that of nitromethane. Rather than a single "average" frequency band, two bands are observed for the selectively deuterated methyl boron difluoride. From the band shapes, the higher energy band was

assigned to the stretching of the CH group when it is in the plane defined by the BF_2 frame. The lower energy methyl fundamental band was assigned to the CH group when it is perpendicular to the frame. The different interpretations of the internal rotational effects on the two molecules with very similar barriers to internal rotation is difficult to rationalize. McKean and Watt[195] suggested that the difference between the methyl CH stretching features of the two molecules is due to a large substituent effect on the methyl CH stretching intensities. However, this argument was not explored and one is unsure how this relates to internal rotational effects.

Using the method of selective deuteration[198], Cavagnat and Lascombe further examined the fundamental CH stretching region of nitromethane and toluene in the gas and solid phases using infrared and Raman spectroscopy. The toluene spectrum was found to be very similiar to that of methyl boron difluoride. Both Sheppard and Woodman[192] along with Mckean and coworkers[195,196] considered the angular variation of the diagonal CH stretching force constant as the dominant torsion-vibration interaction. Cavagnat and Lacombe[197,198] explicitly modelled this torsion-vibration interaction between a single harmonic CH stretching mode and a hindered torsional mode.

Their analysis predicted the most intense methyl CH stretching Raman line to closely correspond to the classical average frequency of the modulated CH stretching mode.

In the course of studying substituent effects in benzene ring systems, Gough and Henry examined the $\Delta v_{CH} = 3$ and 4 regions of toluene and the xylenes[134]. The methyl regions of o-xylene consist of two peaks. *Ab initio* calculations predict a planar, non-geared, minimum energy methyl conformation (see Figure 12.5). The methyl peak positions closely correspond to those predicted from the bondlength-frequency correlation using the predicted equilibrium methyl CH bondlengths. The lower intensity, higher energy peak was assigned as arising from the lone, in-plane, methyl CH oscillator. The higher intensity, lower energy peak was associated with the two oscillators which stagger the ring. The situation is different for toluene, meta-, and para-xylene. Three peaks are observed for these systems. The positions and relative intensities of the highest and lowest energy peaks in the methyl region closely resemble those of o-xylene. Ahmed and Henry[201] observed the same trend in the trimethylbenzenes. Two methyl peaks are observed for 1,2,3 trimethylbenzene while the spectra of the remaining

trimethylbenzenes show three peaks. Henry, Gough, and Sowa[202] reported the same trend in the $\Delta v_{CH} = 3$ region of the monofluorotoluenes. Based on the correspondence between the highest and lowest energy methyl peaks in all the spectra, as in o-xylene, these peaks were assigned to correspond to transitions associated with the minimum energy conformation, in-plane and out-of-plane, CH oscillators. However, the structural interpretation of the methyl CH stretching features cannot account for the central peak observed in the overtone regions of the methylbenzenes and monohalotoluenes. The favoured, tentative, assignment of the central peak was that of a "free-rotor" or averaged CH stretching peak. It is essentially this assignment which is investigated in the remaining sections.

ii.) The Barrier Height Dependence of the Methyl Overtone Features

The aim behind these experimental studies was to attempt to clarify the assignment and the interpretation of the methyl CH stretching overtone regions of molecules which have a low barrier to the internal rotation of the methyl group relative to the remainder of the molecular frame. It was hoped that this goal could be accomplished by examining a wide number of methyl rotor systems with different torsional barrier heights and determining if the overtone features do indeed show a barrier height dependence.

The work of Gough and Henry[132] as well as Ahmed and Henry[201] on methylbenzenes is the most directly related to these studies and will often be refered to in this section. As an extension of the methylbenzene studies, a similar system, the monohalo substituted toluenes were examined. The $\Delta v_{CH}=3$ spectra of ortho, meta, and para fluoro and chloro toluene are presented in Figures 12.1 and 12.2. The $\Delta v_{CH}=3$ spectra of the mono-fluorotoluenes were previously reported by Henry, Gough, and Sowa[202]. Aside from the expected substituent dependent shifts in the position of overtone maxima and the relative

FIGURE 12.1

Gas phase overtone spectra of ortho, meta, and para fluorotoluene in the $\Delta v_{CH} = 3$ region. The spectra were measured at pressures corresponding to the equilibrium vapour pressures of the samples at 86°C and with a 9.75 m gas cell pathlength.

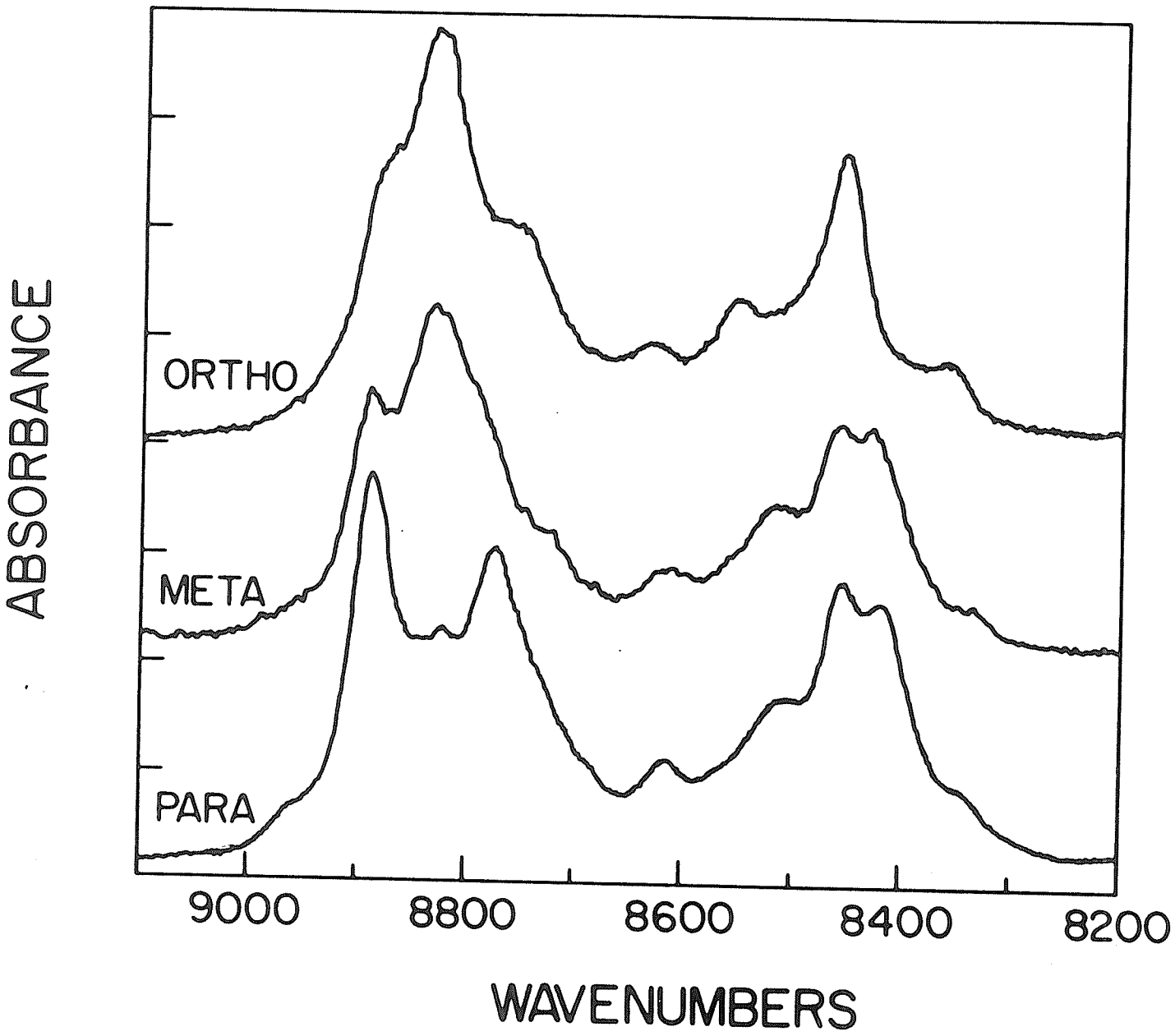
ABSORBANCE
ORTHO
META
PARA
9000
8800
8600
8400
8200
WAVENUMBERS

FIGURE 12.2

Gas phase overtone spectra of ortho, meta, and para chlorotoluene in the $\Delta v_{CH} = 3$ region. The spectra were measured at pressures corresponding to the equilibrium vapour pressures of the samples at 86°C and with a 14.25 m gas cell pathlength.

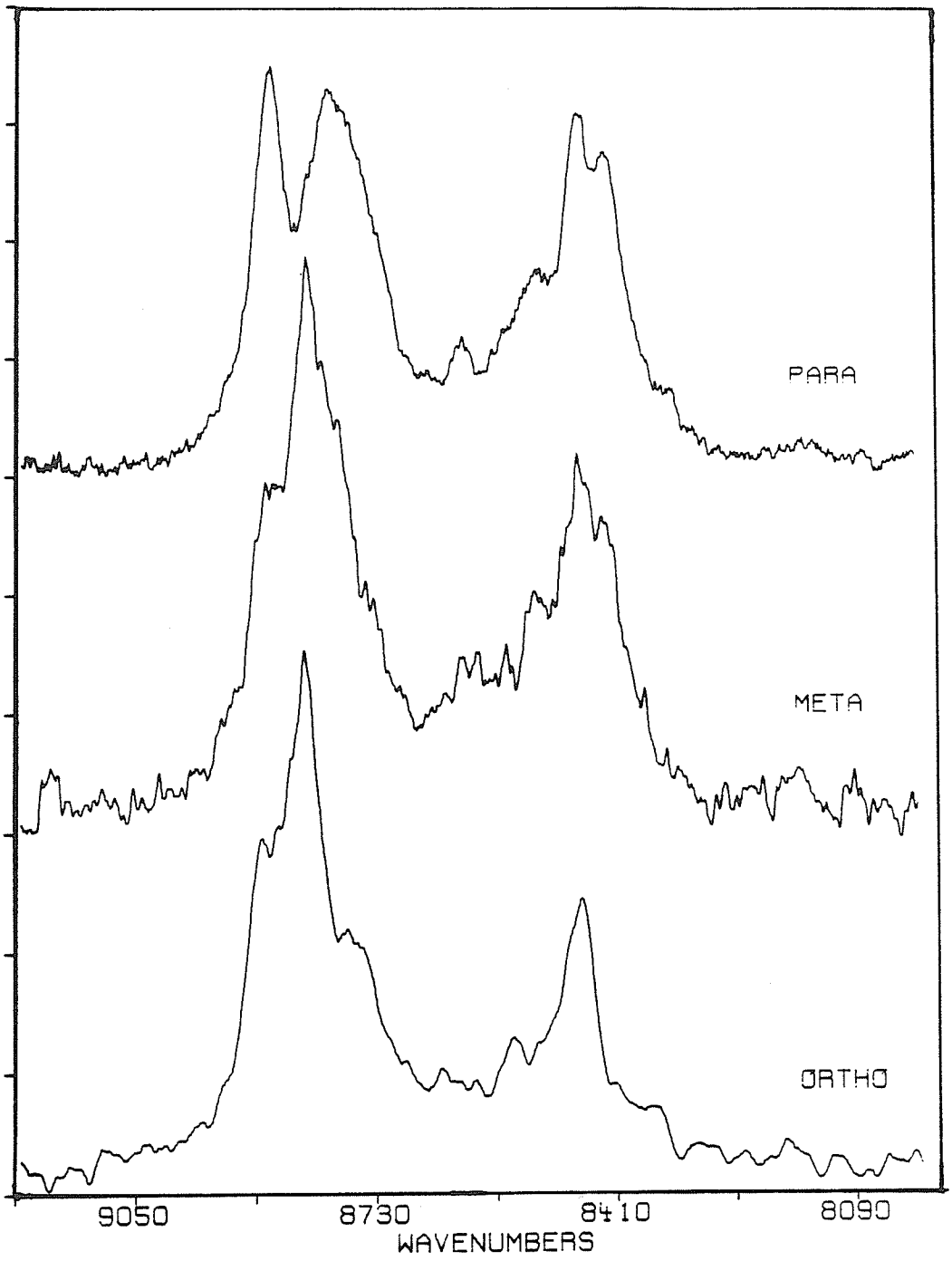
PARA
META
ORTHO
9050
8730
8410
8090
WAVENUMBERS

differences in the intensities of the methyl CH stretching features between mono-, di-, and tri- methyl substituted species, the methylbenzene and mono-halotoluene spectra are very similar.

The aryl regions of the methylbenzenes and halotoluenes have a simple zero order LM interpretation. An aryl CH stretching overtone progression can be identified for each set of chemically equivalent ring oscillators in the molecule. For para-xylene and 1,3,5 trimethylbenzene, there is only one type of aryl CH oscillator and only one aryl overtone progression is observed. Relative to the benzene aryl overtone transition, the corresponding aryl overtone transition in these methylbenzenes is shifted to lower energy. The opposite shift in aryl overtone position was found for the halobenzenes[131]. The oscillators closest to the substitution site were found to be the most affected and the substituent induced shift increased with the number of substituents. In the para-halotoluenes, two intense aryl overtone peaks are observed (see Figure 12.3). The opposing effects of the methyl and halo substituents on the stretching frequencies of adjacent oscillators are responsible for the well resolved aryl features. From the near coincidence of the

FIGURE 12.3

Gas phase overtone spectra of para-fluorotoluene in the $\Delta v_{CH} = 4$ region. The spectrum was measured at the pressure corresponding to the equilibrium vapour pressure of the sample at 86°C and with a 12.75 m gas cell pathlength. The spectrum represents the sum of ten individual scans.

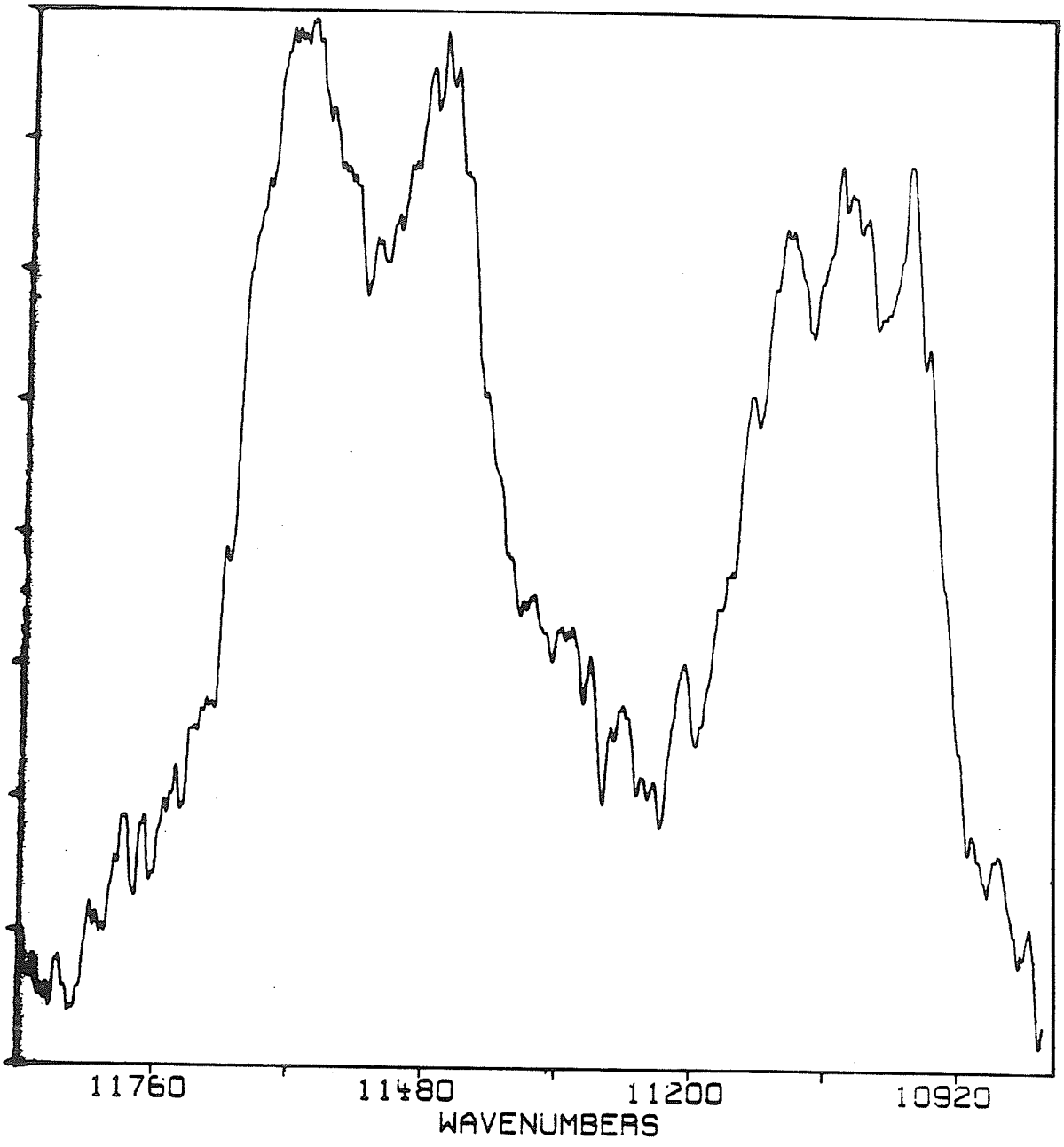
11760
11480
11200
10920
WAVENUMBERS

single aryl CH overtone progression of p-xylene or 1,3,5 trimethylbenzene with the lower energy progression in the p-halo-toluenes, the lower energy overtone is assigned as being associated with the oscillators adjacent to the methyl substituent. LIkewise, the higher energy aryl overtone is assigned to the oscillators ortho to the halo substituent. The single aryl overtone peak of 2,3,5,6 tetra-fluorotoluene (see Figure 12.15) is slightly displaced to the high energy side of the higher energy overtone of p-fluorotoluene. The single overtone peak of p-xylene and 1,3,5 trimethylbenzene are slightly to lower energy of the low energy peak of p-fluorotoluene. The substituent effects on the aryl overtone peak positons of the halotoluenes are in accord with those observed in the halo and methyl benzenes and the aromatic heterocycles.

The aryl overtone regions of the ortho and meta substituted halotoluenes and methylbenzenes are more congested than the para species due to the greater number of chemically nonequivalent aryl oscillators. The Δv_{CH} = 3 and 4 spectra show unresolved contours in the aryl region. At higher overtone levels, congestion typically decreases as the inverse frequency - anharmonicity ratios between

the nonequivalent oscillators detunes the overtones at higher levels of excitation. At $\Delta v_{CH}=5$ (Figure 12.4) three overtone features are partially resolved in both the ortho and meta substituted fluorotoluenes. Although all four aryl oscillators are distinguishable in these molecules , *ab initio* calculations predict only a small structural asymmetry between the oscillators at the 4,5 and 2,5 ring positions of the ortho and meta substituted halotoluenes respectively. Table 12.1 lists the predicted aryl CH bondlengths of the halotoluenes. At the higher overtone levels in the gas phase, subtle differences in CH oscillators result in resolvable spectral features. The correlation between aryl overtone features and the number of chemically nonequivalent aryl oscillators is clearly evident in the methylbenzene, halobenzene and halotoluene spectra. The sensitivity of the energy of the overtone transition to the chemical environment of the CH oscillator has been exploited to give detailed structural and conformational information on various molecules[28,131,133,134,202]. Our results on the halotoluenes are consistent with the bondlength-frequency correlation arguments used in these structural studies.

FIGURE 12.4

Gas phase photoacoustic overtone spectra of ortho, meta, and para fluorotoluene in the $\Delta v_{CH} = 5$ region. The room temperature spectra were measured at 25, 20, and 23 Torr pressure for the ortho, meta, and para substituted species respectively. A 10 cm pathlength photoacoustic gas cell was used.

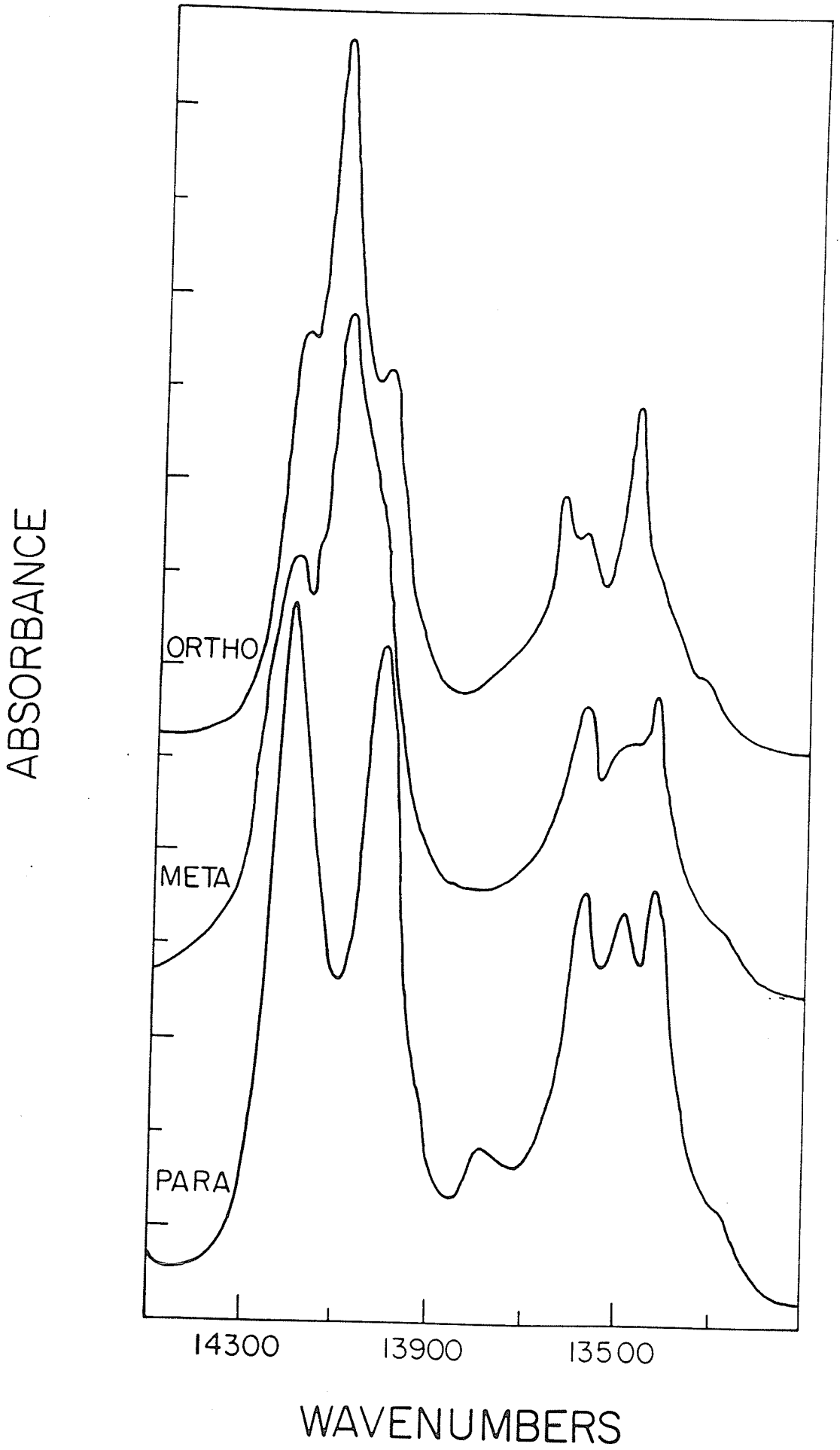
ABSORBANCE
ORTHO
META
PARA
14300
13900
13500
WAVENUMBERS

TABLE 12.1

Predicted 4-21G Aryl CH Bondlengths (Å) of Selected Toluenes

	C(2)H(2)	C(3)H(3)	C(4)H(4)	C(5)H(5)	C(6)H(6)
toluene	1.073	1.072	1.072	1.072	1.073
2-fluoro	-	1.070	1.071	1.071	1.072
3-fluoro	1.070	-	1.069	1.072	1.072
4-fluoro	1.072	1.070	-	1.070	1.072
2-methyl	-	1.073	1.072	1.072	1.073
3-methyl	1.075	-	1.073	1.073	1.073
4-methyl	1.073	1.074	1.074	1.073	-

Two features are notably absent in the aryl CH stretching regions of both the methylbenzenes and halotoluenes. Splittings due to long-range CH stretch - stretch couplings are not resolvable at any level of CH stretch excitation. LM aryl stretch-stretch combinations have little or no intensity relative to the aryl CH stretching overtone transitions. Both of these observations are general. These features were also absent from the aryl regions of the furans and thiophenes. The absence of resolvable coupling splittings and aryl combinations is indicative of the quality of the one-bond coupling approximation and suggestive of a high degree of local mode character for the aryl CH stretching states.

The Δv_{CH} = 3 and 4 methyl overtone regions of the mono halotoluenes resemble those of the methylbenzenes. Two distinct patterns are observed. Ortho substituted molecules yield two major peaks while three major peaks are observed for the meta and para substituted toluenes. A structural interpretation like that used in Chapter 11 for the methyl furans and thiophenes can readily explain two methyl overtone transitions but not three. For methyl substituted furans and thiophenes, *ab initio* calculations predicted

only a single type of rotamer with a substantial barrier to internal rotation. The ortho-halotoluenes behave very similarly. Both microwave results[203,204] and theoretical calculations[205,206] predict a planar geometry with the planar hydrogen opposite to the halo substituent (see Figure 12.5). The reported ground state torsional hindering potential[203,204,207], $V_3 = 2.69$ kJ mol^{-1}, is much larger than meta and para substituted toluenes[207-213]. The larger hindering potential means that the methyl rotor is more localized at the bottom of the potential well. The majority of the transitions originate from the lower portions of the well. At the bottom of the well, the conformationally distinct environments of the methyl oscillators manifest themselves in the CH stretching wavefunctions. Transitions from these lower levels therefore can be associated with chemically nonequivalent oscillators. This is the reasoning behind the structural interpretation of the methyl overtone spectra.

The structural interpretation explains the two methyl overtones observed in the ortho substituted methylbenzenes and halotoluenes. The coincidence of the two methyl overtones of the ortho species with the high and low energy features observed in the

FIGURE 12.5

Minimum energy methyl conformation of the ortho substituted toluenes.

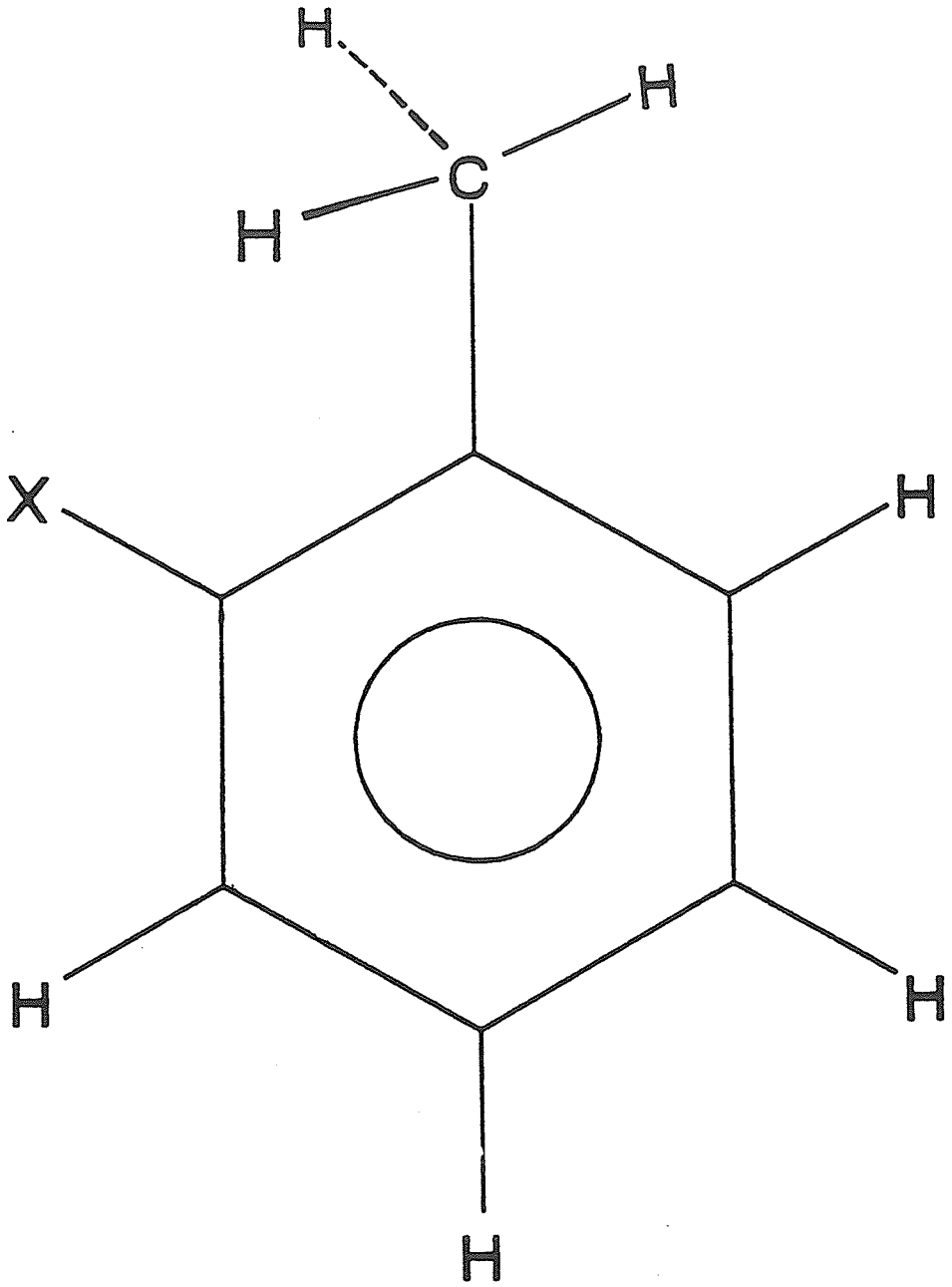
H
H
H
C
X
H
H
H
H

spectra of the meta and para species suggests that these features are due to the distinguishable oscillators of the minimum energy conformer. In this assignment, the origin of the central peak remains uncertain.

Reddy et al[50] postulated that the central methyl peak in the $\Delta v_{CH} = 5$ spectrum of toluene (see Figure 12.6) was due to the presence of a second stable rotamer. However, little evidence exists for the presence of multiple stable conformers of the methylbenzenes and mono-halotoluenes. Neither microwave[203,204,209-213] nor supersonic beam expansion[207,208] spectroscopies have revealed the presence of multiple rotamers. Theoretical calculations[205,206,214-216] are in agreement with the spectroscopic results. It thus seems unlikely that the discrepencies between the methyl regions arise from the presence of two or more conformers in the meta and para substituted molecules.

A Fermi resonance origin for the central peak has also been suggested[134]. The spectroscopic manifestations of Fermi resonances in the overtone regions were studied in some detail in the aryl CH stretching progressions of furan and thiophene. The interactions

FIGURE 12.6

Room temperature, gas phase, photoacoustic overtone spectrum of the $\Delta v_{CH} = 5$ region of toluene. The spectrum was acquired with 24 Torr of sample in a 10 cm pathlength gas cell.

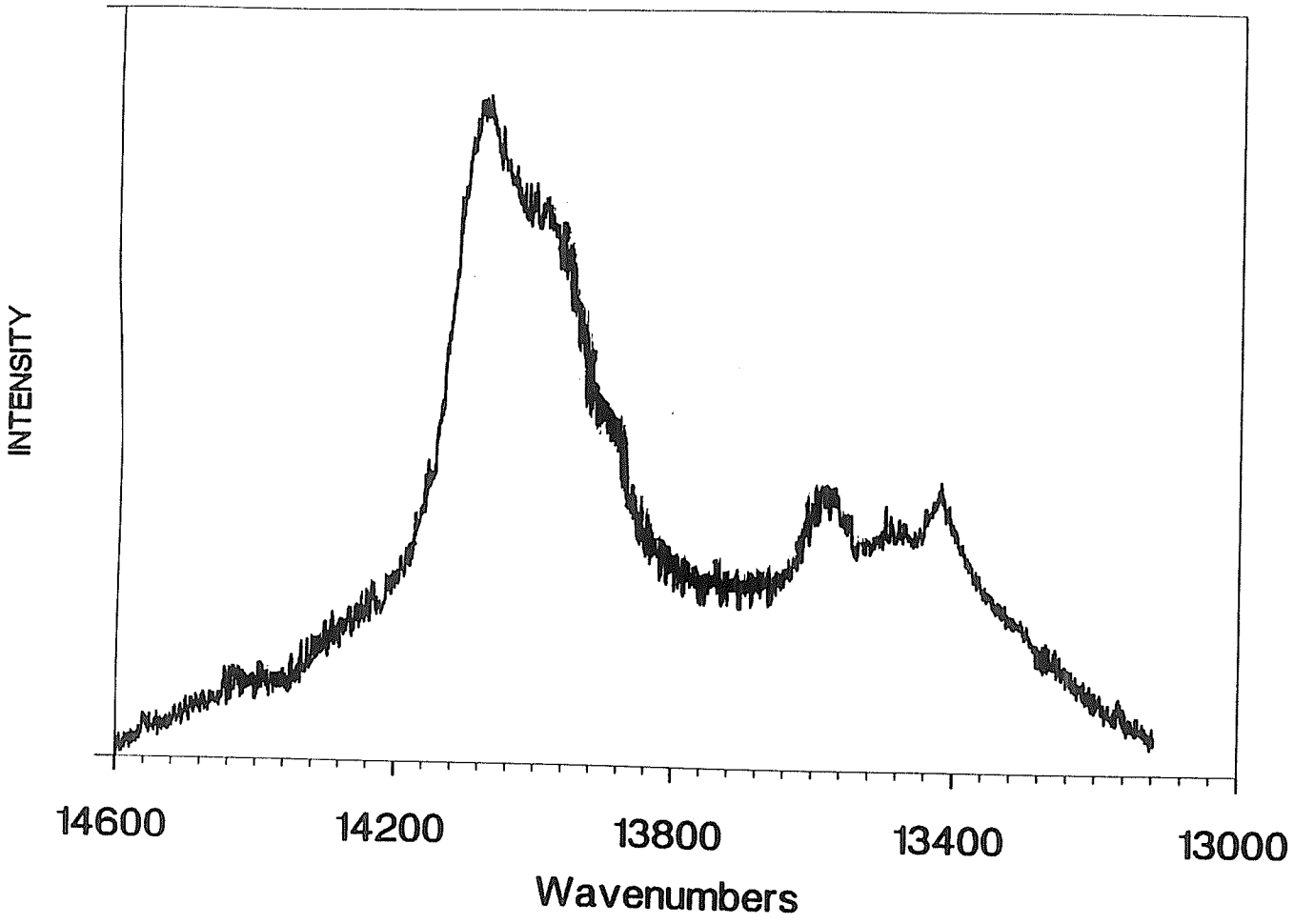
INTENSITY
14600
14200
13800
13400
13000
Wavenumbers

typically tune-in and tune-out of resonance along the overtone progression. However, the central peak in the meta and para substituted toluenes does not show any dramatic tunablity between $\Delta v_{CH} = 3 - 5$. Curiously, a third methyl peak becomes apparent in the gas phase $\Delta v_{CH} = 5$ spectrum of orthofluorotoluene (see Figure 12.4). This same phenomenon is observed in the gas phase $\Delta v_{CH} = 5$ spectra of the methylfurans (see Figure 12.7). In the case of thiophene, small substituent induced shifts in overtone position were sufficient to dramatically change the Fermi resonance structure at a given overtone. It seems unlikely that 2 methylfuran and orthofluorotoluene should have the same Fermi resonance structure at $\Delta v_{CH} = 5$. Nitromethane provides an even better example. Nitromethane has far fewer degrees of freedom and very different mode frequencies compared to the methylbenzenes, halotoluenes, and methyl heterocycles. In particular, the methyl CH stretching frequencies of nitromethane are much greater than most other methyl rotor systems. The different state densities and mode frequencies would seem to make it extremely unlikely for nitromethane to have the same Fermi resonance structure as the

FIGURE 12.7

Room temperature, gas phase, photoacoustic overtone spectrum of the methyl $\Delta v_{CH} = 5$ region of 2 methylfuran. The spectrum was acquired using 100 Torr of sample pressure in a 10 cm pathlength gas cell.

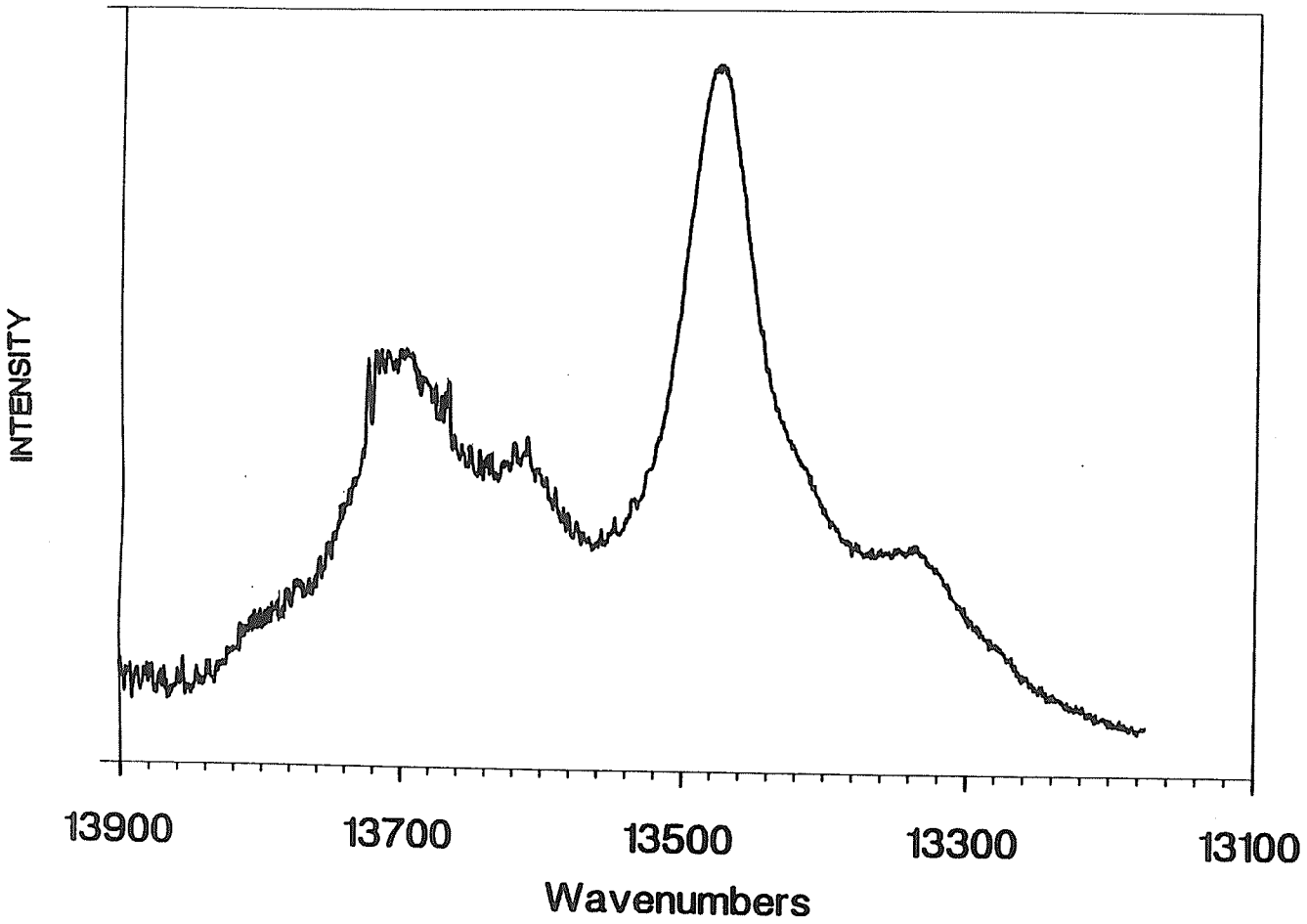
INTENSITY
13900
13700
13500
13300
13100
Wavenumbers

other methyl rotor systems studied. Despite the differences, a central methyl peak is clearly present at the $\Delta v_{CH} \geq 3$ overtone regions of nitromethane (see Figure 12.8). Aside from the shift in positon, the methyl overtone features of nitromethane are very similar to the other low barrier methyl rotor molecules like toluene and para substituted toluenes.

Based on the $\Delta v_{CH} = 3$ and 4 spectra of the methylbenzenes, Gough and Henry[132] favoured assigning the central peak to transitions originating from rotational levels above the torsional barrier. McKean et al[195] and Cavagnat and Lascombe[197] made similar assignments in the fundamental CH stretching region of toluene methylborontrifluoride and nitromethane. These authors suggested that transitions originated from torsional states above the barrier would give rise to an "averaged" methyl CH stretching peak. This interpretation seems consistent with the observations at the $\Delta v_{CH} = 3$ and 4 spectra. However, at $\Delta v_{CH} = 5$ the position of the central peak varies slightly relative to the higher and lower energy peaks.

A systematic pattern observed in the fundamental and overtone methyl CH stretching regions seems to indicate a

FIGURE 12.8

Room temperature, gas phase, photoacoustic overtone spectrum of the $\Delta v_{CH} = 5$ region of nitromethane. The spectrum was acquired with 34 Torr of sample in a 10 cm pathlength gas cell.

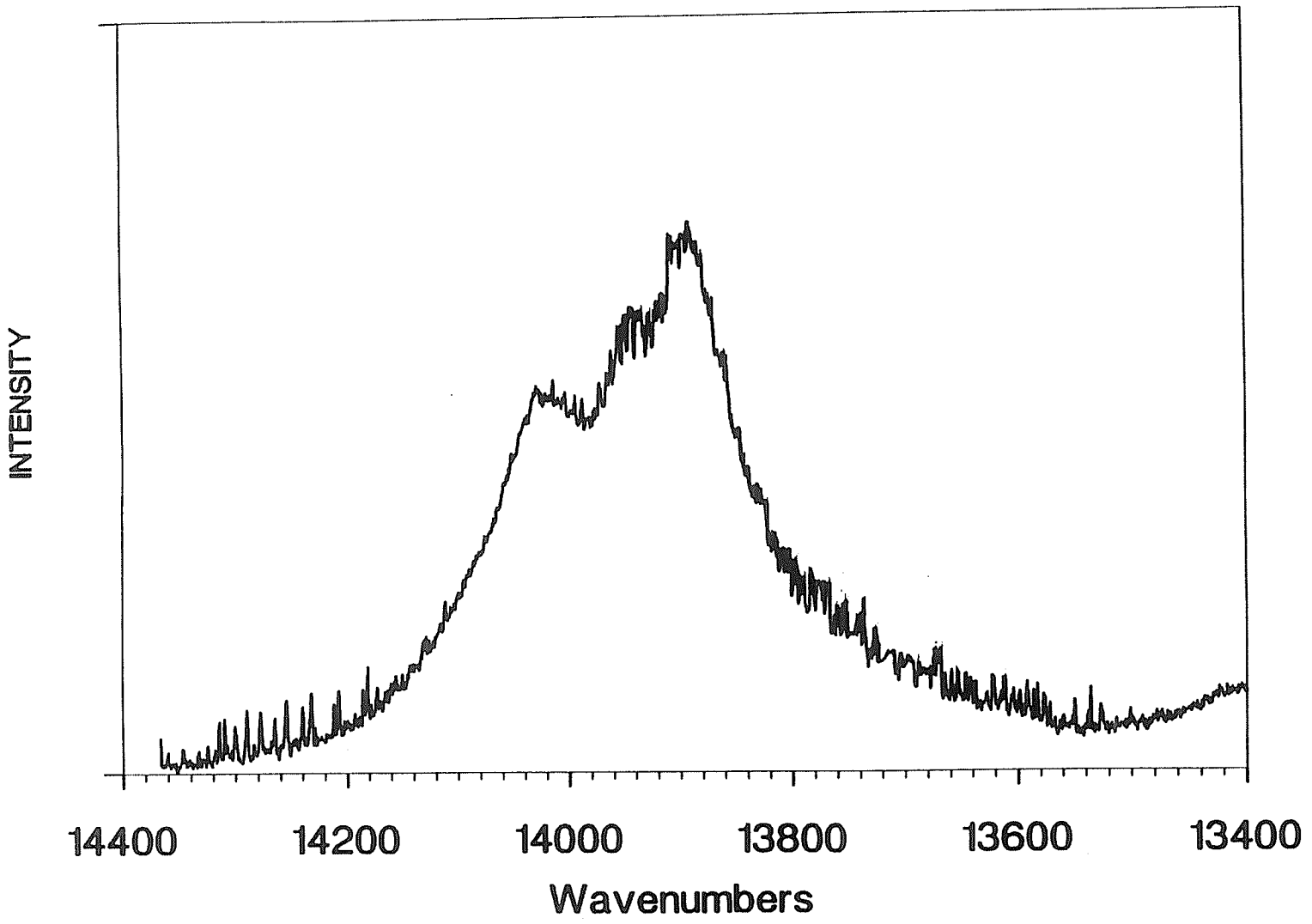
INTENSITY
14400
14200
14000
13800
13600
13400
Wavenumbers

connection between methyl torsion barrier height and the overall contour of the methyl fundamental and overtone regions. In particular, the intensity of the central methyl peak in the $\Delta v_{CH} = 3$ - 5 regions seems to depend on the ground state torsional barrier height. Ortho substituted toluenes, 2 methylpyridine and the methyl heterocycles have a small central peak which only becomes obvious at the higher gas phase overtone regions. The central peak is much more intense in molecules which have low barriers to internal rotation. Molecules with very different structures and properties but with similar barrier heights display similar methyl contours. The five-membered aromatic heterocycle, N-methylpyrrole, has a much lower torsional barrier[217] than the methylfurans and methylthiophenes. Despite the structural similarities between N-methylpyrrole and the methyl furans and thiophenes, the methyl regions of N-methylpyrrole resemble those of low barrier methyl rotor molecules (Figure 12.9).

Assigning the central peak as due to transitions originating from rotational levels above the barrier means that the intensity of the central peak is entirely temperature dependent. In a rotationally

FIGURE 12.9

Gas phase overtone absorption spectrum of N-methylpyrrole in the $\Delta v_{CH} = 3$ region. The spectrum was acquired at 88°C with a 8.25 m pathlength.

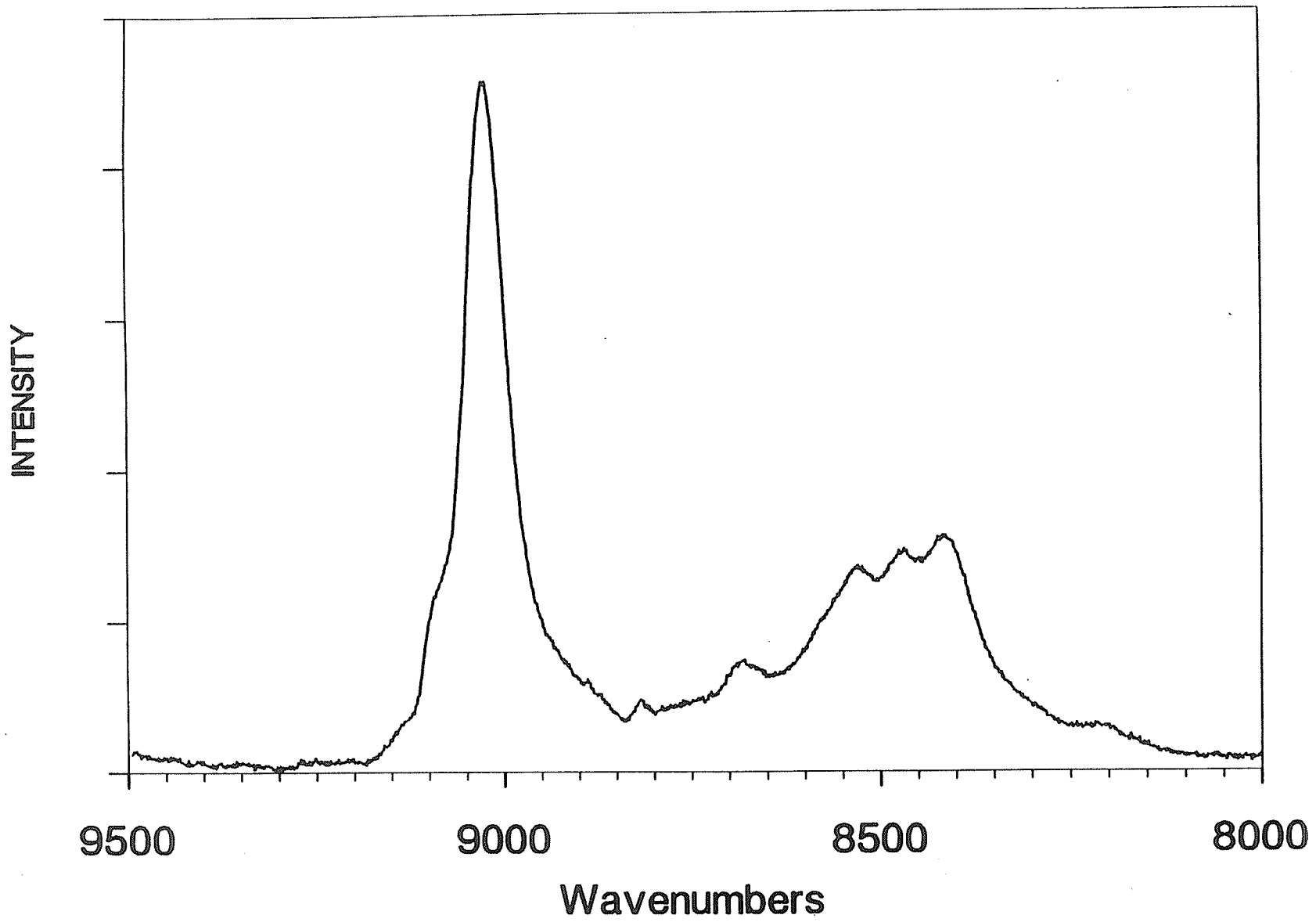
INTENSITY
9500
9000
8500
8000
Wavenumbers

cold sample, the central peak should disappear if the assignment is correct. As mentioned previously, the low absorption cross-sections of the overtone transitions make supersonic expansion overtone spectroscopy exceedingly difficult. No such spectra of methyl rotor systems have been reported. In a variable temperature Raman study of selectively deuterated toluene in the solid phase, Cavagnat and Lascombe showed that the fundamental methyl CH stretching band contour has a temperature dependence. A limited variable temperature overtone study on liquid phase methylbenzenes and halotoluenes gave similar results. Figures 12.10 and 12.11 show the $\Delta v_{CH} = 5$ methyl region of toluene and $\Delta v_{CH} = 3$ and 4 regions of o-bromotoluene recorded at various temperatures. The wider overtone linewidths encountered in the liquid and solid phases add to the spectral congestion. Despite the congestion, changes in the methyl contours can be observed. The contour changes in Figures 12.10 and 12.11 are not dramatic because of the limited temperature range covered in the study. However, the temperature dependence of the methyl contours indicates a hot-band contribution to the intensity of the overtone region. Although the methyl region is congested, the

FIGURE 12.10

Variable temperature liquid phase overtone absorption spectra of the $\Delta v_{CH} = 5$ methyl region of toluene. Bottom, middle and top traces taken at 0^0C, 25^0C, and 100^0C with a 10 cm pathlength cell.

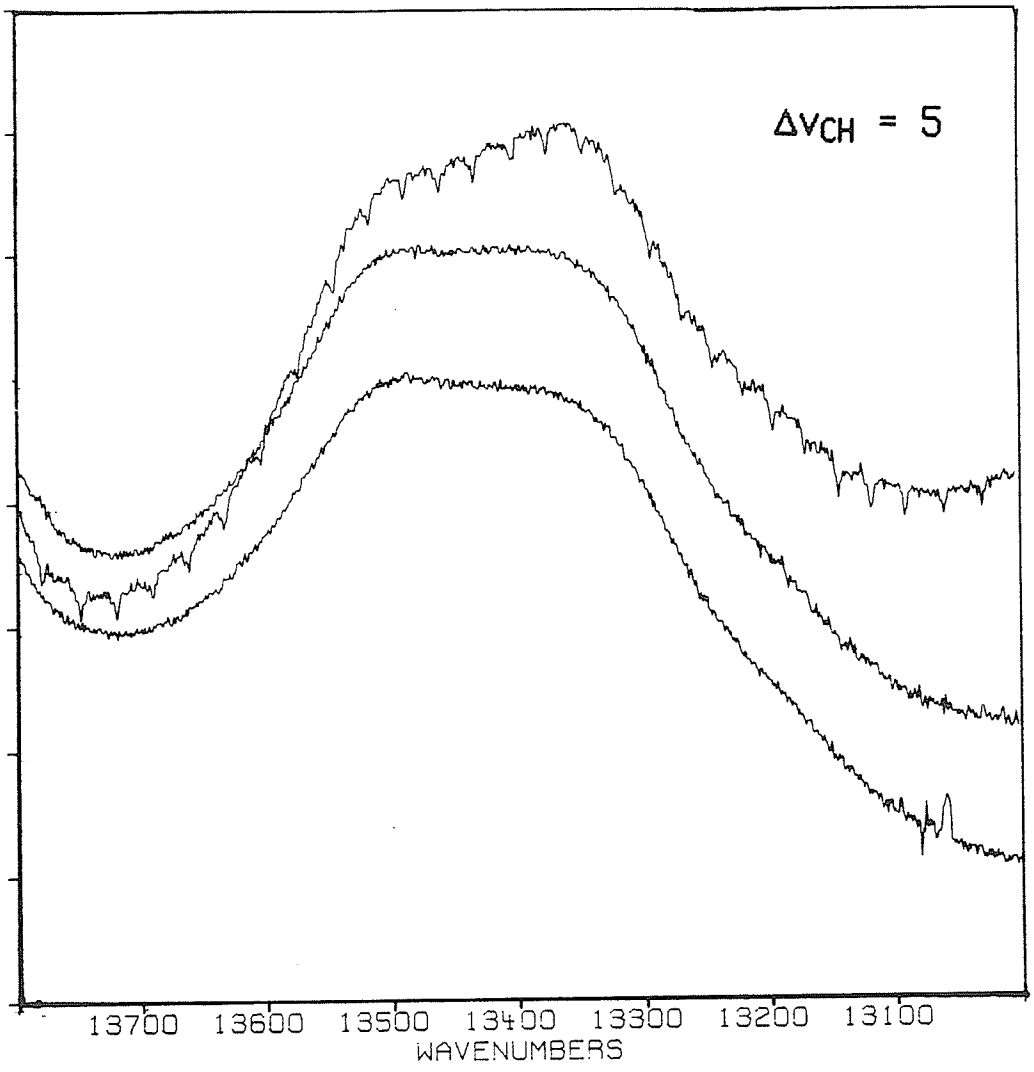
Δv_{CH} = 5
13700
13600
13500
13400
13300
13200
13100
WAVENUMBERS

FIGURE 12.11

Variable temperature liquid phase overtone absorption spectra of the $\Delta v_{CH} = 3$ and 4 methyl regions of o-bromotoluene. The traces in the order from bottom to top traces were respectively taken at 0°C, 25°C, 60°C and 128°C with a 10 cm pathlength cell.

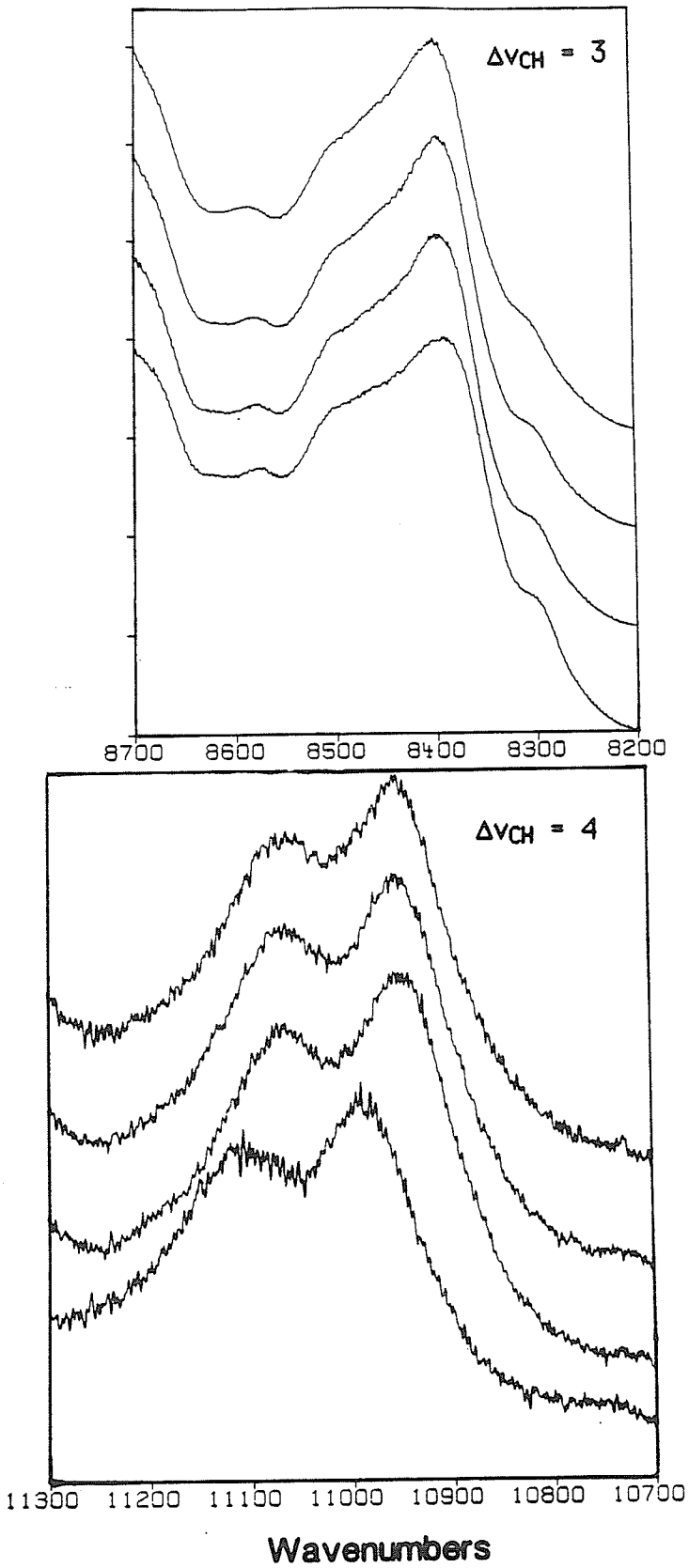
ΔνCH = 3
8700
8600
8500
8400
8300
8200
ΔνCH = 4
11300
11200
11100
11000
10900
10800
10700
Wavenumbers

intensity of the low energy peak relative to the other methyl peaks appears to grow with increasing temperature. From the limited variable temperature study it seems that the lower methyl overtone peak has the greatest hot-band contribution to its intensity. However the results cannot definitively reject the assignment of the central band as a torsional hot-band.

The Δv_{CH} = 3 - 5 methyl overtone regions of a variety of methyl rotor systems were investigated. The methyl CH stretching overtone and fundamental features of these molecules could be divided into two categories depending on whether the molecules had high or low methyl torsional barrier heights. However, in the course of the study a few very important exceptions were encountered. Sections iii and iv discuss two of these exceptional systems and the implications of these results on our overall interpretation of the methyl CH stretching regions.

iii) 2-Butyne, the Homogeneous Rotor Limit

Methyl rotor systems with low torsional barriers are of primary interest in this study. The majority of the methyl rotor molecules studied have been the subject of extensive microwave spectroscopic investigations. From the torsional splittings in the microwave spectrum, the one-dimensional torsional barrier in the ground electronic and vibrational state can be accurately determined. Most of the molecules involved in our study have ground state barriers on the order of kT or lower. At room temperature these systems are rapidly undergoing internal rotation. The vibrational overtone spectra of a number of near "free-rotor" methyl molecules were presented in the previous section. The methyl CH stretching overtone regions of those low barrier molecules were all similar. The $\Delta v_{CH} = 3 - 5$ overtone regions consisted of three major peaks. Here we report a near "free-rotor" system, 2-butyne (dimethylacetylene)[218], that does not display the three peak pattern in the $\Delta v_{CH} = 3 - 5$ methyl overtone regions.

Figures 12.12 and 12.13 display the $\Delta v_{CH} = 3 - 5$ overtone

regions of 2-butyne. The spectra are dominated by a single band which appears to have some unresolved substructure. The 2 butyne spectra are similar to the spectra of neopentane or other tetramethyl systems. This similarity occurs dispite the fact that the molecules have very different ground state methyl torsional barriers. Like the tetramethyl molecules, the high overtone spectra of 2-butyne are consistent with zero order LM predictions. The three equivalent oscillators of the isolated methyl groups give rise to a single CH stretching overtone progression. At the resolution of these spectra, the isolated methyl group approximation holds. The methyl overtone spectra of propyne[180] are nearly identical to the 2-butyne spectra. In the previous section, the two structurally similar molecules, 2 methylfuran and N-methylpyrrole were compared. Dispite their structural similarities, N-methylpyrrole behaved like toluene and nitromethane while 2 methylfuran resembled the ortho substituted toluenes. Why is there an apparent barrier dependence in some systems and a structural dependence in others?

There is one very simple explanation for the behaviour of 2-butyne. 2 Butyne is a double methyl top system with a linear, acetylenic, frame. Any interaction between the tops would be

FIGURE 12.12

Gas phase overtone absorption spectra of the $\Delta v_{CH} = 3$ and 4 regions of 2 butyne. The room temperature spectra were taken with sample pressures of 150 Torr. Pathlengths of 5.25 m and 8.25 m were used at $\Delta v_{CH} = 3$ and 4 respectively.

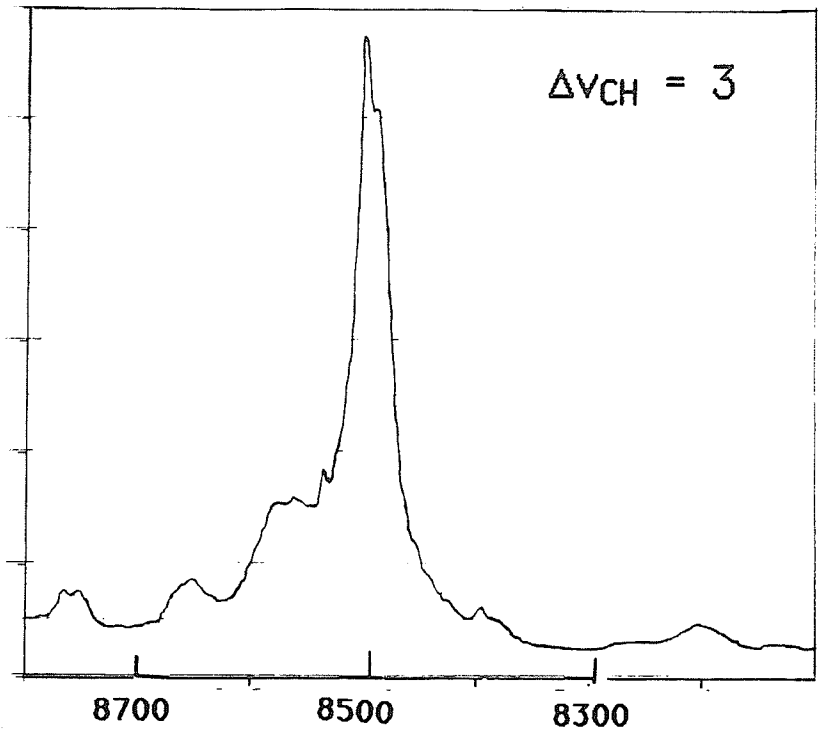

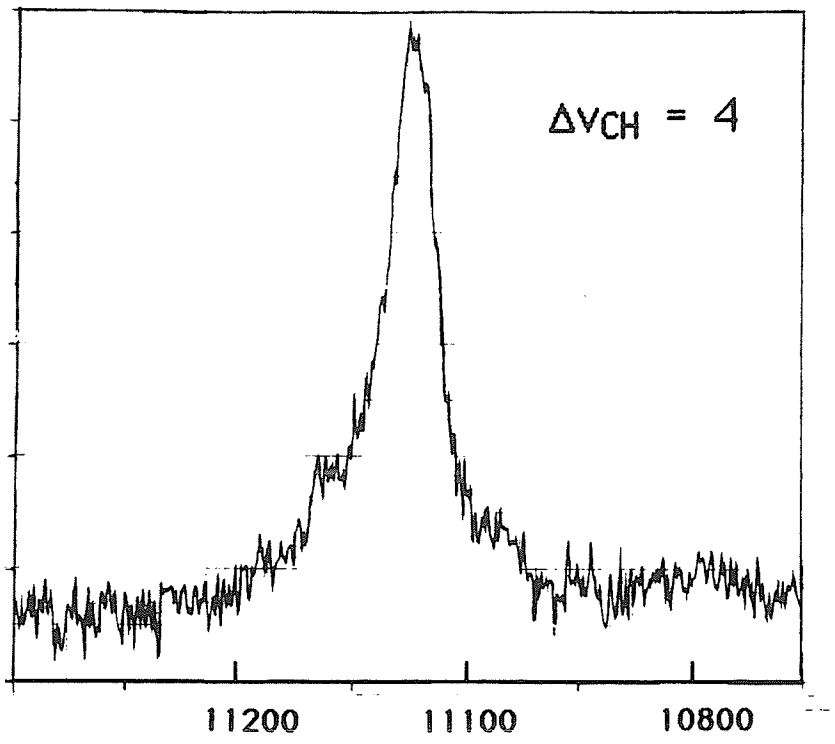

Wavenumbers

FIGURE 12.13

Room temperature, gas phase, photoacoustic overtone spectrum of the $\Delta v_{CH} = 5$ region of 2-butyne. The spectrum was acquired with 250 Torr of sample in a 10 cm pathlength gas cell.

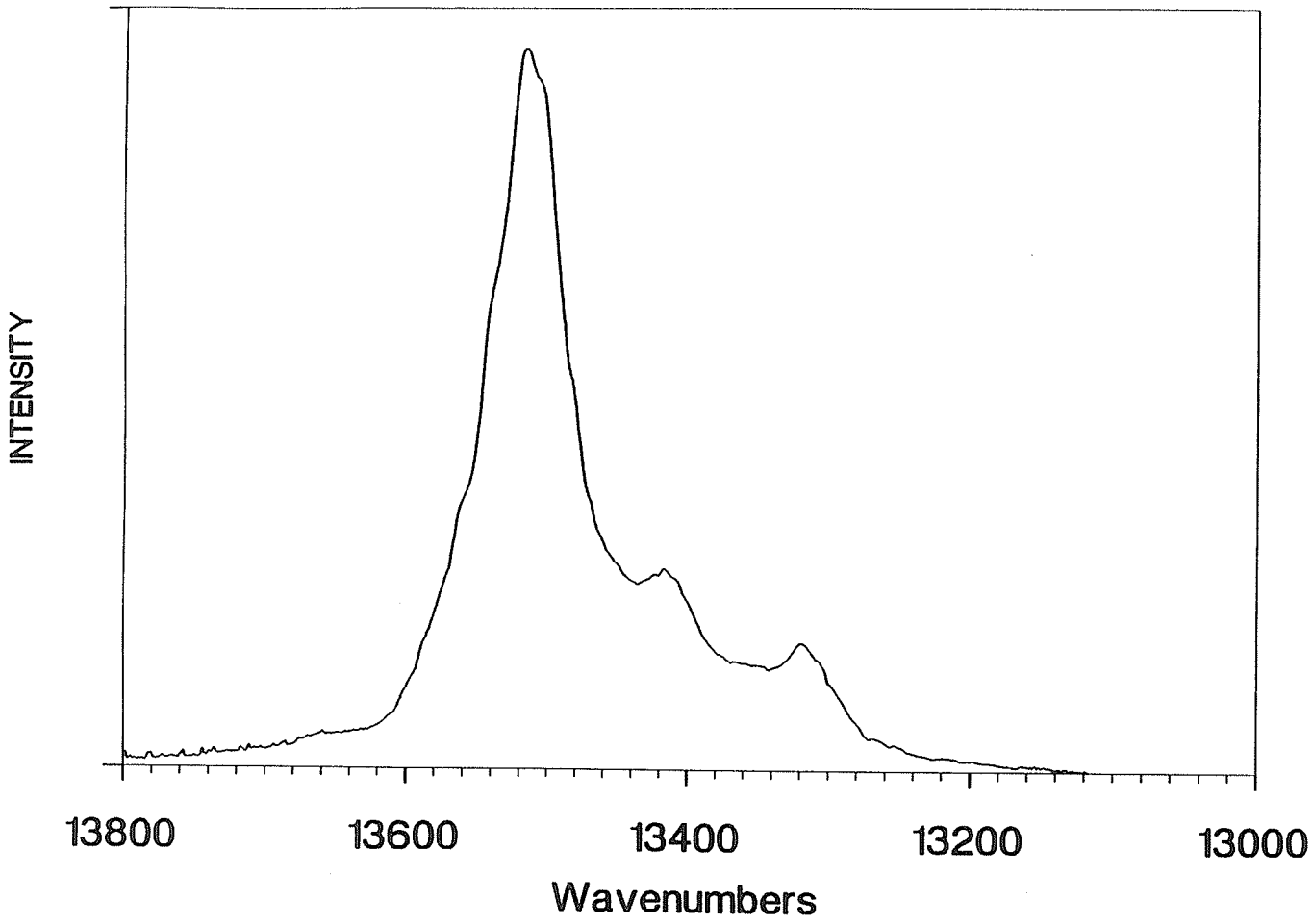
INTENSITY
13800
13600
13400
13200
13000
Wavenumbers

expected to show a dependence on the relative angle between them. However, the length of the linear frame separating the tops is sufficient to effectively isolate the tops from each other. As already mentioned, there are no obvious features arising from the interaction of the methyl rotors observed in the spectra. Owing to the symmetry of the frame with respect to the torsional axis of the methyl group, any frame-top interaction will have no angular dependence. Treating the methyl groups independently ignores any angular variation in the methyl CH stretching parameters. In the homogeneous rotor limit, the methyl rotor experiences no varying torsional hindering potential. To a good approximation, 2-butyne behaves as a homogeneous rotor. Despite the rapid internal rotation, the CH oscillators see a constant chemical environment. The methyl CH stretching overtone spectra of both "rigid" neopentane and "non-rigid" 2-butyne in the homogeneous limit would be the same. The overtone spectra of both molecules can be successfully analysed in terms of three equivalent weakly coupled anharmonic oscillators.

iv.) Line Narrowing in the Methyl Overtone Spectrum

Quite surprisingly, the $\Delta v_{CH} = 3$ methyl overtone region of 2,3,5,6 tetrafluoro and 2,3,4,5,6 pentafluorotoluene are vastly different from toluene, the monohalotoluenes, and the methylbenzenes. The spectra graphically illustrate the subtlety of the nature of the interactions and dynamics at play in the highly vibrationally excited states. The $\Delta v_{CH} = 3$ spectra of 2,3,4,5,6 pentafluorotoluene, 2,3,5,6 tetrafluorotoluene are presented in Figure 12.14. The same region of 2,6 dichlorotoluene is presented in Figure 12.15. Like toluene and para substituted toluenes, 2,3,4,5,6 pentafluorotoluene and 2,3,5,6 tetrafluorotoluenethe have six-fold methyl torsional barriers. Six-fold barriers are typically very low, Penner calculates[216] $V_6 = 99$ J mol^{-1} for pentafluorotoluene using a minimal STO-3G basis set. Schaefer and Penner[215] report STO-3G $V_6 = 467$ J mol^{-1} methyl torsional barrier for 2,6 dichlorotoluene. Based on the spectra of toluene and the other low barrier toluene molecules, three peaks are expected in the methyl overtone regions.

Rather than having three distinct peaks in the methyl overtone region, a progression of peaks is observed at $\Delta v_{CH} = 3$. A sharp

FIGURE 12.14

Gas phase, overtone absorption spectra of the $\Delta v_{CH} = 3$ region of 2,3,4,5,6 penta (bottom trace) and 2,3,5,6 tetra (top trace) fluorotoluene. The spectra were taken at a sample temperature of 60°C and with a 9.75 m pathlength gas cell.

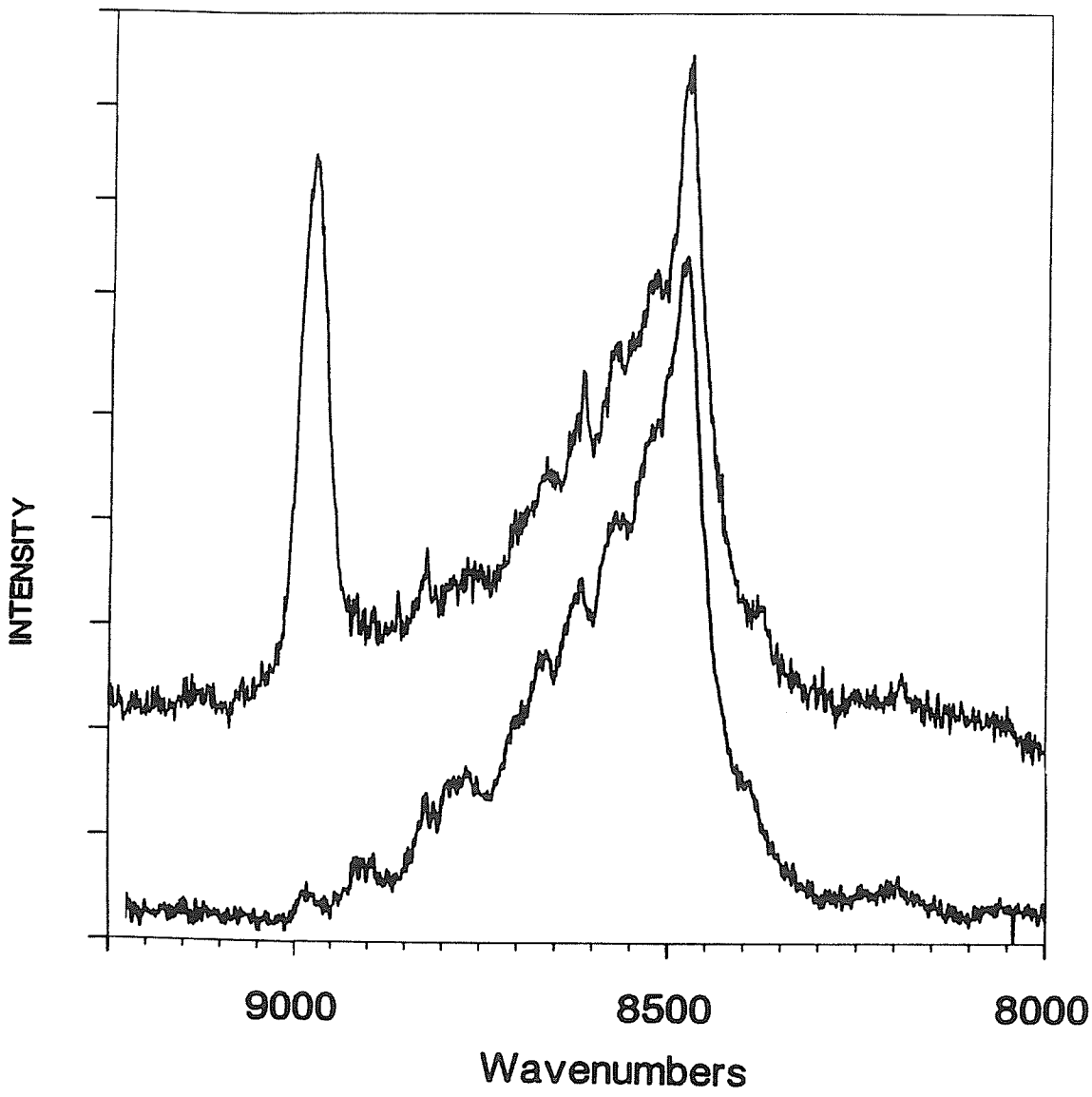
INTENSITY
9000
8500
8000
Wavenumbers

FIGURE 12.15

Gas phase, overtone absorption spectrum of the $\Delta v_{CH} = 3$ region of 2,6 dichlorotoluene. The spectrum was taken at a sample temperature of 80°C and with a 20.25 m pathlength gas cell.

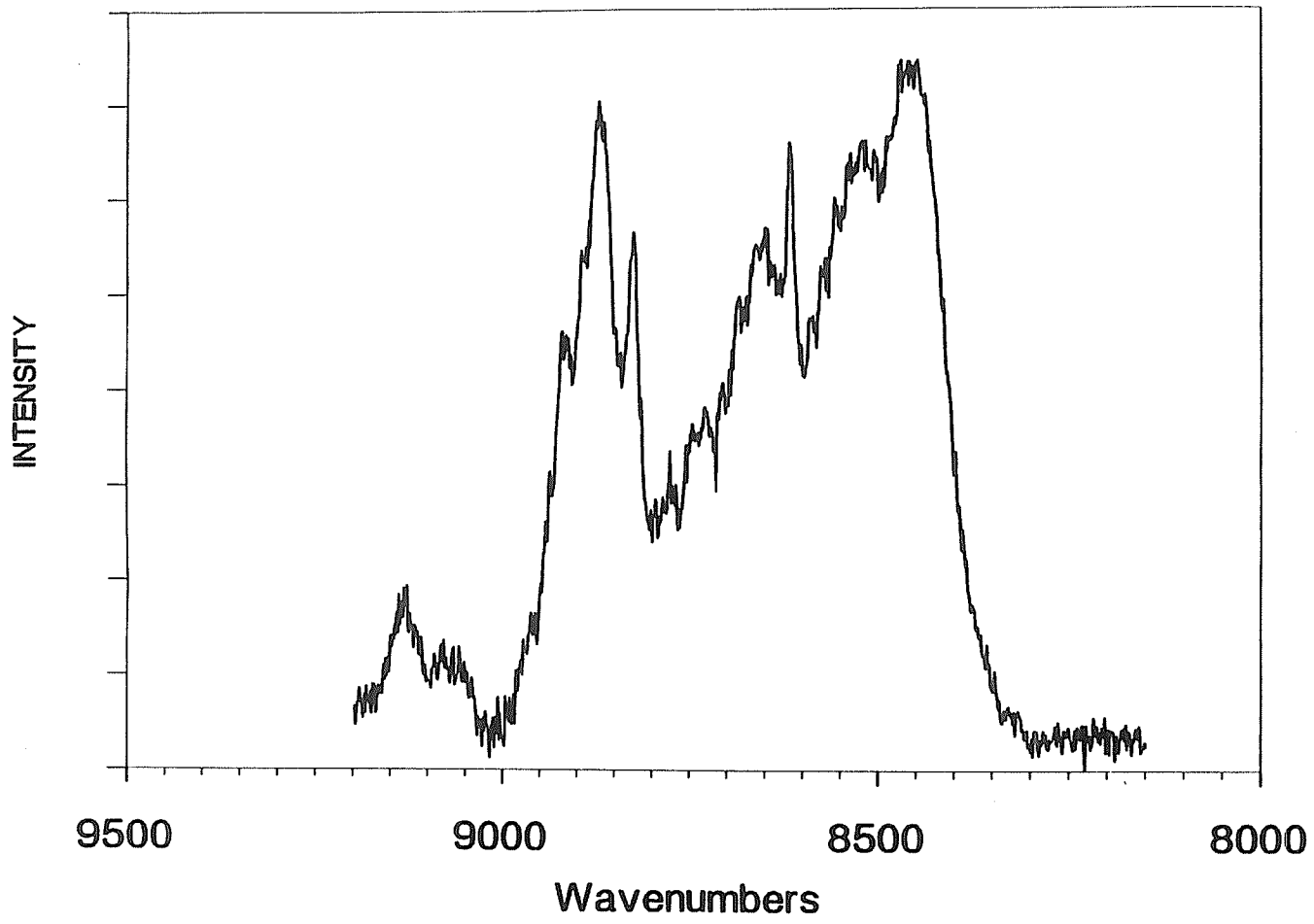
INTENSITY
9500
9000
8500
8000
Wavenumbers

intense peak at around 8497 cm-1 dominates the $\Delta v_{CH} = 3$ methyl region. To the high energy side of the sharp methyl feature there is a series of decreasing intensity peaks. Absent from the overtone spectrum of pentafluorotoluene, is the peak at 8978 cm-1 in the 2,3,5,6 tetrafluorotoluene spectrum. This sharp peak is assigned as the $\Delta v_{CH} = 3$ aryl CH stretching overtone. As observed in the fluorobenzenes, fluoro substituents shift aryl overtone transitions to higher energy. In the tetrafluorotoluene, the aryl overtone is well removed from the methyl CH stretching region. Aside from the aryl overtone, the spectra of penta-fluorotoluene and 2,3,5,6 tetrafluorotoluene are similar. Although some of the fine structure is still resolved in the spectrum of 2,6 dichlorotoluene, an emerging three peak structure is clearly visible. The $\Delta v_{CH} = 3$ spectra of 2,3,4,5,6 pentrafluorotoluene, 2,3,5,6 tetrafluorotoluene, and 2,6 dichlorotoluene seem to represent a series. The penta and tetra fluorotoluene spectra resemble that of 2 butyne. The behaviour of 2,6 dichlorotoluene approaches that observed in toluene and para substituted toluenes.

The unusually narrow $\Delta v_{CH} = 3$ methyl overtone linewidths encountered in the penta and tetra fluorotoluene spectra markedly

reduce the congestion and permit fine structure in the methyl overtone regions to be resolved. The series of peaks to the high energy side of the main methyl peak is suggestive of a torsional progression. Torsional progressions which resemble the $\Delta v_{CH} = 3$ methyl structure are observed in the $S_1 \Leftarrow S_0$ fluorescence excitation or REMPI spectra of cold toluene[208] or p-fluorotoluene[207,218]. Such an interpretation is appealing in that the spectrum can be understood in terms of transitions between hindered rotor states of the adiabatic $v_{CH} = 0$ and $v_{CH} = 3$ surfaces[219]. With sufficient resolution to resolve the torsional structure the methyl torsional barrier height in the $v_{CH} = 3$ state(s) could be determined. Ito and coworkers used such a procedure to determine the S_1 methyl torsional barrier heights in o-, m-, and p-fluorotoluene[207]. Despite the appeal of such an interpretation this model was not explored in detail. The absence of such a progression at $\Delta v_{CH} = 2$ in the penta and tetra fluorotoluenes, the limited data on these toluenes and the differences between the family of toluenes makes the assignment of the methyl regions uncertain. Higher overtone data and preferably overtone data of cold methyl rotor molecules is essential for

definitive assignments to be made in the $\Delta v_{CH} \geq 3$ overtone regions.

In the penta and tetrafluorotoluenes and to a lesser extent in 2,6 dichlorotoluene there is a dramatic decrease in the overtone linewidths at Δv_{CH} = 2 - 3. To the author's knowledge, such an obvious substituent effect on overtone linewidths has not been previously reported. Since sources of overtone linewidth are not clearly established this observation is important. Having only the Δv_{CH} 2 - 3 overtone spectral regions, one can only speculate on the generality of the narrower overtone linewidths of the penta and tetrafluorotoluenes. The narrow linewidths at Δv_{CH} 2 - 3 may be fortuitous in the sense that multiple fluorine substitution may detune these methyl overtones and nearby doorway states. In Chapter 11 Fermi resonant interactions could be tuned-in and out of resonance through substitution. However, it also appears that an interaction between methyl and aryl CH oscillators contributes to the overtone linewidths. From the limited spectroscopic data it is difficult to determine whether again this interaction is through nearby combinations involving ring CH bending modes or now the long range CH stretch - stretch couplings are responsible. One indicator that aryl - methyl CH stretch- stretch couplings may contribute to

overtone linewidth is available from the comparison of the aryl overtone linewidths between 2,3,5,6 tetrafluorotoluene and 1,3,5 trimethylbenzene or between the 2,5 dimethylfuran and 2,5 dimethylthiophene. The aryl $\Delta\nu_{CH} = 2 - 3$ linewidths in the fluorotoluenes are narrower than in the methylbenzenes. Likewise 2,5 di-methylfuran has narrower overtone linewidths the 2,5 dimethylthiophene. The aryl stretching frequencies relative to the methyl frequencies are higher in the fluorotoluenes and than the methyltoluenes. Likewise the frequency difference is greater in the methylfurans than the methylthiophenes. The greater the energy separation between the aryl and methyl stretching region at a given overtone (at least at $\Delta\nu_{CH} = 2 - 3$) the narrower the aryl and methyl overtone linewidths. Note that if stretch-stretch couplings are an operative source of overtone linewidth in the methyltoluenes, the substituent induced frequency shift in tetrafluorotoluene is sufficient to effectively decouple the aryl - methyl interaction. The similar methyl overtone linewidths in the tetra and penta fluorotoluenes can be cited as evidence for the effective decoupling.

The tetra and pentafluorotoluene clearly demonstrate that the density of states in itself does not dictate overtone linewidths.

Even in the lower overtone regions, state densities do not appear to be the singular important factor in IVR. Another aspect that should be noted is the limited effect of nearly free methyl rotation on overtone linewidths. In the low-lying levels of S_1, Parmenter and coworkers[218,220] demonstrated that free methyl rotation has an enormous effect on IVR rates. In the similar molecules, p-difluorobenzene and p-fluorotoluene, methyl internal rotation was considered responsible for the IVR rates in p-fluorotoluene to be two orders of magnitude greater than in p-difluorobenzene. If the overtone linewidths are primarily homogeneously broadened at $\Delta v_{CH} = 3$, methyl torsion appears to play little role in the CH stretching overtone IVR rates in any of the toluenes studied. In a density of states argument this is hard to rationalize. However, if one considers the initial stages of IVR to be more mode specific then the varying effectiveness of methyl torsion as an accelerating group for IVR is understandable. The high frequency CH stretching modes do not efficiently couple to the low frequency methyl torsion (adiabatic separation of fast and slow motion). Methyl torsion states or states built on the methyl torsion act as very poor "door-way" states for the bright overtone states. On the other hand, the

modes which dominate the low lying S_1 vibronic spectrum interact more strongly with the methyl torsion and hence the methyl rotor is a highly effective accelerator of IVR in this region. Direct dynamical studies of the methyl rotor mediated IVR in the mid-infrared would be of interest to see if differences in IVR rates and hence IVR mechanisms exist between S_1 and S_0.

v.) The $\Delta v_{CH} = 2$ Results and Conclusion.

The fundamentals and the intermediate and high overtones of methyl rotor systems have been discussed. Information from the first methyl overtone has been curiously absent in this discussion and other studies. As discussed in Chapter 11, interoscillator coupling leads to degeneracy splittings and intense combinations which complicate the $\Delta v_{CH} = 2$ region. Most of the features in the $\Delta v_{CH} = 2$ region of the methyl substituted furans and thiophenes could be understood in terms of a rigid methyl group of local C_{2v} symmetry. The $\Delta v_{CH} = 2$ region of neopentane and similar molecules have been analysed assuming a rigid C_{3v} methyl group. A careful re-examination of the spectra and the spectra of other methyl rotor systems reveals some inadequacies in both approaches. These inadequacies probably stem from the breakdown of the assumption of a rigid methyl group.

Unlike the high overtones, the $\Delta v_{CH} = 2$ methyl regions are remarkably similar for all the methyl rotor systems studied. Figure 12.16 compares the $\Delta v_{CH} = 2$ spectra of toluene and the

methyltoluenes. Only subtle differences exist between the spectra. The relative intensity of the methyl overtone at ≈ 5760 cm^{-1} to the high energy shoulder (≈ 5810 cm^{-1}) is greater in o-xylene than the other xylenes. In addition, the aryl and methyl features are somewhat sharper in o-xylene than the other methyltoluenes. In the toluenes and xylenes, the methyl substitutent effect on the aryl oscillators shifts the aryl overtone transitions into the methyl CH stretch-stretch $\Delta v_{CH} = 2$ combination region leading to increased congestion in that region. The congestion is considerably reduced in the 2,3,5,6 tetrafluorotoluene spectrum. Once again, narrower linewidths are observed in the tetra and pentafluorotoluene spectra compared to the methylbenzenes. Figure 12.17 compares the $\Delta v_{CH} = 2$ spectrum of p-xylene to 2,3,5,6 tetrafluorotoluene. At $\Delta v_{CH} = 2$ the relative decrease in the overtone linewidths of the fluorotoluenes is not as dramatic as that observed at $\Delta v_{CH} = 3$. At $\Delta v_{CH} = 2$, 2-butyne has much narrower linewidths than the toluenes. Figure 12.18 compares the $\Delta v_{CH} = 2$ spectra of 2-butyne and pentafluorotoluene. The narrow $\Delta v_{CH} = 2$ linewidths reveal splittings and structure not resolved in the other spectra. The additional information present in the 2-butyne spectrum provides insight into the more congested

FIGURE 12.16

Gas phase, overtone absorption spectra of the $\Delta v_{CH} = 2$ region of (from bottom to top) toluene, o-xylene, m-xylene, and p-xylene. The spectra were recorded at 60°C and with a 2.75 m pathlength gas cell.

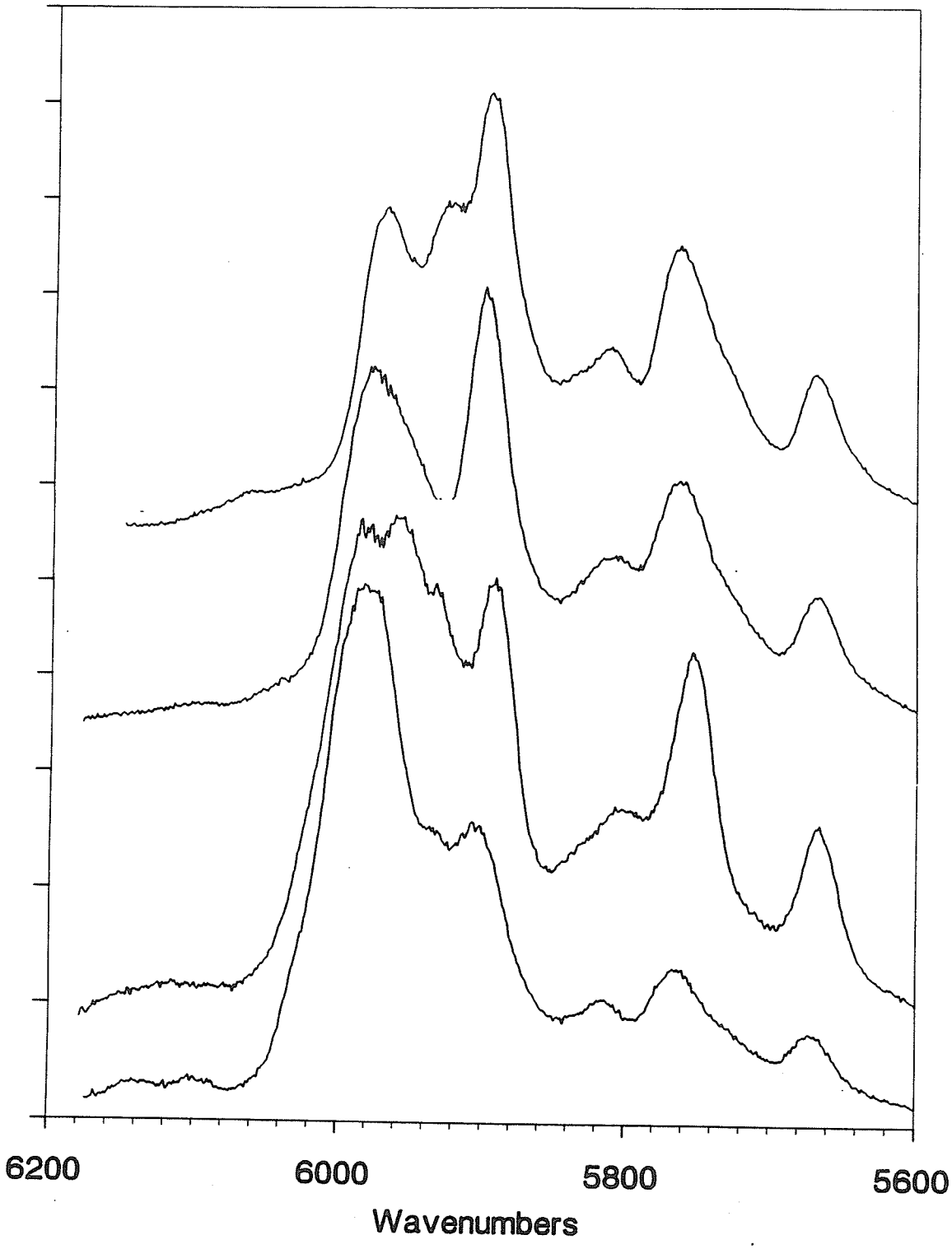
6200
6000
5800
5600
Wavenumbers

FIGURE 12.17

Gas phase, overtone absorption spectra of the $\Delta v_{CH} = 2$ region of 2,3,5,6 tetrafluorotoluene (bottom trace) and p-xylene (top trace). The spectra were recorded at 60°C and with a 2.75 m pathlength gas cell.

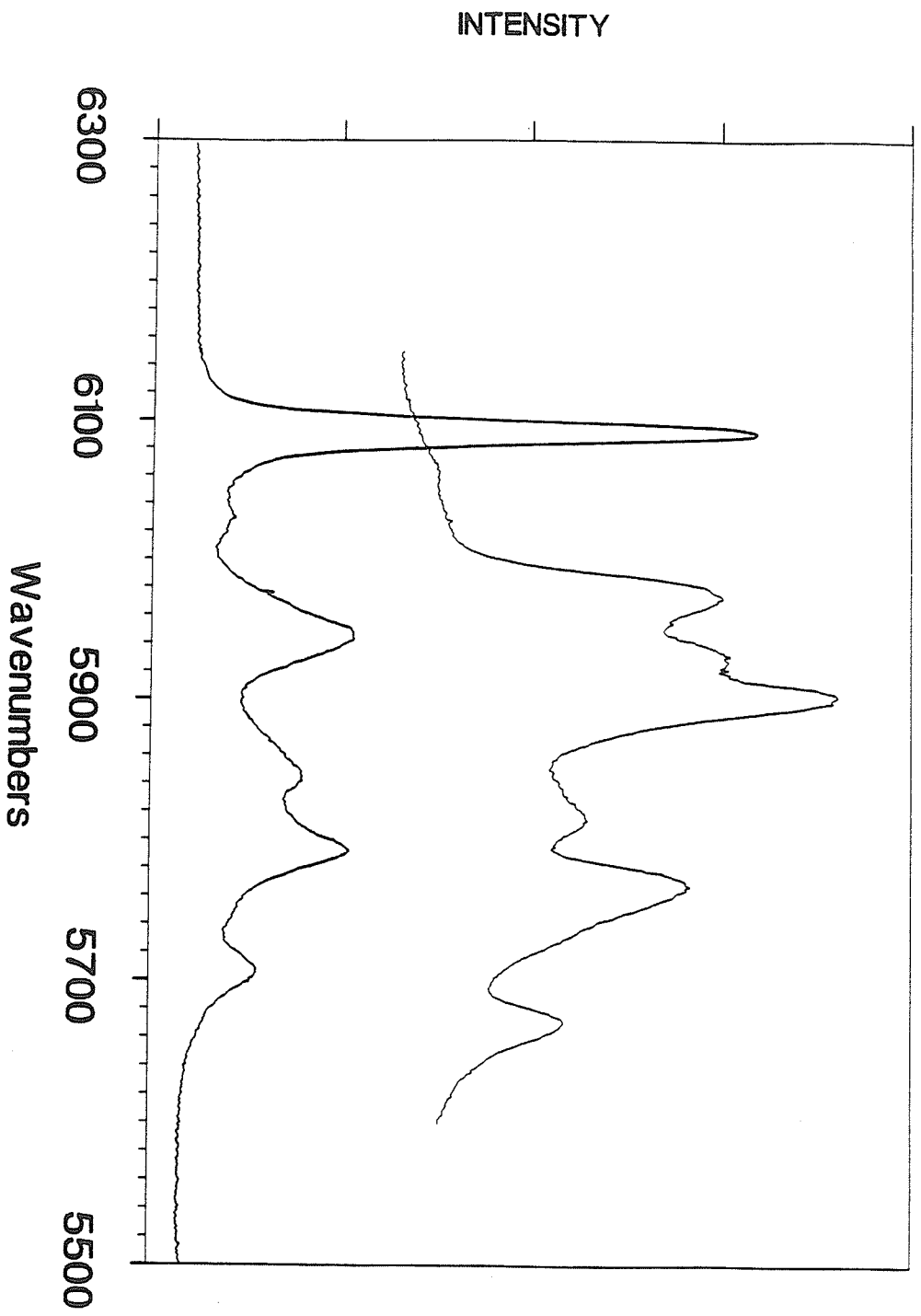
INTENSITY
6300
6100
5900
5700
5500
Wavenumbers

FIGURE 12.18

Gas phase, overtone absorption spectra of the $\Delta v_{CH} = 2$ region of 2,3,4,5,6 pentafluorotoluene (top trace) and 2-butyne (bottom trace). The pentafluorotoluene spectrum was recorded at 60°C with a 5.25 m pathlength gas cell. The 2-butyne spectrum was recorded with 150 torr of sample at room temperature with a cell pathlength of 5.25 m.

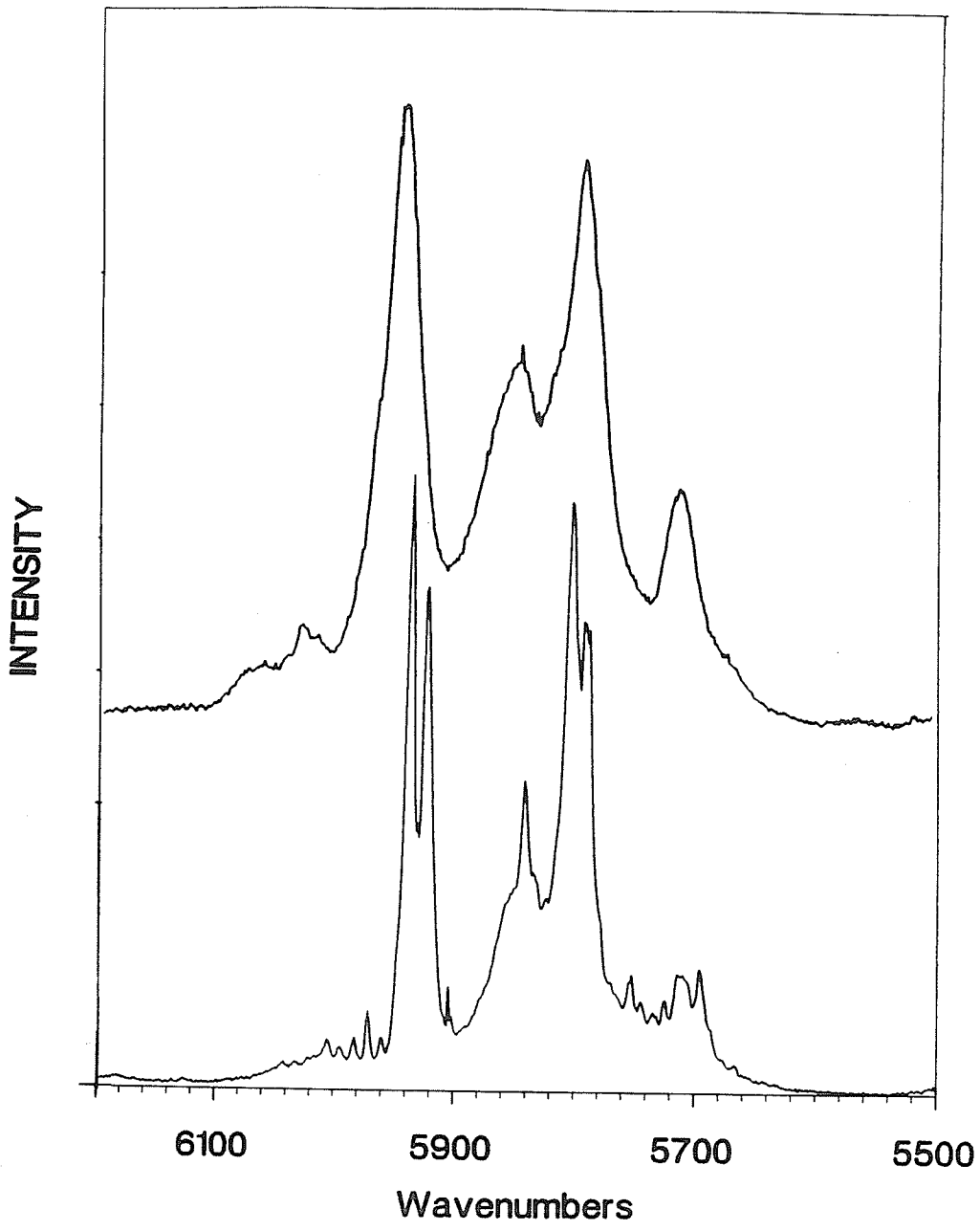
INTENSITY
6100
5900
5700
5500
Wavenumbers

spectra of the other molecules.

The $\Delta v_{CH} \geq 3$ overtone regions of 2-butyne are similar to those of neopentane. The $\Delta v_{CH} = 2 - 5$ spectra of neopentane have been analysed in terms of isolated methyl groups of local C_{3v} symmetry. The $\Delta v_{CH} = 2$ spectra of neopentane-d_9 and 2-butyne are given in Figure 12.19. In the C_{3v} analysis, the peak at $\approx$ 5810 cm^{-1} is unassigned. In both the rigid C_{3v} and C_{2v} treatments, the low energy peak at between 5650 - 5750 cm^{-1} remains unaccounted for. Both of these peaks are associated with the methyl groups. Their intensity grows with the number of methyl substituents (see Figure 12.16). The 2-butyne spectrum reveals extensive structure between 5650 - 5750 cm^{-1}. Similar structure is revealed in the weak high energy band at $\approx$ 6000 cm^{-1}. The low and high energy bands may be a part of a torsional progression or torsional hotband progression. The two doublets centered at $\approx$5925 and $\approx$5795 cm^{-1} correspond to the A_1, E combination and overtone transitions respectively in the C_{3v} analysis. These doublets dominate the spectrum.

The relative magnitude of the doublet splittings between the combination and overtone transitions can be accounted for in the C_{3v}

FIGURE 12.19

Gas phase, overtone absorption spectra of the $\Delta v_{CH} = 2$ region of neopentane-d_9 (bottom trace) and 2-butyne (top trace). The room temperature spectrum of neopentane was acquired with a sample pressure of 435 Torr and a 0.75 m pathlength gas cell. The 2-butyne spectrum was recorded with 150 Torr of sample at room temperature with a cell pathlength of 5.25 m.

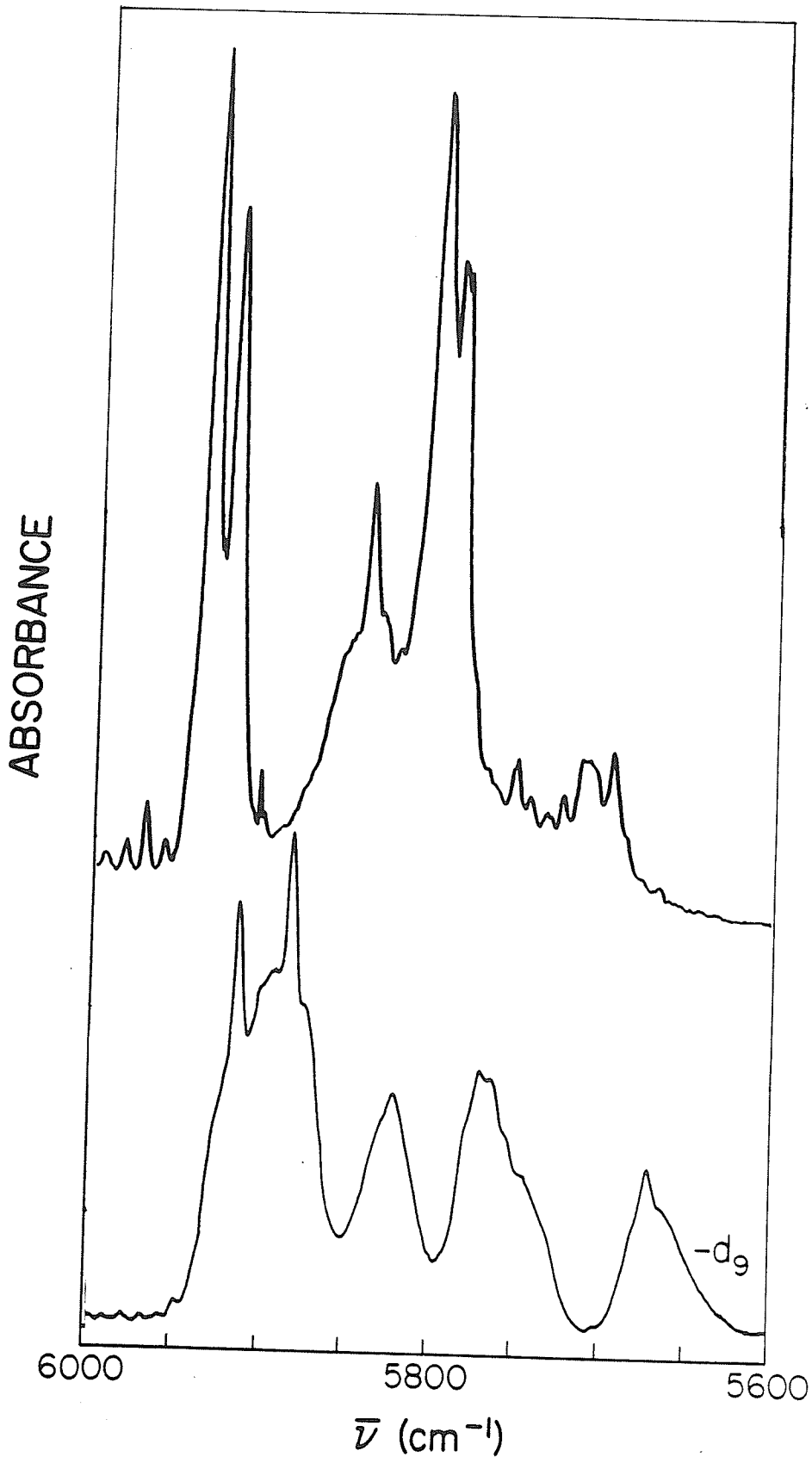
ABSORBANCE
-d9
6000
5800
5600
ν̄ (cm⁻¹)

analysis. Figure 12.20 sketches the C_{2v} and C_{3v} methyl $v_{CH} = 2$ energy level diagrams. The splittings are also understandable within a C_{2v} analysis. In the C_{2v} treatment the lower energy component of the combination doublet is assigned as the $|11\rangle$ $|0\rangle$ combination the higher energy component to the unresolved $|10\rangle_{\pm}|1\rangle$ combination. The C_{2v} analysis can also account for the peak at $\approx$ 5810 cm^{-1} as the $|00\rangle|2\rangle$ overtone. In the higher barrier methyl rotor systems where nonequivalence of the methyl oscillators is expected, a progression involving the 5810 cm^{-1} peak can be identified in the Δv_{CH} = 2 - 5 regions. The intensity of the transitions associated with this progression and the quality of the Birge-Sponer fit is indicative of an overtone progression. As discussed in Chapter 11, the $\Delta v_{CH} \geq 3$ overtone regions of the methyl substituted furans and thiophenes are better understood in terms of a C_{2v} methyl group symmetry. In the same vein, the C_{3v} analysis of neopentane or 2-butyne is much more appropriate at the higher overtones. At $\Delta v_{CH} = 2$ neither analysis seems to be totally correct. However, the spectra of all the methyl rotor systems appear to be better described by the C_{2v} methyl group symmetry.

FIGURE 12.20

Energy level diagram of the v = 2 methyl CH stretching states given by a C_{3v} and C_{2v} intramanifold, one-bond, harmonic coupling extension of the LM model. The C_{3v} LM methyl oscillator frequency and anharmonicity parameters were obtained from the fit to the neopentane overtone progressions[176], ω = 3040 cm^{-1} χ = 59.1 cm^{-1} and the effective intramanifold coupling was obtained from the fundamental degeneracy splitting[176], c = 14.7 cm^{-1}. The zero order C_{2v} parameters were obtained from the 3 methylthiophene overtone progressions, ω_{ip} = 3069 cm^{-1} χ_{ip} = 60.6 cm^{-1} and ω_{op} = 3050 cm^{-1} χ_{op} = 63.3 cm^{-1}. The predicted 3-21G effective intramanifold, interoscillator coupling parameters $c_{ip,op}$ = -23.65 cm^{-1} and $c_{op,op}$ = -18.56 cm^{-1} were used in the analysis.

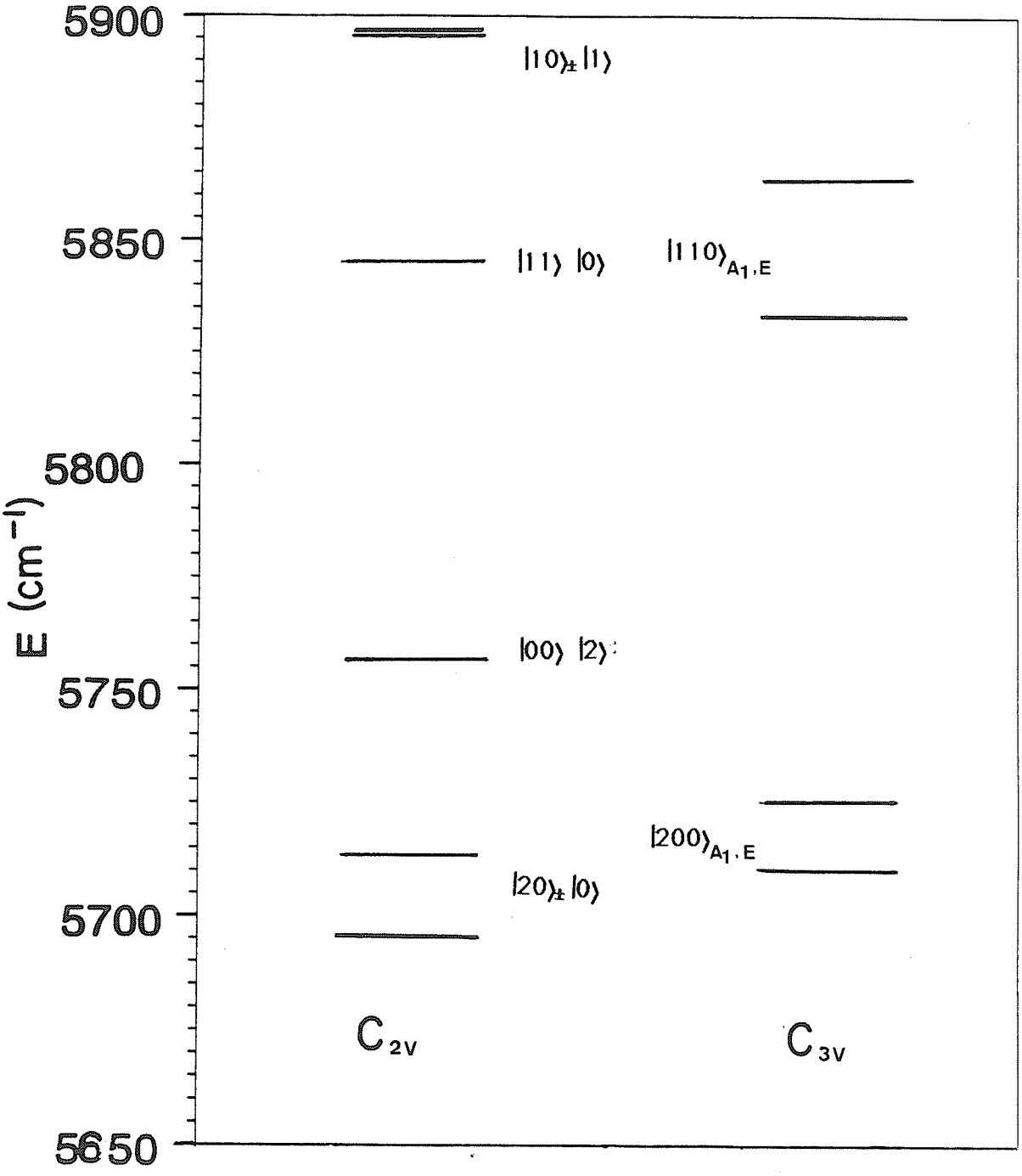
5900
5850
5800
5750
5700
5650
E (cm⁻¹)
|10⟩± |1⟩
|11⟩ |0⟩
|110⟩A1,E
|00⟩ |2⟩
|200⟩A1,E
|20⟩± |0⟩
C2V
C3V

The $\Delta v_{CH} = 2$ spectra of the methyl rotor systems clearly identifies one of the main sources of confusion regarding the assignment and interpretation of the methyl overtones. The assignment of the progression associated with the 5810 cm^{-1} peak as an overtone progression requires acknowledging the conformational nonequivalence of the methyl CH oscillators through the angular dependence of the oscillator frequencies and interoscillator couplings. In the limit of an infinite barrier to internal rotation, the rigid methyl group is described by a local C_{2v} symmetry. At the other limit, the homogeneous rotor limit, methyl CH oscillators see a constant chemical environment. Oscillator frequencies and couplings have no angular dependence. In this limit the methyl CH stretching overtone regions can be analysed assuming a local C_{3v} methyl group symmetry. In this light, it is not surprising that neither analysis rigorously applies. The molecules represent an intermediate case between the rigid molecule limits. However, since most of the molecules studied have relatively low barriers to internal rotation, one might expect the spectra to be more closely described by the homogeneous rotor limit. This does not appear to be the case. Even very small barriers to internal rotation seem to

contribute to the structure of the methyl overtone regions.

- SUMMARY AND FUTURE CHALLENGES

The diverse nature of the work presented in this thesis does not lend itself to an enlightening, concise summary. The work, as presented, partitions into three major sections. The first main section deals with the construction of an intracavity dye laser photoacoustic spectrometer. The exhaustive detail of this section was deliberately aimed to provide enough information to enable one to build or extend the capablilities of a similar instrument. In our case, the enhanced sensitivity of photoacoustic based methods over conventional absorption spectroscopy provides access to the previously inaccessible very weak overtone regions. The photoacoustic spectrometer detailed in Part B has at least one to two orders of magnitude increased sensitivity over the instrumentation previously employed in our laboratory.

The second major section of this thesis concerns the aryl CH stretching overtone spectra of 5-membered aromatic heterocycles. At the outset of the study, it was expected that the aryl overtones of these molecules would behave like those of the substituted benzenes.

Indeed at a qualitative level many similarities are noted. Similar substituent effects and the qualitative inverse frequency - bondlength relationship are observed. However, the quantitative bondlength - frequency correlation developed from the fundamental and overtone CH stretching data of other molecules does not apply to the aromatic heterocycles. The breakdown of the correlation arises from the unusual frequency - anharmonicity ratios encountered in the aromatic heterocycles.

The overtone spectra of the aromatic heterocycles present other features not readily explained by simple local mode models. At $\Delta v_{CH}=4$ the two overtones of furan seem to coalesce. The coalescence can be explained in terms of the Fermi resonance interaction between the CH stretching overtone and a combination built on the next lower CH stretching overtone and the overtone of a lower frequency mode of furan. The perturbations in the thiophene spectrum at $\Delta v_{CH}= 3$ and 4 are more difficult to explain. These perturbations behave like two-state Fermi resonances highly sensitive to the zero order energy match between the interacting states. An assignment of the interacting dark state is not apparent from the available thiophene force field data.

In the third section the methyl overtone regions of various methyl containing molecules are examined. Chapter 11 of this section specifically deals with the methyl overtone regions of methyl substituted furans and thiophenes. These molecules have relatively high barriers to the internal rotation of the methyl group. Like other high barrier methyl systems, most of the features in the methyl CH stretching overtone regions can be explained by considering the methyl rotor as being fixed in its minimum energy conformation. In the methylfurans and methylthiophenes fixing the methyl group results in the in-plane and out-of-plane methyl oscillators becoming distinguishable. Acknowledging the conformational distinguishablity of the oscillators proves quite successful. Using the simple linear dipole approximation and the intramanifold harmonic coupling extension of the local mode model, the relative methyl CH stretching overtone - combination energies and intensities are reasonably well predicted. Intensity predictions improve considerably for the $\Delta v_{CH}=2$ region if the full harmonic coupling model is employed. The ground state mixing contribution to the intensities was cited as the reason for the improvement in the predicted intensities.

Chapter 12 compares the overtone spectra of low and high barrier methyl rotor systems. The high methyl overtone regions $\Delta v_{CH} \geq 3$ of toluene and its substituents as well as many other molecules appear to be dependent on methyl torsional barrier height. There is a strong central peak in the methyl region of low barrier molecules which is virtually absent from the spectra of high barrier molecules. By studying a number of methyl rotor systems over a wide energy range it was hoped to determine the origin of this central peak. Although a definitive assignment of the central peak from the spectroscopic data was not possible, several intriguing results were discovered. Despite the very low barrier, 2-butyne behaved much more like the high barrier neopentane than toluene. The $\Delta v_{CH}=3$ regions of 2,3,5,6 tetra and 2,3,4,5,6 penta fluorotoluene display drastically reduced overtone linewidths with no obvious central peak. The reduced overtone linewidths enable the methyl torsional progression to be observed at this overtone. The broad three peak structure begins to re-emerge in the spectrum of 2,6 dichlorotoluene at this region. These intriguing results suggest that the central methyl peak is not simply due to the rotational "averaged" methyl oscillators.

At $\Delta v_{CH}=2$ the methyl overtone regions of all the methyl rotor systems studied look remarkably similar. This is quite unexpected considering the behaviour at the higher overtones. Neither the C_{2v} nor the C_{3v} rigid methyl group analysis is entirely satisfactory at $\Delta v_{CH}=2$. Clearly more work is required to understand this overtone region and the behaviour of the methyl overtone regions in general. Supersonic jet studies of cold, isolated molecules would be very useful.

The reader of this thesis has probably noticed that the work raises more questions than it attempts to answer. Some of these questions lie at the heart of investigations of highly excited vibrational states. Refinements in vibrational descriptions like the local mode model require high resolution spectra without extensive congestion. Now such spectra can really only be obtained for small molecules. Even fewer molecules lend themselves to supersonic beam expansion spectroscopy. High resolution small molecule spectra are providing insight into the role of Fermi interactions in the XH-stretching overtone regions and even the importance of anharmonic interoscillator coupling. However, it is uncertain whether this information can be generalized to polyatomic systems.

systems. Extrapolating from the small to the large molecule limit seems particularly uncertain when discussing the dynamical aspects of overtone spectroscopy.

The application of time resolved methods to study overtone dynamics represents another major challenge in this field. With time resolved methods, unlike using line width data, one obtains direct dynamical information. With temporal data, the issue of inhomogeneous overtone linebroadening contributions can be bypassed. Technically and financially the femtosecond time scale still represents a challenge. Besides this challenge there is the problem that the experimental method for studying rapid overtone IVR is not established. The high energy vibrational states are not emissive. Therefore time-resolved fluorescence methods which are now so well developed cannot be directly applied. Up-conversion and SEP (stimulated emission pumping) methods appear to be much less promising than initially thought. Aside from some of the major technical problems associated with up-conversion and SEP, disentangling the effects of the various states which are radiatively coupled in these experiments may prove to be the most formidable obstacle facing these experiments.

For the theorist, the challenges in vibrational overtone spectroscopy are abundant. Superior model Hamiltonians for the description of the vibrational motion of polyatomic molecules are required. Work in this area seems to be progressing toward expressing the full kinetic energy operator in optimally separable coordinate systems. Vibrational dynamics particularly in the regime of the quasi-continuum presents a challenging problem. The problem becomes even more difficult if the electronic - vibrational coupling in strong radiation fields is considered. A model of this latter form is required to understand SEP and other related phenomena.

The field of vibrational overtone spectroscopy is a very active area in which some of the fundamental questions still remain unanswered. It is hoped that this thesis represents a small contribution to this field.

APPENDICES

Appendix 1

- Listing of the photoacoustic instrument control program.

Commodore Basic Program to Control PAS Spectrometer

```
10 REM SET PET TO GRAPHICS MODE
20  POKE 59468,12
30 SU%=0:REM INITIALIZE SET-UP VARIABLE
40 REM SET-UP FLUKE DMMs
50  Q0$="124A LOCK-IN":Q1$="128A LOCK-IN":Q2$="POWER METER "
60  R0$="R0 AUTORANGE":R1$="R1  0-200 MV":R2$="R2  0-2    V"
70  R3$="R3  0-20   V":R4$="R4  0-200  V":R5$="R5  0-1000 V"
80 S0$="S0 SLOW   ":S1$="S1 MEDIUM ":S2$="S2 FAST   "
90   B0$=Q0$:B1$=Q2$:B2$=R3$:B3$=R1$:B4$=S1$:B5$=S1$
100 PRINT CHR$(147):REM CLEAR SCREEN AND PRINT TITLES AND HEADINGS
110 PRINT
120 PRINT TAB(18)" PHOTOACOUSTIC DATA COLLECTION PROGRAM"
130 PRINT
140     PRINT     TAB(18)"**************************************"
150 PRINT:PRINT TAB(32)" MAIN MENU"
160 PRINT
170 PRINT TAB(19)"MOTOR CONTROL....."SPC(9)"1"
180 PRINT TAB(19)"DATA INPUT SET-UP ROUTINE."SPC(9)"2"
190 PRINT TAB(19)"DATA COLLECTION....."SPC(9)"3"
200  PRINT TAB(19)"QUIT....."SPC(9)"4"
210 PRINT:PRINT:PRINT "ENTER COMMAND NUMBER"
220 INPUT B1%
230 REM PROCESS COMMAND B1%
240 IF B1%=4 GOTO 380
250 IF (B1%>4)OR(B1%<1) GOTO 350
260 REM BRANCH TO PROPER SUBPROGRAM
270 ON B1% GOSUB 7000,500,5000
280 PRINT CHR$(147)
330 GOTO 120
340 REM ERROR IN COMMAND NUMBER INPUT
350 PRINT:PRINT "ERROR IN COMMAND NUMBER, RE-ENTER"
360 GOTO 180
370 REM IF B1%=Q TERMINATE PROGRAM
380 END
390 REM
400      REM      ************************************************************
410 REM
420 REM      SUBROUTINE: SET-UP
430 REM
```

```
440 REM      THIS ROUTINE INITIALIZES THE PARAMETERS REQUIRED FOR A
450 REM  PHOTOACOUSTIC SCAN.  ONCE THE INITIAL PARAMETERS
460 REM  HAVE BEEN SPECIFIED BY THE USER, DATA COLLECTION,
470 REM  MANIPULATION, AND STORAGE ARE CARRIED OUT AUTOMATICALLY.
480 REM
490       REM       ************************************************************
500 PRINT CHR$(147):PRINT:PRINT TAB(31)" SET-UP ROUTINE "
510 REM
520 REM  SET THE DEFAULT STEP-SIZE AND SCAN DIRECTION PARAMETERS
530 MO%=49:ST%=2:DI%=1:REM HALF-STEP, HIGH TO LOW ENERGY SCAN
532 REM
540 PRINT:PRINT TAB(33)" LASER DYES "
550  PRINT:PRINT TAB(25)"DCM      (600-700 NM)"SPC(5)1
560  PRINT TAB(25)"R6G      (565-640 NM)"SPC(5)2
570  PRINT TAB(25)"R110     (535-590 NM)"SPC(5)3
580  PRINT TAB(25)"MD631    (590-670 NM)"SPC(5)4
590  PRINT TAB(25)"PY2      (680-840 NM)"SPC(5)5
600  PRINT TAB(25)"S9M      (850-960 NM)"SPC(5)6
610 PRINT:PRINT TAB(25)"ESCAPE            "SPC(5)8
620 PRINT:INPUT "ENTER DYE NUMBER: ";B2%
630 IF B2%=8 GOTO 1500
640  ON  B2%  GOSUB  3000,3100,3200,3300,3400,3500,3600
642 REM
644 REM SET-UP STEPPER MOTOR PARAMETERS
646 REM
650 PRINT:INPUT "ENTER STEP-SIZE (F,H) FULL OR HALF: ";SS$
660  IF  SS$="H" THEN ST%=2:MO%=49
670  IF  SS$="F" THEN ST%=1:MO%=57
680 PRINT:INPUT "ENTER NUMBER OF STEPS PER POINT: ";SP%
690 PRINT:PRINT "SCAN DIRECTIONS LOW-HIGH (L), HIGH-LOW (H) ENERGY"
700 INPUT "ENTER SCAN DIRECTION (L,H): ";SD$
710 IF SD$="H" THEN DI%=1
720 IF SD$="L" THEN DI%=0:MO%=MO%-16
722 REM
724 REM SET-UP BIREFRINGENT FILTER SCAN RANGE
726 REM
730 PRINT CHR$(147):PRINT:PRINT TAB(35)DY$
740 PRINT TAB(30)"BIREFRINGENT ANGLES"
750  PRINT TAB(20)" MIN"SPC(5)NA;SPC(13)" MAX"SPC(5)XA
760 PRINT:PRINT TAB(32)"WAVELENGTHS (A)"
770  PRINT TAB(20)" MIN"SPC(5)NW;SPC(10)" MAX"SPC(5)XW
780 PRINT:INPUT "ENTER INITIAL BIREFRINGENT FILTERS SETTING";AI
790 PRINT:INPUT "ENTER FINAL BIREFRINGENT FILTER SETTING";AF
800 IF (AI<NA)OR(AI>XA)GOTO 1400
810 IF (DI%=1)AND(AF<AI) GOTO 1450
820 IF (DI%=0)AND(AF>AI) GOTO 1450
830 IF (AF<NA)OR(AI>XA) GOTO 1400
832 REM
834 REM CALCULATE WAVELENGTHS OF SCAN
836 REM
840   WI=C0+C1*AI+C2*AI^2+C3*AI^3+C4*AI^4
```

```
850  WF=C0+C1*AF+C2*AF^2+C3*AF^3+C4*AF^4
860 PRINT:PRINT TAB(20)" STARTING WAVELENGTH"SPC(8)INT(WI)" A"
870 PRINT:PRINT TAB(20)" FINAL WAVELENGTH"SPC(11)INT(WF)"  A"
872 REM
874 REM CALCULATE INIT. ANGLE, NUMBER OF DATA POINTS AND STEPS
876 REM
880  S1%=INT(ABS(AI-AF)*800)*ST%
890  AI%=INT(AI*1000)
900  DP%=S1%/SP%
910 PRINT:PRINT TAB(20)" NUMBER OF STEPS IN SCAN"SPC(5)S1%
920 PRINT TAB(20)" NUMBER OF DATA POINTS  "SPC(5)DP%
930 PRINT:PRINT:PRINT "HIT ANY KEY TO CONTINUE SET-UP"
940 GET B$:IF B$="" THEN 940
942 REM
992 REM
1000 PRINT CHR$(147):PRINT:PRINT TAB(32)"SET-UP CONTINUED"
1010 PRINT:PRINT TAB(24)" DIGITAL MULTIMETER (DMM) CONTROL"
1020 PRINT:PRINT TAB(30)"DEFAULT DMM PARAMETERS"
1030 PRINT TAB(24)"CHANNEL 9"SPC(11)"CHANNEL 10":PRINT
1040 PRINT TAB(5)"MONITORS     :"SPC(6)B0$SPC(8)B1$
1050 PRINT TAB(5)"VOLT RANGE   :"SPC(6)B2$SPC(8)B3$
1060 PRINT TAB(5)"A/D SPEED    :"SPC(6)B4$SPC(8)B5$
1070 PRINT:PRINT "TO RETAIN THESE SETTINGS, ENTER R"
1080 PRINT:INPUT "TO CHANGE SETTINGS ENTER M,V,A : ";B$
1090 IF B$="M" THEN GOSUB 1700
1100 IF B$="V" THEN GOSUB 1800
1110 IF B$="A" THEN GOSUB 1750
1120 IF B$="R" GOTO 1140
1130 PRINT CHR$(147):GOTO 1010
1132 REM
1134 REM SET UP COMMAND STRINGS FOR DIGITAL MULTIMETERS
1136 REM
1140  C0$=LEFT$(B2$,2)+LEFT$(B4$,2)+"T2"
1150  C1$=LEFT$(B3$,2)+LEFT$(B5$,2)+"T2"
1152 REM
1154 REM  SETUP DISK-DRIVE I/O
1156 REM
1160 PRINT CHR$(147):PRINT:PRINT TAB(31)" DISK FILE CONTROL"
1170 PRINT:INPUT "DO YOU WANT TO STORE PAS DATA ON DISK?: ";Z$:PRINT
1180 IF Z$="N" GOTO 1230
1190 INPUT "ENTER NAME OF SPECTRUM (WITHOUT AN EXTENTION)";Z$
1200 IF LEN(Z$)>12 THEN PRINT "NAME TOO LONG, RE-":GOTO 1050
1202 REM DISKFILES TO BE OPENNED ARE D0$ AND D1$ ON DRIVE 1
1210  D0$="1:"+Z$+".SPE,S,W":D1$="1:"+Z$+".BKG,S,W"
1212 REM SET DISK I/O FLAG TRUE
1220  DD%=-1
1222 REM
1224 REM SETUP LOCKIN TIME CONSTANT
1226 REM
1230 PRINT:PRINT:PRINT TAB(33)" LOCK-IN CONTROL"
1232 REM
```

```
1234 REM SET-UP CONSTANT MULTIPLIERS FOR DMM DATA
1240 IF LEFT$(B2$,2)="R1" THEN Z1=1000000:GOTO 1280
1250 IF LEFT$(B2$,2)="R2" THEN Z1=10000:GOTO 1280
1260 IF LEFT$(B2$,2)="R3" THEN Z1=1000:GOTO 1280
1270 IF LEFT$(B2$,2)="R4" THEN Z1=100
1280 IF LEFT$(B3$,2)="R1" THEN Z2=1000000:GOTO 1330
1290 IF LEFT$(B3$,2)="R2" THEN Z2=10000:GOTO 1330
1300 IF LEFT$(B3$,2)="R3" THEN Z2=1000:GOTO 1330
1310 IF LEFT$(B3$,2)="R4" THEN Z2=100:GOTO 1330
1320  Z1=10:Z2=10
1324 REM SET LOCK-IN TIME CONSTANT
1326 REM
1330 PRINT:INPUT "ENTER LONGEST LOCK-IN TIME CONSTANT (SEC) :";TC
1332 REM
1340 GOTO 1500
1392 REM
1394 REM
1396 REM
1400 PRINT CHR$(147):PRINT:PRINT TAB(37)" ERROR"
1410 PRINT:PRINT TAB(27)"OUT OF RANGE  OF DYE: ";DY$
1420 PRINT:GOTO 760
1450 PRINT CHR$(147):PRINT:PRINT TAB(37)" ERROR"
1460 PRINT:PRINT TAB(22)"MOTOR STEPPING IN OPPOSITE DIRECTION"
1470 PRINT:GOTO 760
1500 RETURN
1692 REM
1694      REM      **********************************************************
1696 REM
1698 REM
1700 PRINT CHR$(147):PRINT:PRINT TAB(28)"VALID DEVICES MONITORED"
1701  Z$="N"
1702 PRINT:PRINT TAB(10)"MODEL 124A LOCK-IN AMPLIFIER"SPC(5)1
1704 PRINT TAB(10)"MODEL 128A LOCK-IN AMPLIFIER"SPC(5)2
1706 PRINT TAB(10)"MODEL 210 PYRO. POWER METER "SPC(5)3:PRINT
1708 INPUT "ENTER CHANNEL NUMBER (9-10) : ";B2%
1709 IF(B2%<9)OR(B2%>10) THEN PRINT "INCORRECT CH., RE-";:GOTO 1708
1710 INPUT "ENTER VALID DEVICE NUMBER  : ";B3%
1711 IF(B3%<1)OR(B3%>3)THEN PRINT "INVALID DEVICE , RE-";:GOTO 1710
1716 REM
1718 IF(B2%=9)AND(B3%=1)THEN B0$=Q0$
1720 IF(B2%=9)AND(B3%=2)THEN B0$=Q1$
1722 IF(B2%=9)AND(B3%=3)THEN B0$=Q2$
1724 REM
1726 IF(B2%=10)AND(B3%=1)THEN B1$=Q0$
1728 IF(B2%=10)AND(B3%=2)THEN B1$=Q1$
1730 IF(B2%=10)AND(B3%=3)THEN B1$=Q2$
1732 IF Z$="Y" GOTO 1745
1734 PRINT:INPUT "DO YOU WANT TO CHANGE THE OTHER CHANNEL? ";Z$
1736 IF Z$="N" GOTO 1745
1738 PRINT:INPUT "ENTER DEVICE # FOR SECOND CHANNEL: ";B3%
1740 IF(B2%=9)THEN B2%=10:GOTO 1726
```

```
1742 IF(B2%=10)THEN B2%=9:GOTO 1718
1744 REM
1745 RETURN
1750 PRINT CHR$(147):PRINT:PRINT TAB(28)"VALID A/D CONVERSION SPEEDS"
1752 PRINT:PRINT TAB(25)"SLOW (395 MS/CONV)"SPC(10)1
1754 PRINT TAB(25)"MEDIUM (45 MS/CONV)"SPC(9)2
1756 PRINT TAB(25)"FAST ( 7 MS/CONV)"SPC(11)3
1758 Z$="N":PRINT
1760 INPUT "ENTER CHANNEL NUMBER (9,10) :";B2%
1762 PRINT:INPUT "ENTER CONVERSION SPEED NO. :";B3%
1764 IF(B2%=9)AND(B3%=1)THEN B4$=S0$:GOTO 1780
1766 IF(B2%=9)AND(B3%=2)THEN B4$=S1$:GOTO 1780
1768 IF(B2%=9)AND(B3%=3)THEN B4$=S2$:GOTO 1780
1770 IF(B2%=10)AND(B3%=1)THEN B5$=S0$:GOTO 1780
1776 IF(B2%=10)AND(B3%=2)THEN B5$=S1$:GOTO 1780
1778 IF(B2%=10)AND(B3%=3)THEN B5$=S2$:GOTO 1780
1779 PRINT "ERROR RE-";:GOTO 1760
1780 IF Z$="Y"GOTO 1790
1782 PRINT:INPUT "DO YOU WANT TO CHANGE THE OTHER CHANNEL ";Z$
1784 IF Z$="N" GOTO 1790
1786 IF B2%=9 THEN B2%=10:GOTO 1762
1788 IF B2%=10 THEN B2%=9:GOTO 1762
1790 RETURN
1792 REM
1794 REM
1796 REM
2950 REM
2960 REM DYE CALIBRATION ROUTINES
2970 REM
2980 REM **** DCM SUBROUTINE ****
2990 REM COEFFICIENTS FOR FITTING POLYNOMIAL
3000 C0=7239.985:C1=-1313.282
3010 C2=380.006 :C3=-44.216869:C4=2.176476
3020 REM MAXIMUM AND MINIMUM BIREFRINGENT FILTER ANGLES
3030 XA=10.5:NA=5.0
3040 REM MAXIMUM AND MINIMUM WAVELENGTH
3050 XW=7142:NW=5966
3060 DY$=" DCM"
3070 RETURN
3080 REM **** R6G SUBROUTINE ****
3090 REM COEFFICIENTS FOR FITTING POLYNOMIAL
3100 C0=5325.434: C1=-21.240763
3110 C2=42.625750: C3=-2.724004: C4=0.017256
3120 REM MAX. AND MIN. BIREFRINGENT FILTER ANGLES
3130 XA=7.25:NA=3.5
3140 REM MAX. AND MIN. WAVELENGTH
3150 XW=6476.0:NW=5660.5
3160 DY$=" R6G"
3170 RETURN
3180 REM **** RH110 SUBROUTINE ****
3190 REM COEFFICIENTS
```

```
3200 C0=0.0: C1=0.0
3210 C2=0.0: C3=0.0: C4=0.0
3220 REM MAX. AND MIN. BIREFRINGENT FILTER ANGLES
3230  XA=4.75:NA=2.75
3240 REM MAX. AND MIN. WAVELENGTH
3250  XW=5913:NW=5566
3260 DY$=" RH110"
3270 RETURN
3280 REM **** MD631 SUBROUTINE ****
3290 REM COEFFICIENTS
3300 C0=0.0: C1=0.0
3310 C2=0.0: C3=0.0: C4=0.0
3320 REM MAX. AND MIN. BIREFRINGENT FILTER ANGLES
3330  XA=20.0:NA=0.0
3340 REM MAX. AND MIN. WAVELENGTH
3350  XW=9999.0:NW=0.0
3360 DY$=" MD631"
3370 RETURN
3380 REM **** PY2 SUBROUTINE ****
3390 REM COEFFICIENTS
3400 C0=0.0: C1=0.0
3410 C2=0.0: C3=0.0: C4=0.0
3420 REM MAX. AND MIN. BIREFRINGENT FILTER ANGLES
3430  XA=10.75:NA=2.75
3440 REM MAX. AND MIN. WAVELENGTH
3450  XW=5913:NW=5566
3460 DY$=" PY 2 "
3470 RETURN
3480 REM **** S 9 M SUBROUTINE ****
3490 REM COEFFICIENTS
3500 C0=0.0: C1=0.0
3510 C2=0.0: C3=0.0: C4=0.0
3520 REM MAX. AND MIN. BIREFRINGENT FILTER ANGLES
3530  XA=12.0:NA=0.0
3540 REM MAX. AND MIN. WAVELENGTH
3550  XW=9999.0:NW=0.0
3560 DY$=" S9M  "
3570 RETURN
3580 REM ****                    ****
3590 REM COEFFICIENTS
3600 C0=0.0: C1=0.0
3610 C2=0.0: C3=0.0: C4=0.0
3620 REM MAX. AND MIN. BIREFRINGENT FILTER ANGLES
3630  XA=12.0:NA=0.0
3640 REM MAX. AND MIN. WAVELENGTH
3650  XW=9999.0:NW=0.0
3660 DY$="      "
3670 RETURN
3680 REM
4900 REM
4910      REM      ************************************************************
```

```
4920 REM
4930 REM  DATA COLLECTION SUBROUTINE
4940 REM
4950 REM      THIS SUBROUTINE COLLECTS DATA FROM DMM'S ON CHANNELS 9
4960 REM  AND 10, STEPS THE STEPPER MOTOR, AND STORES THE DATA ON DISK-
4970 REM
4980 REM  FILES D0$ & D1$ ACCORDING TO THE SET-UP PROCEDURE.
4990 REM
5000 PRINT CHR$(147):PRINT:PRINT TAB(30)" P.A. DATA COLLECTION"
5010 REM
5020 REM OPEN DMM CHANNELS & PRINT COMMAND STRING
5030 REM
5040 OPEN 2,9:PRINT# 2,C0$
5050 OPEN 3,10:PRINT# 3,C1$
5060 REM
5070 REM OPEN DISKFILES IF NECESSARY
5080 REM
5090 IF NOT DD% GOTO 5210
5100 PRINT:PRINT "INSERT DATA DISKETTE INTO DRIVE 1"
5110 PRINT:PRINT "HIT ANY KEY TO BEGIN DATA COLLECTION"
5120 GET B$:IF B$="" THEN 5120
5130 REM OPEN DISKFILES
5140 IF(B0$=Q0$)AND(B1$<>Q0$)THEN OPEN 4,8,2,D0$:OPEN 5,8,3,D1$:GOTO 5210
5150 IF(B1$=Q0$)AND(B0$<>Q0$)THEN OPEN 4,8,2,D1$:OPEN 5,8,3,D0$:GOTO 5210
5160 IF(B0$=Q1$)AND(B1$=Q2$)THEN OPEN 4,8,2,D0$:OPEN 5,8,3,D1$:GOTO 5210
5170 IF(B1$=Q1$)AND(B0$=Q2$)THEN OPEN 4,8,2,D1$:OPEN 5,8,3,D0$:GOTO 5210
5180 REM
5190 REM CLEAR SCREEN AND BEGIN DATA COLLECTION
5200 REM
5210 PRINT CHR$(147):PRINT:PRINT:PRINT:PRINT:PRINT
5220 PRINT TAB(26)" DATA COLLECTION IN PROGRESS":PRINT
5230 PRINT TAB(10)" SCAN WAVELENGTHS: "SPC(5)INT(WI)"A"SPC(5)INT(WF)" A"
5240 PRINT:PRINT TAB(10)"TO ABORT SCAN, HIT ESC KEY"
5250 REM
5260 REM WRITE CONTROL BLOCK ON DISKFILES
5270 REM
5280 IF NOT DD% GOTO 5470
5290 REM
5300 REM WRITE INITIAL BIREFRINGENT ANGLE  AI%
5310 REM
5320 REM     DIRECTION FLAG                  DI%
5330 REM     STEP-SIZE FLAG                  ST%
5340 REM     STEPS PER DATA POINT            SP%
5350 REM     NUMBER OF DATA POINTS           DP%
5360 REM
5370 PRINT# 4,AI%:PRINT# 5,AI%:REM WRITE AI% TO DISKFILES
5380 PRINT# 4,DI%:PRINT# 5,DI%:REM WRITE DI% TO DISKFILES
5390 PRINT# 4,ST%:PRINT# 5,ST%:REM WRIT ST% TO DISKFILES
5400 PRINT# 4,SP%:PRINT# 5,SP%:REM WRITE SP% TO DISKFILES
5410 PRINT# 4,DP%:PRINT# 5,DP%:REM WRITE DP% TO DISKFILES
5420 REM
```

```
5430    REM        **********************
5440 REM  *  DATA COLLECTION LOOP *
5450    REM        **********************
5460 REM
5470 FOR I=1 TO DP%
5480  PRINT# 2,"?"
5490  INPUT# 2,X1
5500  PRINT# 3,"?"
5510  INPUT# 3,X2
5520  X1%=INT(X1*Z1)
5530  X2%=INT(X2*Z2)
5540 IF DD% THEN PRINT# 4,X1%:PRINT# 5,X2%
5550 FOR J=1 TO SP%
5560  POKE 59456,0:POKE 59426,219:POKE 59427,52
5570  POKE 59427,60:POKE 59456,4:POKE 59426,MO%
5580  POKE 59427,52:POKE 59426,MO%+1:POKE 59427,60
5590 NEXT J
5600  T1=TI
5610 GET B$:IF B$=CHR$(27) GOTO 5670
5620  T2=TI:IF  ABS(T2-T1)/60<TC  GOTO 5620
5630 NEXT I
5640 REM
5650 REM CLOSE ALL THE FILES
5660 REM
5670 IF DD% THEN CLOSE 4:CLOSE 5
5680 REM
5690 CLOSE 2:CLOSE 3
5700 REM
5710 REM  END OF SCAN
5720 REM
5730 RETURN
5740 REM
6940       REM        ************************************************************
6950 REM
6960 REM    THIS ROUTINE PERMITS THE USER TO PRE-SET THE BIREFRINGENT
6970 REM  FILTER OF THE DYE-LASER. ALL THE FEATURES OF THE STEPPER MOTOR
6980 REM  (I.E. SLEW,DIRECTION,AND STEP-SIZE) ARE AVAILABLE.
6990       REM        ************************************************************
7000 PRINT  CHR$(147)
7010 REM SET UP STEPPER TO RECEIVE A COMMAND
7020 REM
7030 POKE 59456,0:REM   SET ATN LOW
7040 POKE 59426,219:REM   ADDRESS THE STEPPER
7050 POKE 59427,52:REM SET DAV LOW
7060 REM
7070 REM TERMINATE ADDRESSING MODE, PREPARE STEPPER FOR COMMAND
7080  POKE  59427,60:POKE  59456,4:POKE  59426,255:POKE  59427,52
7090 REM
7100 PRINT TAB(28)" MOTOR CONTROL ROUTINE"
7110 PRINT:PRINT
7120 PRINT  TAB(34)"COMMANDS"
```

```
7130 PRINT
7140 PRINT TAB(14)"SLEW MOTOR CW "SPC(10)1
7150 PRINT TAB(14)"SLEW MOTOR CCW"SPC(10)2
7160 PRINT TAB(14)"STEPPING MODE "SPC(10)3
7170 PRINT TAB(14)"EXIT ROUTINE  "SPC(10)4
7180 PRINT:PRINT:PRINT "ENTER COMMAND NUMBER"
7190 INPUT B2%
7200 IF B2%=4 GOTO 7290
7210 IF (B2%<1)OR(B2%>4) GOTO 7250
7220 ON B2% GOSUB 7320,7390,7430
7230 PRINT CHR$(147)
7240 GOTO 7100
7250 REM ERROR IN COMMAND INPUT
7260 PRINT "ILLEGAL COMMAND NUMBER: RE-ENTER INPUT"
7270 GOTO 7190
7280 REM END OF ROUTINE
7290  POKE 59427,60
7300 RETURN
7310 REM SLEW MOTOR CW
7320  POKE 59426,16
7340 PRINT "HIT ANY KEY TO TERMINATE SLEW"
7350 GET B$:IF B$="" THEN 7350
7360  POKE 59426,255
7370 RETURN
7380 REM SLEW MOTOR CCW
7390  POKE 59426,1
7400 PRINT "HIT ANY KEY TO TERMINATE SLEW"
7410 GET B$:IF B$="" THEN 7410
7420  POKE 59426,255
7430 RETURN
7440 PRINT CHR$(147)
7450 PRINT:PRINT TAB(22)" STEPPING MODE"
7460 PRINT:PRINT TAB(25)"COMMANDS":PRINT
7470 PRINT TAB(18)"HALF STEP CCW "SPC(10)1
7480 PRINT TAB(18)"HALF STEP CW  "SPC(10)2
7490 PRINT TAB(18)"FULL STEP CCW "SPC(10)3
7500 PRINT TAB(18)"FULL STEP CW  "SPC(10)4
7510 PRINT TAB(18)"EXIT ROUTINE  "SPC(10)5
7520 PRINT:PRINT "ENTER COMMAND NUMBER"
7530 INPUT B2%
7540 IF (B2%<1)OR(B2%>4) GOTO 7710
7550 IF B2%=1 THEN CD%=33
7560 IF B2%=2 THEN CD%=49
7570 IF B2%=3 THEN CD%=41
7580 IF B2%=4 THEN CD%=57
7590 PRINT "ENTER THE NUMBER OF STEPS"
7600 INPUT SP
7610 PRINT "HIT ANY KEY TO INITIATE STEPPING"
7620 GET B$:IF B$="" THEN 7620
7630 FOR I=1 TO SP
7640  POKE 59426,CD%+1
```

```
7650 POKE 59426,CD%
7660 NEXT I
7670 PRINT "DO YOU WISH TO STEP THE MOTOR FURTHER IN THIS MODE"
7680 INPUT B$
7690 IF B$="Y" GOTO 7590
7700 GOTO 7440
7710 RETURN
```

APPENDIX 2

- Listing of Photoacoustic Data Analysis Programs, PAS and PASCON

Nicolet Fortran photoacoustic data transfer and analysis programs.

```
C      ************************************************************
C
C           PROGRAM : PAS
C
C           VERSION 6 (10/03/88)
C
C           by M. G. SOWA
C
C     The Photoacoustic AnalySis program is used to display, plot, and manipulate
C  photoacoustic data. The data can be retrieved from an existing file on the
C  NICOLET disk drive or transfered from the SuperPET using the RS232-B port
C  of the Nicolet.
C
C      ************************************************************
C
C  * VARIABLE DICTIONARY (PA related variables)*
C     XxMIN    (x=S,B) :  minimum X axis value for Sample or Background Spectrum.
C     XxMAX      ""    :  maximum                    ""
C     XxSTEP     ""    :  X axis increment           ""
C     IYxMIN     ""    :  minimum Y axis             ""
C     IYxMAX     ""    :  maximum Y axis             ""
C     IxPNTS     ""    :  number of data points      ""
C     IxDAT      ""    :  Sample or Background data points
C      ************************************************************
C  DECLARATION OF VARIABLES
C
C  declare Photoacoustic Data Variables
C
      REAL XSMIN,XSMAX,XSSTEP
C
      REAL XBMIN,XBMAX,XBSTEP
C
      INTEGER ISPNTS,IYSMIN,IYSMAX,ISDAT(8192)
C
      INTEGER IBPNTS,IYBMIN,IYBMAX,IBDAT(8192)
C
C  declare Plotting and Display Variables
C
     REAL XLEN,YLEN,FXF,LXF,STEP
C
     REAL FXFS,LXFS,FXFB,LXFB
C
      INTEGER IFY,ILY,IFYS,ILYS,IFYB,ILYB,IBUF(8192)
```

```
C
      LOGICAL ERROR,SBECK,BBECK,SSPEC,BSPEC
C
       CHARACTER CMD*6,CH*2
C
        CHARACTER XTIT*12,YTIT*9,TITLE*20
C
        CHARACTER AXS*2,TIT*2,PAG*2
C
C
C       **********************************************
C
C  BEGIN PROGRAM
C
C   INITIALIZE PLOTTING AND DISPLAY VARIABLES
C
       XLEN=7.0
       YLEN=5.0
C
       YTIT='INTENSITY'
       TITLE=' '
C
       AXS='YS'
       PAG='YS'
       TIT='NO'
C
       FXF=0.0
       LXF=0.0
       IFY=0
       ILY=0
C
C    INITIALIZE FLAGS
C
      SSPEC = .FALSE.
      BSPEC = .FALSE.
      SBECK = .FALSE.
      BBECK = .FALSE.
C
C    INITIALIZE MANIPULATION VARIABLES
C
       FCS =1.0
       FCB =1.0
       IADD=0
C
C  CLEAR THE RASTER
C
   1  CALL BCLEAR
       CALL BREGS(0,40)
      CALL BWIPE
       DO 10 I=1,40
        PRINT *,
```

```
   10  CONTINUE
C
C  PRINT TITLE AND ENTER COMMAND MODULE
C
       WRITE(*,1000)
      PRINT *,
       WRITE(*,1002)
       WRITE(*,1003)
       WRITE(*,1004)
       WRITE(*,1006)
       WRITE(*,1008)
       WRITE(*,1010)
       WRITE(*,1012)
       WRITE(*,1013)
       WRITE(*,1014)
C
 1000  FORMAT(' ',15X,'PHOTOACOUSTIC ANALYSIS PROGRAM')
 1002   FORMAT('0',5X,'GDx : Get Data file from D0',6X,'(x=S,B)')
 1003   FORMAT(' ',5X,'PDx : Put Data file to   D0',6X,'(x=S,B)')
 1004   FORMAT(' ',5X,'DSx : Display Data file    ',6X,'(x=S,B)')
 1006   FORMAT(' ',5X,'PLx : Plot Data file       ',6X,'(x=S,B)')
 1008   FORMAT(' ',5X,'GRx : Get Data file from RS232B',2X,'(x=S,B)')
 1010   FORMAT(' ',5X,'RAS : Ratio S vs B')
 1012   FORMAT(' ',5X,'ADD : Add S and B')
 1013   FORMAT(' ',5X,'MEN : Display this menu')
 1014   FORMAT(' ',5X,'MON : Return to monitor')
C
      PRINT *,
    2  WRITE(*,1102)
      READ (*,1104) CMD
 1102   FORMAT(' ',5X,'Enter command: ')
 1104   FORMAT(A6)
C
C  DETERMINE THE COMMAND
C
     IF(CMD.EQ.'GDS')GOTO 100
     IF(CMD.EQ.'GDB') GOTO 102
C
     IF(CMD.EQ.'PDS')GOTO 104
     IF(CMD.EQ.'PDB')GOTO 106
C
     IF(CMD.EQ.'GRS')GOTO 110
     IF(CMD.EQ.'GRB')GOTO 112
C
     IF(CMD.EQ.'DSS') GOTO 120
     IF(CMD.EQ.'DSB')GOTO 122
C
     IF(CMD.EQ.'PLS')GOTO 130
     IF(CMD.EQ.'PLB')GOTO 132
C
     IF(CMD.EQ.'RATIO')GOTO 140
```

```
      IF(CMD.EQ.'RAS')GOTO 140
      IF(CMD.EQ.'ADD')GOTO 142
     IF(CMD.EQ.'ZERO')GOTO 144
C
      IF(CMD.EQ.'PAG')GOTO 160
      IF(CMD.EQ.'AXS')GOTO 160
      IF(CMD.EQ.'TIT')GOTO 160
      IF(CMD.EQ.'XSL')GOTO 162
      IF(CMD.EQ.'YSL')GOTO 164
      IF(CMD.EQ.'FCS')GOTO 166
      IF(CMD.EQ.'FCB')GOTO 168
C
      IF(CMD.EQ.'FXF')GOTO 170
      IF(CMD.EQ.'LXF')GOTO 172
      IF(CMD.EQ.'FYA')GOTO 174
      IF(CMD.EQ.'LYA')GOTO 176
      IF(CMD.EQ.'ASS')GOTO 178
      IF(CMD.EQ.'ASB')GOTO 180
C
     IF(CMD.EQ.'MEN')GOTO 1
     IF(CMD.EQ.'MON')GOTO 99
C
      PRINT *,'INVALID COMMAND !'
C
     GOTO 2
C
C        **********************************************
C
C  GET SAMPLE FILE FROM DISK
C
  100   WRITE(*,1110)
 1110   FORMAT('0',5X,'GET SPECTRUM FROM DISK D0')
C
     CALL GETSPE(ISPNTS,ISDAT,IYSMIN,IYSMAX,
    #            XSMIN,XSMAX,XSSTEP,SBECK,ERROR)
C
    IF (ERROR) THEN
       WRITE(*,1112)
     ELSE
      SSPEC = .TRUE.
      FXFS=XSMIN
      LXFS=XSMAX
      IFYS=IYSMIN
      ILYS=IYSMAX
     FXF =FXFS
     LXF =LXFS
     IFY =IFYS
     ILY =ILYS
       WRITE(*,1114)
    ENDIF
C
```

```
 1112  FORMAT(' ',5X,'SPECTRUM UNSUCCESSFULLY LOADED!')
 1114   FORMAT(' ',5X,'SPECTRUM LOADED!')
C
      GOTO 2
C
C        ************************************************
C
C  GET BACKGROUND FILE FROM DISK
C
  102    WRITE(*,1110)
C
       CALL GETSPE(IBPNTS,IBDAT,IYBMIN,IYBMAX,
     #            XBMIN,XBMAX,XBSTEP,BBECK,ERROR)
C
C
      IF (ERROR) THEN
          WRITE(*,1112)
      ELSE
        BSPEC = .TRUE.
        FXFB=XBMIN
        LXFB=XBMAX
        IFYB=IYBMIN
        ILYB=IYBMAX
          WRITE(*,1114)
      ENDIF
C
      GOTO 2
C
C
C        ************************************************
C
C STORE SPECTRUM ON DISK
C     SAMPLE
 104 IF(SSPEC)THEN
C
      CALL PUTSPE(ISPNTS,ISDAT,XSMIN,XSMAX,XSSTEP,SBECK)
C
    ENDIF
C
    GOTO 2
C
C        ************************************************
C    BACKGROUND
 106 IF(BSPEC)THEN
C
      CALL PUTSPE(IBPNTS,IBDAT,XBMIN,XBMAX,XBSTEP,BBECK)
C
    ENDIF
C
    GOTO 2
C
```

```
C          **************************************************
C
C  GET SPECTRUM FROM RS232 PORT B
C     SAMPLE
  110 CALL RECEIV(ISPNTS,ISDAT,IYSMIN,IYSMAX,
     #          XSMIN,XSMAX,XSSTEP,SBECK,ERROR)
C
     IF(ERROR)THEN
        WRITE(*,1112)
     ELSE
      SSPEC=.TRUE.
       FXFS = XSMIN
       LXFS = XSMAX
       IFYS = IYSMIN
       ILYS = IYSMAX
      FXF  = FXFS
      LXF  = LXFS
      IFY  = IFYS
      ILY  = ILYS
        WRITE(*,1114)
     ENDIF
C
     GOTO 2
C
C          **************************************************
C    BACKGROUND
  112 CALL RECEIV(IBPNTS,IBDAT,IYBMIN,IYBMAX,
     #          XBMIN,XBMAX,XBSTEP,BBECK,ERROR)
C
     IF(ERROR)THEN
        WRITE(*,1112)
     ELSE
      BSPEC=.TRUE.
       FXFB = XBMIN
       LXFB = XBMAX
       IFYB = IYBMIN
       ILYB = IYBMAX
        WRITE(*,1114)
     ENDIF
C
     GOTO 2
C
C          **************************************************
C
C  DISPLAY SAMPLE FILE
C
  120  IF(SSPEC) THEN
C
       CALL BREGS(0,7)
      CALL BCLEAR
      CALL BCOLOR('LBLUE','BLUE','YELLOW','GREEN')
```

```
C
      IF (SBECK) THEN
        XTIT = 'WAVENUMBERS'
        CALL INBUF(FXFS,LXFS,XSMIN,XSMAX,XSSTEP,STEP,
     #             ISPNTS,IPNTS,ISDAT,IBUF,-1)
        CALL DSPEC(LXFS,FXFS,IFYS,ILYS,IBUF,IPNTS,
     #             XTIT,YTIT)
      ELSE
        XTIT='FILTER ANGLE'
       IF((FXFS.EQ.XSMIN).AND.(LXFS.EQ.XSMAX))THEN
C
         CALL DSPEC(FXFS,LXFS,IFYS,ILYS,ISDAT,
     #             ISPNTS,XTIT,YTIT)
       ELSE
        CALL INBUF(FXFS,LXFS,XSMIN,XSMAX,XSSTEP,
     #             STEP,ISPNTS,IPNTS,ISDAT,IBUF,1)
        CALL DSPEC(FXFS,LXFS,IFYS,ILYS,IBUF,IPNTS,
     #             XTIT,YTIT)
C
       ENDIF
      ENDIF
C
     ENDIF
C
     GOTO 2
C
C       **************************************************
C    BACKGROUND
  122  IF(BSPEC) THEN
C
       CALL BREGS(0,7)
      CALL BCLEAR
      CALL BCOLOR ('LBLUE','BLUE','YELLOW','GREEN')
C
      IF (BBECK) THEN
        XTIT='WAVENUMBERS'
        CALL INBUF(FXFB,LXFB,XBMIN,XBMAX,XBSTEP,
     #             STEP,IBPNTS,IPNTS,IBDAT,IBUF,-1)
        CALL DSPEC(LXFB,FXFB,IFYB,ILYB,IBUF,IPNTS,
     #             XTIT,YTIT)
      ELSE
        XTIT='FILTER ANGLE'
       IF((FXFB.EQ.XSMIN).AND.(LXFB.EQ.XSMAX))THEN
C
         CALL DSPEC(FXFB,LXFB,IFYB,ILYB,IBDAT,
     #             IBPNTS,XTIT,YTIT)
       ELSE
C
        CALL INBUF(FXFB,LXFB,XBMIN,XBMAX,XBSTEP,
     #             STEP,IBPNTS,IPNTS,IBDAT,IBUF,1)
        CALL DSPEC(FXFB,LXFB,IFYB,ILYB,IBUF,IPNTS,
```

```
     #                XTIT,YTIT)
 C
          ENDIF
         ENDIF
 C
       ENDIF
 C
       GOTO 2
 C
 C        ************************************************************
 C
 C   THIS SECTION PLOTS THE SAMPLE FILE ON THE ZETA PLOTTER.
 C
  130  IF(SSPEC)THEN
 C
 C  initialize  plotter
 C
        CALL PLOTS
 C
        IF(PAG.EQ.'YS')THEN
           CALL FDPLOT(8.5,0.,-3.)
        ENDIF
 C
        IF(AXS.EQ.'YS')THEN
         IF (SBECK) THEN
           XTIT = 'WAVENUMBERS'
           CALL PLAXS(LXFS,FXFS,XLEN,YLEN,IFYS,ILYS,
     #                XTIT,YTIT)
         ELSE
           XTIT = 'FILTER ANGLE'
           CALL PLAXS(FXFS,LXFS,XLEN,YLEN,IFYS,ILYS,
     #                XTIT,YTIT)
         ENDIF
        ENDIF
 C
        IF (SBECK) THEN
          CALL INBUF(FXFS,LXFS,XSMIN,XSMAX,XSSTEP,STEP,
     #               ISPNTS,IPNTS,ISDAT,IBUF,-1)
         CALL PLSPEC(LXFS,FXFS,XLEN,YLEN,IFYS,ILYS,
     #              IPNTS,IBUF)
        ELSE
         IF((FXFS.EQ.XSMIN).AND.(LXFS.EQ.XSMAX))THEN
          CALL PLSPEC(FXFS,LXFS,XLEN,YLEN,IFYS,ILYS,
     #                ISPNTS,ISDAT)
         ELSE
          CALL INBUF(FXFS,LXFS,XSMIN,XSMAX,XSSTEP,STEP,
     #               ISPNTS,IPNTS,ISDAT,IBUF,1)
         CALL PLSPEC(FXFS,LXFS,XLEN,YLEN,IFYS,ILYS,
     #               IPNTS,IBUF)
         ENDIF
 C
```

```
        ENDIF
C
      ENDIF
C
      GOTO 2
C
C       ****************************************
C
C  THIS SECTION PLOTS THE BACKGROUND FILE
C
  132  IF(BSPEC)THEN
C
       CALL PLOTS
C
       IF(PAG.EQ.'YS')THEN
          CALL FDPLOT(8.5,0.,-3.)
       ENDIF
C
       IF(AXS.EQ.'YS')THEN
        IF (BSPEC) THEN
          XTIT = 'WAVENUMBERS'
          CALL PLAXS(LXFB,FXFB,XLEN,YLEN,IFYB,ILYB,
     #               XTIT,YTIT)
        ELSE
          XTIT = 'FILTER ANGLE'
          CALL PLAXS(FXFB,LXFB,XLEN,YLEN,IFYB,ILYB,
     #               XTIT,YTIT)
        ENDIF
       ENDIF
C
       IF (BSPEC) THEN
         CALL INBUF(FXFB,LXFB,XBMIN,XBMAX,XBSTEP,STEP,
     #              IBPNTS,IPNTS,IBDAT,IBUF,-1)
         CALL PLSPEC(LXFB,FXFB,XLEN,YLEN,IFYB,ILYB,
     #              IPNTS,IBUF)
       ELSE
        IF((FXFB.EQ.XBMIN).AND.(LXFB.EQ.XBMAX))THEN
         CALL PLSPEC(FXFB,LXFB,XLEN,YLEN,IFYB,ILYB,
     #               IBPNTS,IBDAT)
        ELSE
         CALL INBUF(FXFB,LXFB,XBMIN,XBMAX,XBSTEP,STEP,
     #              IBPNTS,IPNTS,IBDAT,IBUF,1)
         CALL PLSPEC(FXFB,LXFB,XLEN,YLEN,IFYB,ILYB,
     #              IPNTS,IBUF)
        ENDIF
       ENDIF
C
     ENDIF
C
     GOTO 2
C
```

```
C        **************************************************
C
C  THIS SECTION RATIOS THE SAMPLE FILE AGAINST THE BACKGROUND FILE.
C  THE RATIOED SPECTRUM CAN THEN BE DISPLAYED, PLOTTED,
C AND/OR STORED ON DISK.
C
 140 IF((SSPEC).AND.(BSPEC))THEN
C
     IF(ISPNTS.NE.IBPNTS)GOTO 24
     IF(XSMIN.NE.XBMIN)  GOTO 24
     IF(XSMAX.NE.XBMAX)  GOTO 24
C
       PRINT *,'Ratio in progress!'
      IADD=0
       IFYS=20000
        ILYS=-524287
C
       IF(IBMIN.LT.1) IADD=1-IBMIN
C
      DO 20 I=1,ISPNTS
C
        TMP1=FCS*FLOAT(ISDAT(I))
        TMP2=FCB*FLOAT(IBDAT(I)+IADD)
         IBUF(I)=IFIX(TMP1/TMP2)
       IF(IBUF(I).GT.ILYS) ILYS=IBUF(I)
       IF(IBUF(I).LT.IFYS) IFYS=IBUF(I)
C
  20  CONTINUE
C
     CALL BREGS(0,7)
C
     CALL DSPEC(FXFS,LXFS,ISXMIN,ISMAX,ISDAT,ISPNTS,
    #           XTIT,YTIT)
     CALL BDRAW(IBUF,ISPNTS,IFYS,ILYS,0)
C
      PRINT *,
       WRITE(*,1150)
      READ (*,1152) CH
C
 1150    FORMAT(' ',5X,'Abort Ratio (Y/N) : ')
 1152   FORMAT(A2)
C
    IF(CH.EQ.'N')THEN
C
       DO 22 I=1,ISPNTS
         ISDAT(I)=IBUF(I)
  22   CONTINUE
C
      ISXMIN=IFYS
      ISMAX=ILYS
C
```

```
      ELSE
C
        IFYS=ISXMIN
        ILYS=ISMAX
C
      ENDIF
C
       PRINT *,
C
    ENDIF
C
    GOTO 2
C
   24 PRINT *,'Incompatible Sample and Background!'
C
    GOTO 2
C
C       ************************************************************
C
C THIS SECTION ADDS SAMPLE*FCS WITH BACKGROUND*FCB.
C THE SCALING FACTORS FCS AND FCB CAN BE SET IN THE PROGRAM BY
C  ENTERING FCS AND/OR FCB.
C
  142 IF((SSPEC).AND.(BSPEC))THEN
C
      IF(ISPNTS.NE.IBPNTS) GOTO 22
      IF((XSMIN.NE.XBMIN).OR.(XSMAX.NE.XBMAX))GOTO 22
C
        ISMAX=-524287
       ISXMIN= 20000
C
       DO 30 I=1,ISPNTS
C
         TMP1    =FCS*FLOAT(ISDAT(I))
         TMP2    =FCB*FLOAT(IBDAT(I))
         ISDAT(I)=IFIX(TMP1+TMP2)
         IF(ISDAT(I).GT.ISMAX) ISMAX=ISDAT(I)
         IF(ISDAT(I).LT.ISXMIN) ISXMIN=ISDAT(I)
C
   30  CONTINUE
C
      IFYS=ISXMIN
      ILYS=ISMAX
C
    ENDIF
C
    GOTO 2
C
C       ************************************************
C
C    THIS SECTION ZEROES THE SAMPLE FILE
```

```
C
 144  IF(SSPEC)THEN
C
        DO 40 I=1,ISPNTS
          ISDAT(I)=ISDAT(I)-IYSMIN
  40    CONTINUE
C
        IYSMAX=IYSMAX-IYSMIN
        IYSMIN=0
       IFYS =IYSMIN
        ILYS =IYSMAX
C
     ENDIF
C
     GOTO 2
C
C        **********************************************************
C
C   THIS SECTION SETS PLOTTING FLAGS FOR PAGING, AXIS  PLOTTING, AND TITLE PRINTING
C
  160   WRITE(*,1210) CMD
       READ(*,1212) CH
C
 1210    FORMAT(' ',2X,A6,2X,'YS OR NO',5X)
 1212    FORMAT(A2)
C
     IF((CH.EQ.'YS').OR.(CH.EQ.'NO')) THEN
C
       IF(CMD.EQ.'PAG')PAG=CH
       IF(CMD.EQ.'AXS')AXS=CH
       IF(CMD.EQ.'TIT')TIT=CH
C
     ENDIF
C
     GOTO 2
C
C        **********************************************
C
C   THIS SECTION ALTERS THE X SCALE LENGTH IN PLOTS
C
  162   WRITE(*,1220) CMD,XLEN
     READ *, XLEN
C
 1220    FORMAT(' ',2X,A6,2X,F8.2,2X)
C
     GOTO 2
C
C        **********************************************
C   THIS SECTION ALTERS THE Y SCALE LENGTH IN PLOTS
C
  164   WRITE(*,1220) CMD,YLEN
```

```
      READ *,YLEN
C
      GOTO 2
C
C        **************************************************
C   THIS SECTION ALTERS SAMPLE SCALE FACTOR FCS
C
  166   WRITE(*,1220) CMD,FCS
      READ *,FCS
C
      IF (FCS.EQ.0.0) FCS = 1.0
C
      GOTO 2
C
C        **************************************************
C   BACKGROUND SCALE FACTOR
  168   WRITE(*,1220) CMD,FCB
      READ *,FCB
C
      IF (FCB.EQ.0.0) FCB = 1.0
C
      GOTO 2
C
C        **************************************************
C   THIS SECTION ALTERS THE STARTING FILTER ANGLE
C
  170  WRITE(*,1220) CMD,FXF
     READ *,FXF
C
     IF (FXF.NE.0.0) THEN
      FXFS=FXF
      FXFB=FXF
     ENDIF
C
     GOTO 2
C
C        **************************************************
C  ALTERS THE LAST FILTER ANGLE
  172  WRITE(*,1220) CMD,LXF
     READ *,LXF
C
     IF (LXF.NE.0.0) THEN
      LXFS=LXF
      LXFB=LXF
     ENDIF
C
     GOTO 2
C
C        **************************************************
C   SET FIRST Y VALUE FOR DISPLAY
  174 WRITE(*,1230) CMD,IFY
```

```
 1230  FORMAT(' ',2X,A6,2X,I5,2X)
       READ *,IFY
       IFYS=IFY
       IFYB=IFY
C
       GOTO 2
C
C          **************************************************
C SET LAST Y VALUE FOR DISPLAY
  176  WRITE(*,1230)  CMD,ILY
       READ *,ILY
       ILYS=ILY
       ILYB=ILY
C
       GOTO 2
C
C          **************************************************
C AUTOSCALE SPECTRUM
C    SAMPLE
  178 IF(SSPEC)THEN
C
       FXFS=XSMIN
       LXFS=XSMAX
       IFYS=IYSMIN
       ILYS=IYSMAX
C
      ENDIF
C
      GOTO 2
C
C          **************************************************
C  BACKGROUND
  180 IF(BSPEC)THEN
C
       FXFB=XBMIN
       LXFB=XBMAX
       IFYB=IYBMIN
       ILYB=IYBMAX
C
      ENDIF
C
      GOTO 2
C
C          **************************************************
C
   99  CONTINUE
C
       STOP
       END
```

```
C      ************************************************************
C
C            PROGRAM : PASCON
C
C             VERSION 6 (2/04/88)
C
C             M. G. SOWA
C
C      The Photoacoustic Conversion program is used to convert photoacoustic data into
C a format compatible with NIRCAP and FTIR36 software.  In order to convert the
C spectra, the dye laser must first be wavelength calibrated.  An existing calibration
C file can be called from disk, or a new one can be created.  Once the calibration is carried
C out and the PAS data is loaded, the WAVENUMBER CONVERSION process can be initiated.
C Once completed, the converted data can be stored and loaded into NIRCAP or FTIR36
C
C      ************************************************************
C
C DECLARATION OF VARIABLES
C
C  declare Photoacoustic Data Variables
C
      REAL XSMIN,XSMAX,XSSTEP
C
      INTEGER ISPNTS,ISYMIN,ISYMAX,ISDAT(16384)
C
C  declare Cubic Spline Variables
C
      REAL SPLX(50),SPLY(50),SPLA(50),SPLB(50),SPLC(50)
C
     INTEGER ISPL,IOPT
C
C  declare BECKMA Conversion Variables
C
      INTEGER IPNTS,IFRST,ILAST,INX,PINX,IER,IERMS,IBUF(8192)
C
      REAL WAVNUM(8192),WMIN,WMAX,WTEST,TMP1,TMP2,TMP3,SPACE
C
     LOGICAL ERROR,SBECK,SSPEC,SCONV,SCAL,CFILE
C
      CHARACTER CMD*15,FILE*15,CH*1
C
     CHARACTER DYEFIL*15
C
C
      COMMON /SPLDAT/ ISPL,SPLX,SPLY,SPLA,SPLB,SPLC
C
C      ************************************************************
C
C  BEGIN PROGRAM
C
C   INITIALIZE FLAGS
```

```
C
      SSPEC = .FALSE.
      SBECK = .FALSE.
      SCONV = .FALSE.
      SCAL  = .FALSE.
      CFILE = .FALSE.
C
C CLEAR THE RASTER
C
   2  CALL BCLEAR
      CALL BREGS(0,40)
      CALL BWIPE
C
      DO 3 I=1,40
        PRINT *,
   3  CONTINUE
C
C  PRINT TITLE AND ENTER COMMAND MODULE
C
       WRITE(*,1000)
      PRINT *,
       WRITE(*,1002)
       WRITE(*,1004)
       WRITE(*,1006)
       WRITE(*,1008)
       WRITE(*,1010)
       WRITE(*,1012)
       WRITE(*,1014)
       WRITE(*,1016)
       WRITE(*,1018)
C
 1000  FORMAT(' ',17X,'PHOTOACOUSTIC CONVERSION PROGRAM')
 1002   FORMAT('0',17X,'Get Data File from D0       : GDS')
 1004   FORMAT(' ',17X,'Put Data File to   D0       : PDS')
 1006   FORMAT(' ',17X,'Wavelength Calibration      : WAV')
 1008   FORMAT(' ',17X,'Get Calibration File        : GETPAR')
 1010   FORMAT(' ',17X,'Store Calibration File      : STOPAR')
 1012   FORMAT(' ',17X,'Edit Calibration File       : EDPAR')
 1014   FORMAT(' ',17X,'Print Calibration File      : PRT')
 1016   FORMAT(' ',17X,'Convert P.A. file to FTIR   : CONV')
 1018   FORMAT(' ',17X,'Return to Monitor           : MON')
C
     PRINT *,
   4   WRITE(*,1102)
      READ (*,1104) CMD
 1102   FORMAT(' ',5X,'Enter command: ')
 1104   FORMAT(A15)
C
C  DETERMINE THE COMMAND
C
    IF(CMD.EQ.'GDS')GOTO 100
```

```
      IF(CMD.EQ.'PSS')GOTO 104
      IF(CMD.EQ.'PDS')GOTO 104
C
      IF(CMD.EQ.'GETPAR')GOTO 110
      IF(CMD.EQ.'STOPAR')GOTO 112
      IF(CMD.EQ.'PRT')  GOTO 114
      IF(CMD.EQ.'CAL')  GOTO 160
      IF(CMD.EQ.'EDPAR') GOTO 180
      IF(CMD.EQ.'CONV') GOTO 200
      IF(CMD.EQ.'MEN')GOTO 2
      IF(CMD.EQ.'MON')GOTO 99
C
      PRINT *,'INVALID COMMAND !'
C
      GOTO 4
C
C     ************************************************************
C
C  GET SAMPLE FILE FROM DISK
C
  100 WRITE(*,1110)
 1110 FORMAT('0',5X,'GET DATA FILE FROM DISK D0')
C
    CALL GETSPE(ISPNTS,ISDAT,IYSMIN,IYSMAX,XSMIN,XSMAX,XSSTEP,SBECK,ERROR)
C
    IF (ERROR) THEN
       WRITE(*,1112)
    ELSE
     SSPEC = .TRUE.
     IF (SBECK) THEN
      SCONV = .TRUE.
       SCAL  = .TRUE.
     ENDIF
       WRITE(*,1114)
    ENDIF
C
 1112 FORMAT(' ',5X,'File Unsuccessfully Loaded!')
 1114 FORMAT(' ',5X,'SPECTRUM LOADED!')
C
    GOTO 4
C
C     ************************************************************
C
C STORE SPECTRUM ON DISK
C
 104 IF (SSPEC) THEN
C
    CALL PUTSPE(ISPNTS,ISDAT,XSMIN,XSMAX,XSSTEP,SBECK)
C
   ENDIF
C
```

```
      GOTO 4
C
C          ************************************************************
C
C       This section gets a Dye Laser Calibration Parameter file from the disk drive.
C
  110 IF (CFILE) THEN
        WRITE(*,1120) DYEFIL
        WRITE(*,1122)
        READ (*,1124) CH
       IF (CH.EQ.'Y') GOTO 6
       GOTO 4
      ENDIF
C
  1120 FORMAT(' ',5X,'Active Calibration Parameter File :',1X,A15)
  1122 FORMAT(' ',5X,'Use Active File ? (Y/N) : ')
  1124 FORMAT(A1)
C
    6 CALL GETPAR(FILE)
      CFILE = .TRUE.
      DYEFIL=FILE
C
      GOTO 4
C
C          ************************************************************
C
C       This section stores a Dye Laser Calibration File to the disk drive.
C
  112 IF (CFILE) THEN
        CALL STOPAR(DYEFIL)
        ENDIF
C
     GOTO 4
C
C          ************************************************************
C
C       This section prints out the Dye Laser Calibration Parameters to the screen.  If the
C baud rate is 300 bps, the parameters can be listed on the teletype.
C
  114 IF (CFILE) THEN
        CALL PRTPAR(DYEFIL)
        ENDIF
C
     GOTO 4
C
C          ************************************************************
C
C       This section creates or gets a file of wavenumber calibration points for the dye laser
C
  160 PRINT *,
        WRITE(*,1600)
```

```
          PRINT *,
 1600 FORMAT(' ',17X,'WAVELENGTH CALIBRATION OF DYE LASER')
C
     IF(CFILE)THEN
        WRITE(*,1120) DYEFIL
         WRITE(*,1122)
        READ (*,1124) CH
C
      IF(CH.EQ.'N') GOTO 12
C
        WRITE(*,1130)
        READ(*,1124) CH
C
 1130    FORMAT(' ',5X,'Edit Active File? (Y/N) : ')
C
      IF(CH.EQ.'N') GOTO 4
      IF(CH.EQ.'Y') GOTO 180
C
    ENDIF
C
    12 WRITE(*,1140)
       WRITE(*,1142)
      PRINT *,
       WRITE(*,1144)
      READ (*,1124) CH
C
 1140 FORMAT(' ',5X,'Get Existing Calibration File : G')
 1142 FORMAT(' ',5X,'Create New Calibration File   : N')
 1144 FORMAT(' ',5X,'Enter G or N : ')
C
    IF((CH.NE.'G').AND.(CH.NE.'N')) GOTO 12
C
    IF(CH.EQ.'G')GOTO 110
C
    IF(CH.EQ.'N')THEN
        WRITE(*,1600)
       PRINT *,
     CALL GETXY
       PRINT *,
     DYEFIL='NEW'
        WRITE(*,1130)
       READ(*,1124) CH
     IF(CH.EQ.'N') GOTO 190
     CFILE = .TRUE.
     GOTO 180
   ENDIF
C
   GOTO 4
C
C       ************************************************************************
C
```

```
C  edit calibration parameters
C
 180 IF (CFILE) THEN
       CALL PRTPAR(DYEFIL)
       CALL EDPAR
     ENDIF
C
C  select endpoint strategy for cubic spline interpolation
C
 190 IOPT =1
     TMP1 =0.
     TMP2 =0.
C
      WRITE(*,1620)
      WRITE(*,1622)
      WRITE(*,1624)
      WRITE(*,1626)
      WRITE(*,1628)
      WRITE(*,1630)
      WRITE(*,1632)
C
1620 FORMAT('0',20X,'CUBIC SPLINE FITTING PROCEDURE')
1622 FORMAT('0',24X,'ENDPOINT STRATEGIES')
1624 FORMAT(' ',20X,'Specify 2nd Derivatives : Opt 1')
1626 FORMAT(' ',20X,'Constant 2nd Derivatives: Opt 2')
1628 FORMAT(' ',20X,'Linear 2nd Derivatives  : Opt 3')
1630 FORMAT(' ',20X,'Specify 1st Derivatives : Opt 4')
1632 FORMAT('0',5X,'Enter Opt : ')
C
     READ *,IOPT
C
    IF((IOPT.EQ.1).OR.(IOPT.EQ.4))THEN
C
      WRITE(*,1634)
     READ *,TMP1
      WRITE(*,1636)
     READ *,TMP2
C
1634 FORMAT(' ',5X,'Enter derivative at 1st pnt  : ')
1636 FORMAT(' ',5X,'Enter derivative at last pnt : ')
C
    ENDIF
C
C  call spline fitting procedure
C
     CALL SPLFIT(IOPT,TMP1,TMP2)
C
     PRINT *,
      PRINT *,'wavelength calibration complete'
     PRINT *,
C
```

```
      GOTO 4
C
C     ************************************************************
C
C  Convert Spectrum to a format suitable for the FTIR Software.  This involves converting
C Birefringent Filter Angles to Wavenumbers according to the Cubic Spline Calibration
C Parameters.  The Photoacoustic signal is then made linear in wavenumber and converted
C to FTIR36 format
C
  200 IF((SSPEC).AND.(CFILE))THEN
C
       PRINT *,
      PRINT *,'   WAVELENGTH CONVERSION'
C
C  CALCULATE CORRESPONDING WAVENUMBER READING FOR EACH PA DATA POINT
C
       CALL WAVCON(IER,ISPNTS,IFRST,ILAST,XSMIN,XSMAX,XSTEP,WAVNUM)
C
     IF (IER.LT.0)THEN
        WRITE(*,1700)
        WRITE(*,1702)
       ERROR=.TRUE.
    ELSE
       ERROR=.FALSE.
        IERMS=IER/100
       IF(IERMS.EQ.1)THEN
          WRITE(*,1704)
         IER=IER-100
       ENDIF
        IERMS=IER/10
       IF(IERMS.EQ.1)THEN
          WRITE(*,1706)
         IER=IER-10
       ENDIF
        IF(IER.EQ.1)WRITE(*,1708)
    ENDIF
C
C  LINEARIZE DATA IN WAVENUMBERS & WITH APPROPRIATE BECKMA RESOLUTION
C
     IF(IER.EQ.0)THEN
        IF(WAVNUM(IFRST).GT.WAVNUM(ILAST))THEN
          K=ILAST
          DO 30 I=IFRST,ILAST
             IBUF(I)=ISDAT(K)
             K=K-1
30       CONTINUE
       ENDIF
       WMIN=WAVNUM(IFRST)
        WMAX=WAVNUM(ILAST)
         PINX=IFIX((WAVNUM(ILAST)/SPACE)+.5)
         INX=IFIX((WAVNUM(IFRST)/SPACE)+.5)
```

```
          IPNTS=PINX-INX+1
          ISDAT(1)=IBUF(IFRST)
          ISDAT(IPNTS)=IBUF(ILAST)
           J=1
           DO 33 I=IFRST+1,ILAST-1
           PINX=INX
             INX=IFIX((WAVNUM(I)/SPACE)+.5)
          IF(PINX.EQ.INX)GOTO 33
            IF(INX.GT.(PINX+1))THEN
               DO 32 K=PINX+1,INX-1
                 J=J+1
                   ISDAT(J)=IBUF(I-1)
   32         CONTINUE
             ENDIF
               J=J+1
                ISDAT(J)=IBUF(I)
   33    CONTINUE
       ENDIF
C
 1700 FORMAT('0',5X,'P.A. SPECTRUM AND WAVELENGTH CALIBRATION FILE ARE INCOMPATIBLE')
 1702 FORMAT(' ',5X,'CALIBRATION ABORTED')
 1704 FORMAT('0',5X,'ERROR ENCOUNTERED IN SPLINT ROUTINE')
 1706 FORMAT('0',5X,'PA DATA EXTENDS BEYOND CALIBRATION RANGE')
 1708 FORMAT('0',5X,'PA DATA BEGINS PRIOR TO CALIBRATION RANGE')
C
       ENDIF
C
      GOTO 4
C
C        **********************************************************
C
  99  CONTINUE
       STOP
      END
```

- General Subroutines for the PAS and PASCON programs.

```
*****************
*  I/O Routines  *
*****************
```

```
C       ************************************************
C *
C * SUBROUTINE GETSPE
C *
C *     This subroutine gets a Photoacoustic or FTIR - Beckma spectra from disk.
C * The routine is able to determine if the FTIR - Beckma files have been stored
C * in a truncated format using the special put commands PSx (x=S,D,B).
C * The files are assumed to be stored on drive D0.
C *
C       ************************************************
C
      SUBROUTINE GETSPE(IPNTS,IDATA,IYMIN,IYMAX,XMIN,XMAX,XSTEP,BECKMA,ERR)
C
      INTEGER IPNTS,IDATA(1),IYMIN,IYMAX
C
      INTEGER IXMIN,IXMAX,IFSB(352)
C
      REAL XMIN,XMAX,XSTEP
C
      LOGICAL BECKMA,ERR
C
      CHARACTER CHAR*1,FILE*15
C
        DATA  SPACE,HALF,FULL/1.2207,6.25E-4,1.25E-3/
C
C       ************************************************************
C main line
C
      ERR = .TRUE.
      BECKMA = .FALSE.
C
      IXMIN = 1
      IXMAX = 16384
C
      IPNTS = 16384
      ISTEP = 0
C
    2 WRITE(2,1000)
      READ (1,1010) FILE
      WRITE(2,1020) FILE
      READ (1,1030) CHAR
C
    IF (CHAR .EQ. 'Y') THEN
```

```
      CALL DEFINE(13,FILE)
C read in file status block
      READ(13) IFSB(1)
      READ(13) IFSB(2)
C
C       determine if it is an FTIR/BECKMAN file
C
      IF ((IFSB(2).EQ.1234321).OR.(IFSB(2).EQ.342225))THEN
       BECKMA = .TRUE.
C         read in remainder of file status block
        DO 10 I=3,352
         READ(13) IFSB(I)
 10     CONTINUE
C
C set the min. & max. freq. of special put files
C
        IF (IFSB(234) .GT. 0) THEN
          IXMIN = IFSB(234)
          IXMAX = IFSB(235)
         IPNTS = IXMAX - IXMIN
         XMIN  = SPACE * FLOAT(IXMIN)
          XMAX  = SPACE * FLOAT(IXMAX)
        XSTEP = SPACE
       ENDIF
C
     ELSE
C         read in Photoacoustic file status block
       READ(13) IFSB(3)
       READ(13) IFSB(4)
       READ(13) IPNTS
C
       IF (IFSB(3) .EQ. 1) THEN
         XSTEP = FULL * FLOAT(IFSB(4))
       ELSE
         XSTEP = HALF * FLOAT(IFSB(4))
       ENDIF
C
       IF (IFSB(2) .EQ. 1) THEN
          XMIN  = FLOAT(IFSB(1))/1000.0
         XMAX  = FLOAT(IPNTS)*XSTEP + XMIN
       ELSE
          XMAX  = FLOAT(IFSB(1))/1000.0
         XMIN  = XMAX - FLOAT(IFSB(1))*XSTEP
       ENDIF
C
     ENDIF
C
C read in data
C
       IYMAX = 0
       IYMIN = 99999
```

```
        DO 20 I=1,IPNTS
          READ(13) IDATA(I)
            IF (IDATA(I) .EQ. (-524287-1)) IDATA(I) = 0
          IF (IDATA(I) .LT. IYMIN) IYMIN = IDATA(I)
          IF (IDATA(I) .GT. IYMAX) IYMAX = IDATA(I)
  20    CONTINUE
C
      ERR = .FALSE.
C
      CALL IOEXIT
      CALL ENBLKB
C
    ELSE
C
       WRITE(2,1040)
      READ (1,1030) CHAR
     IF (CHAR .EQ. 'Y') GOTO 2
C
    ENDIF
C
C       ************************************************************
C
 1000 FORMAT(' ','Enter Filename : ')
 1010 FORMAT(A15)
 1020 FORMAT(' ','Get file ',A15,'from D0   (Y/N)? : ')
 1030 FORMAT(A1)
 1040 FORMAT(' ','Re-Enter Filename (Y/N)? : ')
C
C       ************************************************************
C
    RETURN
    END
C
C
C       ********************************************************
C *
C * SUBROUTINE PUTSPE
C *
C *     This subroutine writes a Photoacoustic or FTIR - Beckma spectrum to disk.
C *  The routine stores the  FTIR - Beckma files in a truncated format if possible.
C *  The format is consistent with that obtained with the special put commands in
C *  Beckma or FTIR (PSx x=S,D,B etc.).  The spectral files are stored on the D0 drive.
C *
C       ********************************************************
C
    SUBROUTINE PUTSPE(IPNTS,IDATA,XMIN,XMAX,XSTEP,BECKMA)
C
C
     INTEGER IPNTS,IDATA(1),IFSB(352)
C
    REAL XMIN,XMAX,XSTEP
```

```
C
      LOGICAL BECKMA
C
       CHARACTER CHAR*1,FILE*15
C
         DATA  SPACE,HALF,FULL/1.2207,6.25E-4,1.25E-3/
C
C          ************************************************************
C main line
C
     2 WRITE(2,1000)
       READ (1,1010) FILE
       WRITE(2,1020) FILE
       READ (1,1030) CHAR
C
      IF (CHAR .EQ. 'Y') THEN
        CALL ALLOC(12,FILE,1056)
C
C write the BECKMAN/FTIR or Photoacoustic data file to disk
C
       IF (BECKMA) THEN
C          set up file status block
          DO 4 I=11,352
    4       IFSB(I) = -1
C
          IFSB(1) = 64
          IFSB(2) = 342225
          IFSB(3) = 1
          IFSB(4) = 1
          IFSB(5) = 1
          IFSB(6) = 3
          IFSB(7) = 1
          IFSB(8) = 1
          IFSB(9) = 1
          IFSB(10)= 0
          IFSB(15)= 128
          IFSB(16)=64
          IFSB(17)= 1
C
          IXMIN = IFIX(XMIN/SPACE) + 352
          IXMAX = IFIX(XMAX/SPACE) + 352
C
          IFSB(234)= IXMIN
          IFSB(235)= IXMAX
C
C          write the file status block to disk
          DO 6 I=1,352
    6       WRITE(12) IFSB(I)
C
       ELSE
C          write out the Photoacoustic file status block
```

```
          IFSB(1) = IFIX((XMIN*1000))
          IFSB(2) = 1
          IFSB(3) = 0
          IFSB(4) = IFIX((XSTEP/HALF))
          IFSB(5) = IPNTS
C
          IFSB(351) = MOD(IFSB(4),2)
          IF (IFSB(351) .EQ. 0) THEN
            IFSB(3) = 1
            IFSB(4) = IFSB(4)/2
        ENDIF
C
         DO 8 I=1,5
  8        WRITE(12) IFSB(I)
C
      ENDIF
C
C write the data to disk.
C
         DO 20 I=1,IPNTS
           WRITE(12) IDATA(I)
 20      CONTINUE
C
        CALL IOEXIT
        CALL ENBLKB
C
     ELSE
C
        WRITE(2,1040)
        READ (1,1030) CHAR
       IF (CHAR .EQ. 'Y') GOTO 2
C
     ENDIF
C
C       ************************************************************
C
 1000 FORMAT(' ','Enter Filename : ')
 1010 FORMAT(A15)
 1020 FORMAT(' ','Store file ',A15,' to D0  (Y/N)? : ')
 1030 FORMAT(A1)
 1040 FORMAT(' ','Re-Enter Filename (Y/N)? : ')
C
C       ************************************************************
C
    RETURN
    END
C
C
C       ************************************************************
C *
C * SUBROUTINE RECEIVe
```

```
C *
C *      This subroutine receives a Photoacoustic or FTIR/Beckma spectrum from the RS-232 B
C * port.  An appropriate sending program must be running on the machine sending the file.
C *
C       ************************************************************
C
      SUBROUTINE RECEIV(IPNTS,IDATA,IYMIN,IYMAX,XMIN,XMAX,XSTEP,BECKMA,ERR)
C
C
      INTEGER IPNTS,IDATA(1),IYMIN,IYMAX
      INTEGER IXMIN,IXMAX,IFSB(352)
C
      REAL XMIN,XMAX,XSTEP
C
      LOGICAL BECKMA,ERR
C
        DATA  SPACE,HALF,FULL/1.2207,6.25E-4,1.25E-3/
C
C       ************************************************************
C main line
C
C  choose the data port and set the baud rate
C
      CALL SETRATE
C
      ERR = .TRUE.
      BECKMA = .FALSE.
C
       IYMIN = 99999
        IYMAX = (-524287-1)
      IXMIN = 1
       IXMAX = 16384
C
      IPNTS = 16384
     ISTEP = 0
C
      CALL RS232B(IFSB(1))
      CALL RS232B(IFSB(2))
C
C       determine if it is an FTIR/BECKMAN file
C
      IF ((IFSB(2).EQ.1234321).OR.(IFSB(2).EQ.342225))THEN
C       read in remainder of file status block
       DO 10 I=3,352
        CALL RS232B(IFSB(I))
  10  CONTINUE
C
C set the min. & max. freq. of special put files
C
       IF (IFSB(234) .GT. 0) THEN
        IXMIN = IFSB(234)
```

```
          IXMAX = IFSB(235)
          IPNTS = IXMAX - IXMIN
          DO 20 I = 1,IPNTS
            CALL RS232B(IDATA(I))
              IF (IDATA(I).EQ.(-524287-1)) IDATA(I) = 0
            IF (IDATA(I).LT. IYMIN) IYMIN = IDATA(I)
            IF (IDATA(I).GT. IYMAX) IYMAX = IDATA(I)
   20     CONTINUE
         BECKMA=.TRUE.
          XMIN  = SPACE * FLOAT(IXMIN)
          XMAX  = SPACE * FLOAT(IXMAX)
         XSTEP = SPACE
         ERR = .FALSE.
        ELSE
         ERR = .TRUE.
        ENDIF
C
      ELSE
C       read in Photoacoustic file status block
        CALL RS232B(IFSB(3))
        CALL RS232B(IFSB(4))
        CALL RS232B(IPNTS)
C
        DO 30 I=1,IPNTS
          CALL RS232B(IDATA(I))
          IF (IDATA(I).LT. IYMIN) IYMIN = IDATA(I)
          IF (IDATA(I).GT. IYMAX) IYMAX = IDATA(I)
   30   CONTINUE
C
        IF (IFSB(3) .EQ. 1) THEN
          XSTEP = FULL * FLOAT(IFSB(4))
        ELSE
          XSTEP = HALF * FLOAT(IFSB(4))
        ENDIF
C
        IF (IFSB(2) .EQ. 1) THEN
           XMIN  = FLOAT(IFSB(1))/1000.0
          XMAX  = FLOAT(IPNTS)*XSTEP + XMIN
        ELSE
           XMAX  = FLOAT(IFSB(1))/1000.0
          XMIN  = XMAX - FLOAT(IFSB(1))*XSTEP
        ENDIF
C
        ERR = .FALSE.
C
      ENDIF
C
C       ************************************************************
C
    RETURN
    END
```

```
C
C       **********************************************************
C *
C * SUBROUTINE SETRATE
C *
C *     This subroutine sets the RS-232 data port and the baud rate for that particular port.
C *
C       **********************************************************
C
      SUBROUTINE SETRAT
C
C
      INTEGER IBAUD,IBD,ITMP
C
       CHARACTER PORT*1,CHAR*1
C
C       **********************************************************
C main line
C
       PORT = 'B'
       IBAUD= 1200
      IPORT= 2
C
       WRITE(*,1000) PORT
C
    20 WRITE(*,1010) IBAUD
        WRITE(*,1040)
       READ (*,1030) CHAR
C
      IF (CHAR .EQ. 'Y') THEN
          WRITE(*,1050)
        READ *,ITMP
        IF (ITMP.EQ.300) IBAUD = 300
        IF (ITMP.EQ.600) IBAUD = 600
        IF (ITMP.EQ.1200)IBAUD = 1200
        IF (ITMP.EQ.2400)IBAUD = 2400
        IF (ITMP.EQ.4800)IBAUD = 4800
        IF (ITMP.EQ.9600)IBAUD = 9600
        IF (ITMP.NE.IBAUD)WRITE(*,1060)
       GOTO 20
     ENDIF
C
C  set the baud rate
C
       IF (IBAUD.EQ.300) IBD = 1
       IF (IBAUD.EQ.600) IBD = 2
       IF (IBAUD.EQ.1200)IBD = 3
       IF (IBAUD.EQ.2400)IBD = 4
       IF (IBAUD.EQ.4800)IBD = 5
       IF (IBAUD.EQ.9600)IBD = 6
C
```

```
A      SETBDB=623702
A     MEMA IBD
A    SETBDB
C
C
C       ************************************************************
C
 1000 FORMAT('0',5X,'ACTIVE RS-232 PORT : ',A1)
 1010 FORMAT('0',5X,'CURRENT  BAUD RATE : ',I5)
 1030 FORMAT(A1)
 1040 FORMAT(' ','Do you want to change the baud rate   : ')
 1050 FORMAT('0','Enter desired baud rate : ')
 1060 FORMAT('0','Invalid Baud Rate!!')
C
C       ************************************************************
C
    RETURN
    END
C
C       ************************************************************
C       SUBROUTINE RS232B
C         Subroutine reads an integer number from  RS 232 port B.
C       ************************************************************
C
    SUBROUTINE RS232B(INUM)
C
    INTEGER INUM,ITMP,ISGN,IERR
C
     ITMP = 0
    IERR = 0
    ISGN = 0
C
A     ZERM  INUM
A DLOOP,RSINF
A      JMP   DLOOP
A      RSIN
A       SNQ   (215
A     JMP   DONE
A      SNQ   (255
A      JMP   MINUS
A       AMMA  (260
A      ACCM  ITMP
A     JPM   ERROR
A       AMMA  (12
A     JPP   ERROR
A      LAX   (12
A     ZERA
A     MULT
A     INUM
A     JPZ   DOK
A     JMP   ERROR
```

```
A DOK,  TMQAC
A       APMA  ITMP
A       ACCM  INUM
A       JMP   DLOOP
A ERROR,MONM IERR
A       JMP   DLOOP
A MINUS,MONM ISGN
A       JMP   DLOOP
A DONE, MONM ITMP
C
      IF(ISGN.NE.0) INUM = -INUM
C
     RETURN
     END
```

```
*******************
* Graphics Routines *
*******************
```

```
C
C      ******************************************
C
C      SUBROUTINE : DSPEC (Display Spectrum)
C
C     This subroutine displays a spectrum on the screen
C
C      ******************************************
C
C
      SUBROUTINE DSPEC(FXF,LXF,IFY,ILY,IBUF,IPNTS,XTIT,YTIT)
C
C
      REAL FXF,LXF,XTIC,YTIC,YTOP,YBOT
C
      INTEGER IFY,ILY,IBUF(8000),IPNTS
C
       CHARACTER XTIT*12,YTIT*9
C
C
       DATA SEVEN,FOUR/7.0E0,4.0E0/
C
C
C       *****************************************************
C
C  CAL. SCALING FACTORS AND DRAW X&Y AXIS
C
     YBOT=FLOAT(IFY)
     YTOP=FLOAT(ILY)
C
     XTIC=(LXF-FXF)/SEVEN
     YTIC=(YTOP-YBOT)/FOUR
```

```
C
      CALL BAXIS(1.0,1.0,XTIT,12,7,0,FXF,XTIC,0)
      CALL BAXIS(1.0,1.0,YTIT,9,4,1,YBOT,YTIC,0)
C
C DRAW THE DISPLAY BUFFER INTO DISPLAY
C
      CALL BDRAW(IBUF,IPNTS,IFY,ILY,0)
C
C
C     ************************************************************
C
      CALL BPIXEL (0)
C
C
C
C     ************************************************************
C
      RETURN
C
      END
C
C
C     ************************************************************
C
C   SUBROUTINE PLot AXiS
C
C   THIS SUBROUTINE PLOTS THE X AND Y AXIS
C
C     ************************************************************
C
      SUBROUTINE PLAXS(FXF,LXF,XLEN,YLEN,IFY,ILY,XTIT,YTIT)
C
      REAL FXF,LXF,XLEN,YLEN,YBOT,YTOP,XTIC,YTIC
C
      INTEGER IFY,ILY
C
      CHARACTER XTIT*12,YTIT*9
C
C
      YBOT=FLOAT(IFY)
      YTOP=FLOAT(ILY)
C
      YTIC=(YTOP-YBOT)/YLEN
      XTIC=(LXF-FXF)/XLEN
C
C PLOT X AXIS
C
      CALL FAXIS(1.,.5,XTIT,12.,XLEN,0.,FXF,XTIC,4.,2.)
C
C PLOT Y AXIS
C
```

```
        CALL FAXIS(1.,.5,YTIT,9.,YLEN,90.,YBOT,YTIC,4.,2.)
C
C
      RETURN
C
      END
C
C       ************************************************************
C
C       SUBROUTINE:  PLot SPECtrum
C
C      THIS SUBROUTINE PLOTS THE PAS DATA ON THE ZETA PLOTTER.  THIS
C ROUTINE SPECIFICALLY PLOTS THE SIGNAL VS BIREFRINGENT FILTER ANGLE DATA.
C
C       ************************************************************
C
C
      SUBROUTINE PLSPEC(FXF,LXF,XLEN,YLEN,IFY,ILY,IPNTS,IBUF)
C
C
      REAL FXF,LXF,XLEN,YELN,X,Y,XSTEP,YSCALE
C
      INTEGER IFY,ILY,IPNTS,IBUF(8000)
C
C       ************************************************************
C
C BEGIN ROUTINE
C
      XSTEP=XLEN/FLOAT(IPNTS)
      YSCALE=YLEN/FLOAT(ILY-IFY)
C   RESET ORIGIN
       CALL FDPLOT(1.,.5,-3.)
C
      DO 10 I=1,IPNTS
C
        X=FLOAT(I)*XSTEP
        Y=FLOAT(IBUF(I)-IFY)*YSCALE
C
        CALL FDPLOT(X,Y,2.)
C
  10  CONTINUE
C
C   RETRUN PLOTTER PEN TO ORIGIN
C
        CALL FDPLOT(-1.,-.5,-3.)
C
C   END SUBROUTINE
C
     RETURN
C
     END
```

```
C
C
C              ************************************************************
C
C     SUBROUTINE  INBUF
C
C     THIS SUBROUTINE PUTS FTIR/BECKMAN OR PHOTOACOUSTIC DATA INTO A
C  DISPLAY/PLOT BUFFER.  THIS BUFFER CAN BE USED TO WINDOW IN ON CERTAIN
C AREAS OF THE RECORDED DATA.
C
C              ************************************************************
C
C
      SUBROUTINE INBUF(FXF,LXF,XMIN,XMAX,XSTEP,STEP,IPNTS,ICNT,IDAT,IBUF)
C
C
      REAL FXF,LXF,STEP,XMIN,XMAX,XSTEP,XBUF,XDAT1,XDAT2
C
      INTEGER IPNTS,ICNT,IDAT(IPNTS),IBUF(IPNTS),IDIR
C
C
C              ************************************************************
C
C
      J=0
      ICNT=IFIX((LXF-FXF)/XSTEP)
C
      IF(ICNT.GT.8192)THEN
         STEP=(LXF-FXF)/8100.0
        ICNT=IFIX((LXF-FXF)/STEP)
     ELSE
       STEP=XSTEP
     ENDIF
C
     XBUF =FXF-STEP
C
      DO 30 I=1,ICNT
C
      XBUF=XBUF+STEP
C
      IF((XBUF.GE.XMIN).AND.(XBUF.LE.XMAX))THEN
C
   10   XDAT1=XMIN +(XSTEP*J)
        XDAT2=XDAT1+XSTEP
       IF((XBUF.GE.XDAT1).AND.(XBUF.LE.XDAT2))GOTO 20
         IF(XBUF.LT.XDAT1) J=J-1
         IF(XBUF.GT.XDAT1) J=J+1
         IF(XBUF.GT.XDAT2) J=J+1
C
       GOTO 10
C
```

```
  20     IF((XBUF.GT.XDAT1).AND.(XBUF.LT.XDAT2))THEN
            IBUF(I)=IFIX(FLOAT(IDAT(J)+IDAT(J+1))/2.0)
         ELSE
           IF(XBUF.EQ.XDAT1) IBUF(I)=IDAT(J)
           IF(XBUF.EQ.XDAT2) IBUF(I)=IDAT(J+1)
         ENDIF
C
      ELSE
C
         IBUF(I)=0
C
      ENDIF
C
  30  CONTINUE
C
     RETURN
     END
```

- Specialized PASCON subroutines.

```
                    ********************************
                    *   calibration parameter routines *
                    ********************************

C           ************************************************************
C *
C * SUBROUTINE GETPAR
C *
C  *  This subroutine gets Cubic Spline Calibration parameters which have been previously
C  *  stored on disk.  Only the filename DYEPAR is explicitly passed to the subroutine.
C  * The variables in the Common Block /SPLDAT/ is used by the subroutine.
C *
C           ************************************************************
C
C
      SUBROUTINE GETPAR(FILE)
C
C
        REAL SPLX(50),SPLY(50),SPLA(50),SPLB(50),SPLC(50)
C
      INTEGER ISPL
C
       CHARACTER CH*1,FILE*15
C
C
       COMMON /SPLDAT/ ISPL,SPLX,SPLY,SPLA,SPLB,SPLC
C
C
C           ************************************************************
C
C
C
     2 WRITE(2,1000)
       READ (1,1010) FILE
       WRITE(2,1020) FILE
       READ (1,1030) CHAR
C
      IF (CHAR .EQ. 'Y') THEN
C
       CALL DEFINE(13,FILE)
        READ (13,1100) ISPL
C
       DO 10,I=1,ISPL
          READ(13,1110) SPLX(I),SPLY(I),SPLA(A),SPLB(I),SPLC(I)
  10 CONTINUE
C
       CALL IOEXIT
       CALL ENBLKB
```

```
C
      ELSE
C
         WRITE(2,1040)
        READ (1,1030) CHAR
       IF (CHAR .EQ. 'Y') GOTO 2
C
      ENDIF
C
C        ************************************************************
C
 1000 FORMAT(' ','Enter Filename : ')
 1010 FORMAT(A15)
 1020 FORMAT(' ','Get file ',A15,'from D0   (Y/N)? : ')
 1030 FORMAT(A1)
 1040 FORMAT(' ','Re-Enter Filename (Y/N)? : ')
 1100 FORMAT(' ',I4)
 1110 FORMAT(' ',5(F12.4))
C
C        ************************************************************
C
      RETURN
      END
C
C              ************************************************************
C  *
C  * SUBROUTINE STOPAR
C  *
C  *  This subroutine stores the the dye laser calibration parameter file to disk.
C  *  Common Block /SPLDAT/ is used by the subroutine.
C  *
C              ************************************************************
C
C
      SUBROUTINE STOPAR(DYEPAR)
C
C
        REAL SPLX(50),SPLY(50),SPLA(50),SPLB(50),SPLC(50)
C
      INTEGER ISPL
C
       CHARACTER CH*1,DYEPAR*15
C
C
       COMMON /SPLDAT/ ISPL,SPLX,SPLY,SPLA,SPLB,SPLC
C
C              ************************************************************
C
     2 WRITE(2,1020) DYEPAR
       READ (1,1030) CH
C
```

```
      IF(CH.EQ.'Y')THEN
C
        CALL ALLOC(12,DYEPAR,1056)
        WRITE(12,1100) ISPL
        DO 10 I=1,ISPL
          WRITE(12,1110) SPLX(I),SPLY(I),SPLA(I),SPLB(I),SPLC(I)
   10   CONTINUE
C
      CALL IOEXIT
      CALL ENBLKB
C
      ELSE
C
        WRITE(2,1040)
        READ (1,1030) CH
       IF(CH.EQ.'N') THEN
         WRITE(2,1000)
         READ (1,1010) DYEPAR
        GOTO 2
       ENDIF
C
      ENDIF
C
C       **********************************************************************
C
 1000 FORMAT(' ','Enter Filename : ')
 1010 FORMAT(A15)
 1020 FORMAT(' ','Store file ',A15,' to D0 (Y/N)? : ')
 1030 FORMAT(A1)
 1040 FORMAT(' ','Return to Command menu (Y/N)? : ')
 1100 FORMAT(' ',I4)
 1110 FORMAT(' ',5(F12.4))
C
C       **********************************************************************
C
      RETURN
      END
C
C             ************************************************************
C *
C * SUBROUTINE PRTPAR
C *
C  *  This subroutine prints the Dye Laser Calibration Parameters to the screen.
C  *  If the baud rate is set to 300 bps the parameters can be listed on the teletype.
C  *  Common Block /SPLDAT/ is used by the subroutine.
C  *
C             ************************************************************
C
      SUBROUTINE PRTPAR(DYEPAR)
C
C
```

```
      REAL SPLX(50),SPLY(50),SPLA(50),SPLB(50),SPLC(50)
C
    INTEGER ISPL
C
    CHARACTER DYEPAR*15
C
    COMMON /SPLDAT/ ISPL,SPLX,SPLY,SPLA,SPLB,SPLC
C
C           ************************************************************
C
C
    PRINT *,
     WRITE(*,1000)
    PRINT *,
    WRITE(*,1004) DYEPAR
     WRITE(*,1010)
    PRINT *,
C
 1000 FORMAT('0',18X,'WAVELENGTH CALIBRATION PARAMETERS')
 1004 FORMAT(' ',18X,' PARAMETER FILE : ',A15)
 1010  FORMAT('  ',2X,'I',6X,'X',12X,'Y',12X,'A',12X,'B',12X,'C')
C
    DO 10,I=1,ISPL
C
      WRITE(*,1100) I,SPLX(I),SPLY(I),SPLA(A),SPLB(I),SPLC(I)
 1100  FORMAT(' ',I3,5(F12.4,1X))
C
  10 CONTINUE
C
    PRINT *,
C
   RETURN
   END
C
C
C           ************************************************************
C  *
C * SUBROUTINE GETXY
C  *
C  *  This subroutine allows the input of wavelength calibration points from the keyboard.
C  *  These points can later be editted, printed out, and then used in a cubic spline
C  *  interpolation procedure.    Common Block /SPLDAT/ is used by the subroutine.
C  *
C           ************************************************************
C
   SUBROUTINE GETXY
C
C
      REAL SPLX(50),SPLY(50),SPLA(50),SPLB(50),SPLC(50)
C
   INTEGER ISPL
```

```
C
      CHARACTER CH*1
C
C
      COMMON /SPLDAT/ ISPL,SPLX,SPLY,SPLA,SPLB,SPLC
C
C               ************************************************************
C
       WRITE(*,1000)
      READ *,ISPL
      PRINT *,
      PRINT *,
C
 1000 FORMAT(' ',5X,'Enter the number of calibration points ( max 50) : ')
C
      DO 10 I=1,ISPL
C
        WRITE(*,1004) I
       READ *,SPLX(I)
        WRITE(*,1006)
       READ *,SPLY(I)
       PRINT *,
      CALL BWIPE
      CALL BCLEAR
C
 1004   FORMAT(' ','FILTER ANGLE ',I2,' : ')
 1006   FORMAT(' ','WAVENUMBERS     : ')
C
  10 CONTINUE
C
C
     RETURN
     END
C
C
C               ************************************************************
C  *
C * SUBROUTINE EDPAR
C  *
C  *  This subroutine allows for editting of the Dye Laser Calibration Parameters.  The editted X-Y
C  *  data points can then be fit to a piecewise Cubic spline using the subroutine SPLFIT.
C  *  Common Block /SPLDAT/ is used by the subroutine.
C  *
C               ************************************************************
C
    SUBROUTINE EDPAR
C
C
      REAL SPLX(50),SPLY(50),SPLA(50),SPLB(50),SPLC(50)
C
    INTEGER ISPL,IVALUE
```

```
C
      CHARACTER CH*1
C
C
      COMMON /SPLDAT/ ISPL,SPLX,SPLY,SPLA,SPLB,SPLC
C
C               ************************************************************
C
      PRINT *,
   10 WRITE(*,1000)
      READ (*,1010) IVALUE
C
     IF(IVALUE.GT.ISPL)THEN
        WRITE(*,1020) ISPL
       GOTO 10
     ENDIF
C
     IF(IVALUE.EQ.0) GOTO 20
C
      WRITE(*,1030) SPLX(IVALUE),SPLY(IVALUE)
      PRINT *,'Enter new values : '
      READ (*,1040) SPLX(IVALUE),SPLY(IVALUE)
       PRINT *,'continue editting? (Y/N) : '
      READ (*,1050) CH
C
     IF(CH.EQ.'Y') GOTO 10
C
   20 PRINT *,
C
 1000 FORMAT(' ',5X,'Enter Parameter Number to be editted : ')
 1010 FORMAT(I3)
 1020 FORMAT(' ',5X,'There are only',I3,' parameters')
 1030 FORMAT(' ',20X,F7.4,',',F10.4)
 1040 FORMAT(' ',F7.4,F10.4)
 1050 FORMAT(A1)
C
C
     RETURN
     END
C
C         ************************************************************************
C *  SUBROUTINE WAVCON
C *         Generates the wavelength for each PA data point using the Cubic spline parameters
C         ************************************************************************
     SUBROUTINE WAVCON(IER,IPTS,IWF,IWL,XMIN,XMAX,XSTEP,X)
C
     INTEGER IER,IPTS,IWF,IWL,IT,ISPL
C
      REAL SPLX(50),SPLY(50),SPLA(50),SPLB(50),SPLC(50)
     REAL XMIN,XMAX,XSTEP,SMIN,SMAX,XTP,F,HALF,X(1)
C
```

```
      LOGICAL BIN
C
        DATA  HALF/6.25E-4/
C
C
       COMMON /SPLDAT/ ISPL,SPLX,SPLY,SPLA,SPLB,SPLC
C
C
C       ***************************************************************
C
       IER = -1
       IT= 1
       IWF=1
       BIN = .TRUE.
       SMIN=SPLX(1)
       SMAX=SPLX(ISPL)
       IF(SMIN.GT.SMAX)THEN
         XTP=SMAX
         SMAX=SMIN
         SMIN=XTP
       ENDIF
C
       IF((XMIN.LT.SMAX).AND.(XMAX.GT.SMIN))THEN
        IER = 0
        IF(XMAX.GT.(SMAX+HALF)) IER = 10
        IF(XMIN.LT.(SMIN-HALF)) IER = IER + 1
C
        I=0
   20   I = I + 1
        IF(I.EQ.1)F=XMIN
        IF(I.GT.1)F=F+XSTEP
C
        IF((I.GT.IPTS).OR.(F.GT.SMAX)) GOTO 40
        IF(F.LT.(SMIN-HALF))GOTO 20
C
C GET INTEPOLATING INDEX
C
        CALL SPLINT(F,XTP,IT,BIN)
C
       IF(XTP.LT.ZERO)GOTO 40
C
        IF (BIN) THEN
          IWF = I
          BIN = .FALSE.
        ENDIF
C
        X(I)=XTP
C
      GOTO 20
C
   40 IWL =I-1
```

```
      IF(IWL.LT.IWF) IER=-1
C
      ENDIF
C
      RETURN
      END
C
C     ********************************************************
C SPLINT
C   GET INTERPOLATING INDEX THROUGH LINEAR OR BINARY SEARCH AND
C USING INDEX DETERMINE WAVELENGTH.
C     ********************************************************
C
      SUBROUTINE SPLINT(F,XT,IT,BIN)
C
      INTEGER IT,ITP1,ITM1,I,J,ISPL
      REAL SPLX(50),SPLY(50),SPLA(50),SPLB(50),SPLC(50)
      REAL F,FL,FH,FP1L,FP1H,FM1L,FM1H,DF,XT
      LOGICAL BIN
C
      DATA HALF/6.25E-4/
C
      COMMON /SPLDAT/ ISPL,SPLX,SPLY,SPLA,SPLB,SPLC
C
C     ************************************************************
C
C BINARY AND LINEAR SEARCH FOR ARRAY INDEX
C
      I=1
      J=ISPL
   10 ITP1 = IT+1
      ITM1 = IT-1
      FL = SPLX(I)-HALF
      FH = SPLX(I)+HALF
      FP1L = SPLX(ITP1)-HALF
      FP1H = SPLX(ITP1)+HALF
      FM1L = SPLX(ITM1)-HALF
      FM1H = SPLX(ITM1)+HALF
C
      IF(ITP1.GT.ISPL) GOTO 99
      IF(ITM1.LT.0) GOTO 99
      IF((F.GT.FL).AND.(F.LT.FH)) GOTO 70
      IF((F.GT.FP1L).AND.(F.LT.FP1H)) GOTO 60
      IF((F.GT.FM1L).AND.(F.LT.FM1H)) GOTO 50
      IF((F.GE.SPLX(IT)).AND.(F.LT.SPLX(ITP1)))GOTO 40
      IF(ITM1.EQ.0) GOTO 20
      IF(F.EQ.SPLX(ITM1))GOTO 50
      IF((F.GT.SPLX(ITM1)).AND.(F.LT.SPLX(IT))) GOTO 30
C
   20 IF(BIN)THEN
      IF(F.LT.SPLX(IT)) J=IT
```

```
        IF(F.GT.SPLX(IT)) I=IT
          IT=(I+J)/2
        IF(J.GT.I+1) GOTO 10
        IT = ITM1
      ELSE
        IF(F.GT.FH) IT=ITP1
        IF(F.LT.FL) IT=ITM1
       GOTO 10
      ENDIF
C
   30 IT=ITM1
   40 DF = F-SPLX(IT)
         XT=SPLY(IT)+DF*(SPLC(IT)+DF*(SPLB(IT)+DF*SPLA(IT)))
      GOTO 100
C
   50 IT=ITM1
     GOTO 70
   60 IT=ITP1
   70 XT=SPLY(IT)
     GOTO 100
C
   99 XT=-9999.9
C
  100 RETURN
      END
```

REFERENCES

1. see for example : Woodin R. L. and Kaldor A., Adv. Chem. Phys. **47**(2),3,(1981) and references therein.
2. a) Rice S. A., Adv. Chem. Phys. **47**(1),117,(1981)
   b) Felker P. M. and Zewail A. H., Adv. Chem. Phys. **70**(1),265,(1988).
3. Born M. and Oppenheimer R., Annal. der Physik **84**,457,(1927).
4. Carney G. D., Sprandel L. L., and Kern C. W., Adv. Chem. Phys. **37**,305,(1978).
5. Tennyson J., Comput. Phys. Rep. **4**,1,(1986).
6. Wilson E. B., Decius J. C. and Cross P., "Molecular Vibrations", McGraw-Hill, N.Y., (1955).
7. Califano S., "Vibrational States", John Wiley & Sons, London, (1976).
8. Podolsky B., Phys. Rev. **32**,812,(1928).
9. Kemble E.C., "The Fundamental Principles of Quantum Mechanics", McGraw-Hill, N.Y., (1937).
10. Nauts A. and Chapuisat X., Mol Phys **55**,1287,(1985).
11. Neto N., Chem. Phys. **91**,89,(1984).
12. Cohen-Tannoudji C., Dio B., and Laloe F., "Quantum Mechanics,Vol 1", Hermann, Paris, (1977).

(references continued)

13. Abramowitz M. and Stegun I. A. (editors), "Handbook of Mathematical Functions", Dover Pub. Inc., N.Y., (1972).

14. Levine I. N., "Molecular Spectroscopy", John Wiley & Sons, N.Y., (1975).

15. Curnutte B. and Spangler J. in, "Methods of Expereimental Physics : Spectroscopy", (Williams D. ed) Academic Press, N.Y., (1976).

16. Gelbart W. M., Stannard P. R., and Elert M. L., Inter. J. Quantum. Chem. **14**,703,(1978).

17. Ellis J. W., Trans. Farad. Soc. **26**,888,(1929).

18. Freymann R., Ann. de. Phys. 10e serie, t. xx,243,(1933).

19. Siebrand W. and Williams D. F., J. Chem. Phys. **49**,1860,(1968).

20. Henry B. R. and Siebrand W., J. Chem. Phys. **49**,5369,(1968).

21. Hayward R. J. and Henry B. R., J. Mol. Spec. **57**,221,(1975).

22. Hayward R. J. and Henry B. R., Chem. Phys. **12**, 387,(1976).

23. for a review of the early developments see:

    a) Henry B. R., Acc. Chem. Res. **10**,207,(1977).

    b) Henry B. R. in, "Vibrational Spectra and Structure", (Durig J. R. ed.) Elsevier, N.Y., (1981).

24. Morse P. M., Phys. Rev. **34**,57,(1929).

25. Ter Haar D., Phys. Rev. **70**,222,(1946).

(references continued)

26. Sage M. L., Chem. Phys. **35**,375,(1978).

27. Wallace R., Chem. Phys. Lett. **37**,115,(1976).

28. Henry B. R., Acc. Chem. Res. **20**,429,(1987).

29. Mortensen O. S., Henry B. R., and Mohammadi M. A., J. Chem. Phys. **75**,4800,(1981).

30. Halonen L. and Child M. S., Mol. Phys. **46**,239,(1982).

31. Mortensen O. S. in, "Time Resolved Vibrational Spectroscopy", (Atkinson G. H. ed.) Academic Press, N.Y., (1983).

32. Child M. S. and Halonen L., Adv. Chem. Phys. **62**,1,(1984).

33. Henry B. R., Tarr A. W., Mortensen O. S., Murphy W. F., and Compton D. A. C., J Chem Phys. **79**,2583,(1983).

34. a) Ahmed M. K. and Henry B. R., J. Phys. Chem. **90**,1081,(1986).
b) Ahmed M. K. and Henry B. R., J. Phys. Chem. **91**,5194,(1987).
c) Ahmed M. K. and Henry B. R., Can. J. Chem. **66**,628,(1988).

35. Ahmed M. K. and Henry B. R., J. Phys. Chem. **91**,3741,(1987).

36. Kellman M. E., J. Chem. Phys. **76**,4528,(1982).

37. Lehmann K. K., J. Chem. Phys. **79**,1098,(1983).

38. Mills I. M. and Robiette A. G., Mol. Phys. **56**,743,(1985).

(references continued)

39. a) Baggott J. E., Clase H. J., and Mills I. M., Spectrochimica Acta **42A**,319,(1986).

b) Baggott J. E., Law D. W., Lightfoot P. D., and Mills I. M., J. Chem. Phys. **85**,5414,(1986).

40. a) Bell A. G., Proc. Am. Assoc. Adv. Sci. **29**,115,(1880).

b) Bell A. G., Philos. Mag. **11**,510,(1881).

41. Tyndall J., Proc. Roy. Soc. London **31**,307,478,(1881).

42. Roentgen W. C., Philos. Mag. **11**,308,(1881).

43. Viengerov M. L., Dokl. Akad. Nauk SSSR **19**,687,(1938).

44. Luft K. F., Z. Tech. Phys. **24**,97,(1943).

45. Gorelik G., Dokl. Akad. Nauk SSSR **54**,779,(1946).

46. Kerr E. L. and Atwood J. G., Appl. Opt. **7**,915,(1969)

47. Kreuzer L. B., J. Appl. Phys. **42**,2934,(1971).

48. Stella G., Gelfand J., and Smith W. H., Chem. Phys. Lett. **39**,146,(1976).

49. Reddy K. V., Bray R. G., and Berry M. J. in, (1978). "Advances in Laser Chemistry", (Zewail A. H., ed.) Springer-Verlag, Berlin, (1978).

50. Reddy K. V., Heller D. F., and Berry M. J., J. Chem. Phys. **76**,2814,(1982).

51. Leite R. C. C., Moore R. S., and Whinnery J. R., Appl. Phys. Lett. **5**,141,(1964).

(references continued)

50. Reddy K. V., Heller D. F., and Berry M. J., J. Chem. Phys. **76**,2814,(1982).

51. Leite R. C. C., Moore R. S., and Whinnery J. R., Appl. Phys. Lett. **5**,141,(1964).

52. a) Swofford R. L., Long M. E., and Albrecht A. C., J. Chem. Phys. **65**,179,(1976).

b) Long M. E., Swofford R. L., and Albrecht A. C., Science **191**,183,(1976).

c) Swofford R. L., Burberry M. S., Morrell J. A., and Albrecht A. C., J. Chem. Phys. **66**,5245,(1977).

53. Boccara A. C., Fournier D., Jackson W., and Amer N.M., Opt. Lett. **5**,377,(1980).

54. Reddy K. V., Rev. Sci. Instrum. **54**,422,(1983).

55. Fraim F. W., Murphy P. V., and Ferran R. J., J. Acoust. Soc. Am. **53**,1601,(1973).

56. "Optoacoustic Spectroscopy and Detection", (Pao Y.-H. ed.) Academic Press, N.Y., (1977).

57. Rosencwaig A., Adv. Electron. Electron Phys. **46**,207,(1978).

(references continued)

58. Rosencwaig A., "Photoacoustics and Photoacoustic Spectroscopy", Wiley, N.Y., (1980).

59. a) Tam A.C. in, "Ultrasensitive Laser Spectroscopy", (Kliger D., ed.) Academic Press, N. Y., (1983).

b) Patel C. K. N. and Tam A. C., Rev. Mod. Phys. **53**,517,(1981).

c) Tam A. C., Rev. Mod. Phys. **58**,381,(1986).

60. "Photothermal Investigations of Solids and Fluids", (Sell J. A., ed.) Academic Press Inc., San Diego, (1988).

61. "Photoacoustic and Thermal Wave Phenomena in Semiconductors", (Mandelis A., ed.) Elsevier Science Publishing Co. Inc., N. Y., (1987).

62. Kreuzer L. B. in, "Optoacoustic Spectroscopy and Detection", (Pao Y.-H., ed.) Academic Press, N. Y., (1977).

63. Stettler J. D. and Witriol N. M. in, "Optoacoustic Spectroscopy and Detection", (Pao Y.-H., ed.) Academic Press, N. Y., (1977).

64. Morse P. M. and Ingard K. U. in, "Encyclopedia of Physics", (Flugge S.,ed.) Vol XI/1 Springer-Verlag, Berlin, (1961).

65. Rosengren L.-G., Appl. Opt. **14**,1960,(1975).

(references continued)

66. Kogelnik H. W., Ippen E. P., Dienes A., and Shank C. V., IEEE J. Quant. Electron. **8**,373,(1972).

67. Leutwyler S., Schumacher E., and Woste L., Opt. Commun. **19**,197,(1976).

68. Wellegehausen B., Laepple L., and Welling H., Appl. Phys. **6**,335,(1975).

69. Teschke O., Whinnery J. R., and Diennes, IEEE J. Quant. Electron. **12**,513,(1976).

70. Johnston T. F., Brady R. H. Jr., and Proffitt W., Appl. Opt. **21**,2307,(1982).

71. Baving H. J., Muuss H., and Skolaut W., Appl. Phys. **B29**,19,(1982).

72. Holtom G. and Teschke O., IEEE J. Quant. Electron. **10**,577,(1974).

73. Bloom A. L., J. Opt. Soc. Am. **64**,447,(1974).

74. Preuss D. R. and Gole J. L., Appl. Opt. **19**,702,(1980).

75. Wong J. S., Ph.D. Thesis, U.C. Berkeley, 1981.

76. Yeh P., Appl. Opt. **21**,3806,(1982).

(references continued)

77. Sessler G. M. and West J. E., J. Acoust. Soc. Am. **53**,1589,(1973).

78. Baines D. C., Appl. Acoust. **15**,117,(1982).

79. Hieftje G. M., Anal. Chem. **44**,81A,(1972).

80. Blair D. P. and Sydenham P. H., J. of Phys. **E6**,621,(1975).

81. Fisher and Jensen, "PET and the IEEE-488 Bus (GPIB)", Osborne/McGraw-Hill, Berkeley, (1980).

82. Yob G., Microcomputing, July (1980).

83. Tilden M. D., EDN, Oct 27 (1983).

84. Ashworth H. A. and Augustine R. L., Rev. Sci. Instrum. **52**,105,(1981).

85. a) SAS Version 5.16, SAS Institute Inc., Box 8000, Cary N.C.
b) GLM procedure of SAS Version 5.16

86. Gerald C. F.,"Applied Numerical Analysis",ed. 3, Addison Wesley, Reading Mass., (1984).

87. Spath H., "Spline Algorithms for Curves and Surfaces", Utilitas Mathematica Pub. Inc., Winnipeg Man., (1974).

(references continued)

88. Camy-Peyret C, Flaud J. M., Mandin J. Y., Chevillard J. P., Brault J., Ramsay D. A., Vervloet M. and Chauville J., J. Mol. Spec. **113**,208,(1985).

89. Mandin J. Y., Chevillard J. P., Camy-Peyret C., and Flaud J. M., J. Mol. Spec. **116**,167,(1986).

90. Smith D. F. and Overend J., Spectrochimica Acta. **28A**,471,(1972).

91. Peterson M. R. and Poirer R. A., MONSTERGAUSS, Department of Chemistry, University of Toronto, Toronto, Ontario, Canada, 1981.

92. Binkley J. S., Frisch M. J., Defrees D. J., Raghavachari K, Whiteside R. A.,Schlegel H.B., Pople J. A., GAUSSIAN 82, Department of Chemistry, Carnegie Mellon University, Pittsburgh, P. A., U.S.A., 1983.

(references continued)

93. Frisch M. J., Binkley J. S., Schlegel H. B., Raghavachari K., Melius C. F., Martin R. L., Stewart J. J. P., Bobrowicz F. W., Rohlfing C. M., Kahn L. R., Defrees D. J., Seeger R., Whiteside R. A., Fox D. J., Fluder E. M., and Pople J. A., GAUSSIAN 86, Carnegie-Mellon Quantum Chem. Publ. Unit, Pittsburgh, P. A., U.S.A., 1987.

94. Davidson W. C., Math. Programming **9**,1,(1975).

95. Murtagh B. A. and Sargent R. W., Comput. J. **13**,185,(1972).

96. Pulay P., Fogarasi G., Pang F., and Boggs J. E., J. Am. Chem. Soc. **101**,2550,(1979).

97. Schafer L., Van Alsenoy C., Scarsdale J. N., J. Mol. Struct. (Theochem) **86**,349,(1982).

98. Boggs J. E. and Cordell F. R., J. Mol. Struct. (Theochem) **76**,329,(1981).

99. McKean D. C., Boggs J. E., and Schafer L., J. Mol. Struct. (Theochem) **116**,313,(1984).

100. "Internal Rotation in Molecules", (Orville-Thomas W. J., ed.) Wiley, N. Y., (1974).

(references continued)

101. Helgaker T. and Jorgensen P., Adv. Quantum Chem. **19**,183,(1988).

102. a) Fogarasi G. and Pulay P., In "Vibrational Spectra and Structure", (Durig J. R., ed.) Vol 14, p 125, Elsevier, Amsterdam, (1985).

b) Pulay P., Adv. Chem. Phys. **69**(2),241,(1987).

c) Pulay P. in, "The Force Method in Chemistry", (Deb B. M., ed.), Van Nostrand-Reinhold, N.Y., (1981).

d) Fogarasi G. and Pulay P., Ann. Rev. Phys. Chem. **35**,191,(1984).

103. Michalska D., Schaad L. J., Carsky P., Andes Hess B., and Ewig C. S., J. Comp. Chem. **9**,495,(1988).

104. a) Bleicher W. and Botschwina P., Mol. Phys. **30**,1029,(1975).

b) Botschwina P., Meyer W., and Semkow A.M., Chem. Phys. **15**,25,(1976).

c) Botschwina P., Mol. Phys. **47**,241,(1982).

105. Amos R. D., Adv. Chem. Phys. **69**(1),99,(1987).

106. Mortensen O. S., Ahmed M. K., Henry B. R., and Tarr A. W., J. Chem. Phys. **82**,3903,(1985).

(references continued)

107. Tarr A. W., Swanton D. J., and Henry B. R., J. Chem. Phys. **85**,3463,(1986).

108. Tarr A. W. and Zerbetto F., Chem Phys. Lett. **154**,273,(1989).

109. Carney G. D. and Porter R. N., J. Chem. Phys. **65**,3547,(1976).

110. Bacskay G. B., Saebo S., and Taylor P. R., Chem. Phys. **90**,215,(1984).

111. Williams I. H., J. Mol. Struct. (Theochem) **94**,275,(1983).

112. Eckart C., Phys. Rev. **47**,552,(1935).

113. Sayetz A., J. Chem. Phys. **6**,383,(1939).

114. Hout R. F., Levi B. A., and Hehre W. J., J. Comput. Chem. **3**,234,(1982).

115. Swanton D. J., Bacskay G. B., and Hush N. S., J. Chem. Phys. **84**,5715,(1986).

116. Green J. H. S. and Harrison D. J., Spectrochim. Acta. **33A**,843,(1977) and references therein.

117. Scott D. W., J. Mol. Spec. **37**,77,(1971) and references therein.

118. Scott D. W., J. Mol. Spec. **31**,451,(1969) and references therein.

119. Paliani G. and Cataliotti R., Spectrochim. Acta. **37A**,707,(1981).

(references continued)

120. Paliani G. and Cataliotti R., Spectrochim. Acta. **38A**,751,(1982).

121. Navarro R. and Orza J.M., An. Quim. **A75**,557,(1983).

122. Mizugai Y. and Katayama M., Chem. Phys. Lett. **73**,240,(1980).

123. Cataliotti R. and Paliani G., Can. J. Chem. **54**,2451,(1976).

124. Wong J. S. and Moore C. B., J. Chem. Phys. **77**,603,(1982).

125. McKean D. C., Chem. Soc. Rev. **7**,399,(1978) and references therein.

126. Mizugai Y., Katayama M., J. Am. Chem. Soc. **102**,6424,(1980).

127. Barnes J. and Fulweiler W. H., J. Am. Chem. Soc. **49**,2034,(1927).

128. Freymann R., Comptes Rendus **194**,1471,(1932).

129. Allard G., Comptes Rendus **194**,1495,(1932).

130. Mizugai Y., Katayama M., and Nakagawa N., J. Am. Chem. Soc. **103**,5061,(1981).

131. Gough K. M., Ph.D. Thesis, University of Manitoba,(1984).

132. Gough K. M. and Henry B. R., J. Phys. Chem. **87**,3433,(1983).

133. Gough K. M. and Henry B. R., J. Am. Chem. Soc. **106**,2781,(1984).

134. Gough K. M. and Henry B. R., J. Phys. Chem. **88**,1298,(1984).

(references continued)

135. Jaffe H.H. and Jones H.L., Advanc. Heterocylic Chem. **3**,209,(1964).

136. Freeman F., J. Chem. Educ. 140,(1970).

137. Clementi S., Linda P. and Marino G., J. Chem. Soc. **B**,1153,(1970).

138. Morizur J. P. and Pascal Y., Bull. Soc. Chim. Fr. **7**,2296,(1966).

139. Peron J. J., Lebas J. M., and Saumagne P., C.R. Acad. Sci. Paris **267B**,586,(1968).

140. Angelelli J. M., Katritzky A. R., Pinzelli R. F., and Topsom R. D., Tetrahedron **28**,2037,(1972).

141. Badger R. M., J. Chem. Phys. **2**,128,(1934) and **3**,710,(1935).

142. Huggins M. L., J. Chem. Phys. **3**,473,(1935) and **4**,308,(1936).

143. Sutherland G. B. B. M., J. Chem. Phys. **8**,161,(1940).

144. Linnett J. W., Trans. Faraday Soc. **36**,1123,(1940) and **38**,1,(1942).

145. Varshni Y. P., J. Chem. Phys. **28**,1078 and 1081,(1958).

146. Goodisman J., "Diatomic Interaction Potential Theory", Academic Press, N. Y., Vols 1 and 2, (1975), and references therein.

(references continued)

147. Borkman R. F. and Parr R. G., J. Chem. Phys. **48**,1116,(1968).

148. Swanton D. J. and Henry B. R., J. Chem. Phys. **86**,4801,(1987) and references therein.

149. Mata F., Martin M. C., and Sorensen G. O., J. Mol. Struct **48**,157,(1978).

150. Nygaard L., Nielson J. F., Kirchheiner J., Maltesen G., Rastrup-Andersen J., and Sorensen G. O., J. Mol. Struct **3**,491,(1969).

151. Bak B., Christensen D., Hansen-Nygaard L., and Rastrup-Andersen J., J. Mol. Spec. **7**,58,(1961).

152. Bak B., Christensen D., Dixon W. B., Hansen-Nygaard L., Rastrup-Andersen J., Schottlander M., J. Mol. Spec. **9**,124,(1962).

153. Fermi E., Z. Phys. **71**,250,(1931).

154. a.) Sage M. L. and Jortner J., Chem. Phys. Lett. **62**,451,(1979).
b.) Sage M. L. and Jortner J., Adv. Chem. Phys. **47**,293,(1981).

155. Mukamel S., J. Phys. Chem. **88**,832,(1984).

156. a.) Heller D. F. and Mukamel S., J. Chem. Phys. **70**,463,(1979).
b.) Heller D. F., Chem. Phys. Lett. **61**,583,(1979).

157. Stannard P. R. and Gelbart W., J. Phys. Chem. **85**,3592,(1981).

(references continued)

158. a.) Cerjan C. J., Shi S. -H., and Miller W. H., J. Phys. Chem. **86**,2244,(1982).

b.) Shi S. and Miller W. H., Theor. Chim. Acta. **68**,1,(1985).

159. a.) Nagy P. J. and Hase W. L., Chem. Phys. Lett. **54**,73,(1978).

b.) Nagy P. J. and Hase W. L., Chem. Phys. Lett. **58**,482,(1978).

160. a.) Sibert III E. L., Reinhardt W. P., and Hynes J. T., Chem. Phys. Lett. **92**,455,(1982).

b.) Sibert III E. L., Reinhardt W. P., and Hynes J. T., J. Chem. Phys. **81**,1115,(1984).

161. Sibert III E. L., Hynes J. T., and Reinhardt W. P., J. Chem. Phys. **81**,1135,(1984).

162. a.) Hutchinson J. S., Reinhardt W. P., and Hynes J. T., J. Chem. Phys. **79**,4247,(1983).

b.) Hutchinson J. S., Hynes J. T., and Reinhardt W. P., Chem. Phys. Lett.**108**,353,(1984).

c.) Uzer T., Hynes J. T., and Reinhardt W. P., J. Chem. Phys. **85**,5791,(1986).

(references continued)

163. a.) Holme T. A. and Hutchinson J. S., J. Chem. Phys. **84**,5455,(1986).

b.) Hutchinson J. S. and Marshall K. T., J. Chem. Soc. Fara. Trans. 2, **84**,1535,(1988).

c.) Hutchinson J. S., Adv. Chem. Phys. **73**,637,(1989) and references therein.

164. a.) Lami A. and Villani G., J. Chem. Phys. **90**,3559,(1989).

b.) Lami A. and Villani G., J. Chem. Phys. **88**,5186,(1988).

165. Hofmann P., Gerber R. B., Ratner M. A., Baylor L. C., and Weitz E., J. Chem. Phys. **88**,7434,(1988) and **89**,6557,(1988).

166. a.) Dubal H. -R. and Quack M., Mol. Phys. **53**,257,(1984).

b.) Dubal H. -R., and Quack M., J. Chem. Phys. **81**,3779,(1984).

c.) von Puttkamer K., Dubal H. -R., and Quack M., Fara. Discuss. Chem. Soc. **75**,197,(1983).

167. Douketis D., Anex D., Ewing G. and Reilly J. P., J. Phys. Chem. **89**,4173,(1985).

(references continued)

168. a.) West G. A., Mariella R. P. Jr., Pete J. A., Hammond W. B., Heller D. F., J. Chem. Phys. **75**,2006,(1981).

b.) McGinley E. S. and Crim F. F., J. Chem. Phys. **85**,5741,(1986).

c.) McGinley E. S. and Crim F. F., J. Chem. Phys. **85**,5748,(1986).

169. a.) Dubal H. -R. and Crim F. F., J. Chem. Phys. **83**,3863,(1985).

b.) Ticich T. M., Rizzo R. R., Dubal H. -R., and Crim F. F., J. Chem. Phys. **84**,1508,(1986).

170. Likar M. D., Baggott J. E., and Crim F. F., J. Chem. Phys. **90**,6266,(1989).

171. a.) Page R. H., Shen Y. R., and Lee Y. T., Phys. Rev. Lett. **59**,1293,(1987).

b.) Page R. H., Shen Y. R. and Lee Y. T., J. Chem. Phys. **88**,4621,(1988).

172. Crofton M. W., Stevens C. G., Klenerman D., Gutow J. H., and Zare R. N., J. Chem. Phys. **89**,7100,(1988).

173. a.) Perry J. W. and Zewail A. H., J. Chem. Phys. **80**,5333,(1984).

b.) Perry J. W. and Zewail A. H., J. Phys. Chem. **86**,5197,(1982).

174. Fermi E., "Nuclear Physics", University of Chicago Press, Chicago Il.,(1950), p142.

(references continued)

175. Tarr A. W. and Henry B. R., Chem. Phys. Lett. **112**,295,(1984).

176. Tarr A. W., Ph.D. Thesis, University of Manitoba,(1986).

177. Tarr A. W. and Henry B. R., J. Chem. Phys. **84**,1355,(1986).

178. a.) Findsen L. A., and Fang H. L., Swofford R. L., and Birge R. R., J. Chem. Phys. **84**,16,(1986).

b.) Fang H. L. and Compton D. A. C., J. Phys. Chem. **92**,6518,(1988).

c.) Fang H. L. and Compton D. A. C., J. Phys. Chem. **92**,7185,(1988).

d.) Fang H. L., Swofford R. L., and Compton D. A. C., Chem. Phys. Lett. **108**,539,(1984).

e.) Fang H. L., Meister D. M. and Swofford R. L., J. Phys. Chem. **88**,410,(1984).

f.) Fang H. L. and Swofford R. L., Appl. Opt. **21**,55,(1982).

179. Manzanares I. C., Yamasaki N. L. S., and Weitz E., J. Phys. Chem. **91**,3959,(1987).

180. Baylor L. C., Weitz E., and Hofmann P., J. Chem. Phys. **90**,615,(1989).

(references continued)

181. Henry B. R., Goswami P. C., and Swanton D. J., Chem. Phys. Lett. **144**,527,(1988).

182. Henry B. R., Mohammadi M. A., Hanazaki I., and Nakagaki R., J. Phys. Chem. **87**,4827,(1983).

183. Norris W. G. and Krisher L. C., J. Chem. Phys. **51**,403,(1969).

184. a.) Ogata T. and Kozima K., J. Mol. Spec. **42**,38,(1972).

b.) Ogata T. and Kozima K., Bull. Chem. Soc. Jap. **44**,2344,(1971).

185. a.) Pozdeev N. M., Gunderova L. N., Shapkin A. A., Opt. Spektrosk. **28**,254,(1970).

b.) Pozdeev N. M., Latypova R. G., and Gunderova L. N., Zh. Struct. Khim. **17**,362,(1976).

186. Khalique A. M., Ph.D. Thesis, University of Manitoba (1987).

187. a.) Handy N. C., Gaw J. F., and Simandiras E. D., J. Chem. Soc. Fara. Trans. 2, **83**,1577,(1987).

b.) Amos R. D., J. Chem. Soc. Fara. Trans. 2, **83**,1597,(1987).

c.) Amos R. D., Gaw J. F., and Handy N. C., J. Chem. Soc. Fara. Trans. 2, **84**,1247,(1988) and references therein.

(references continued)

188. Botschwina P., J. Chem. Soc. Fara. Trans. 2, **84**,1263,(1988) and references therein.

189. Wollrab J. E., "Rotational Spectra and Molecular Structure", Academic Press, N.Y., (1967).

190. Lister D. G., Macdonald J. N., and Owen N. L.,"Internal Rotation and Inversion", Academic Press, N.Y.,(1978).

191. Jones W. J. and Sheppard N., Proc. Roy. Soc. **A304**,135,(1968).

192. Sheppard N. and Woodman C. M., Proc. Roy. Soc. Lond. **A313**,149,(1969).

193. a.) Dempster A. B., Powell D. B., and Sheppard N., Spectrochimica. Acta. **31A**,245,(1974).

b.) Dempster A. B., Powell D. B., and Sheppard N., Spectrochimica. Acta. **28A**,373,(1972).

c.) Leech R. C., Powell D. B., and Sheppard N., Spectrochimica Acta **21A**,559,(1965).

d.) Leech R. C., Powell D. B., and Sheppard N., Spectrochimica Acta **22A**,1,(1965).

194. Reed P. R. and Lovejoy R. W., Spectrochimica. Acta. **26A**,1087,(1970).

(references continued)

195. McKean D. C. and Watt R. A., J. Mol. Spec. **61**,184,(1976).

196 McKean D. C., Becher H. J. and Bramsiepe F, Spectrochimica. Acta. **33A**,951,(1977).

197. a.) Cavagnat D. and Lascombe J., J. Mol. Struct. **80**,363,(1982).

b.) Cavagnat D. and Lascombe J., J. Mol. Spec. **92**,141,(1982).

c.) Cavagnat D. and Lascombe J., J. Chem. Phys. **76**,4336,(1982).

d.) Cavagnat D., Brom H. and Nugteren P. R., J. Chem. Phys. **87**,801,(1987).

198. Lascombe J., Cavagnat D., Lassegues J. C., Rafilipomanana C., and Biran C., J. Mol. Struct. **113**,179,(1984).

199. a.) Tannenbaum E., Myers R. J., and Gwinn W. D., J. Chem. Phys. **25**,42,(1956).

b.) Cox P. A. and Waring S., J. Chem. Soc. Fara. Trans. 2, **68**,1060,(1972)

c.) Sorensen G. O., Pedersen T., Dreizler H., Guarnieri A., and Cox P. A., J. Mol. Struct. **97**,77,(1983).

200. a.) Naylor R. E. and Wilson E. B., J. Chem. Phys. **26**,1057,(1957).

b.) Langridge-Smith P. R. R., Stevens R., and Cox P. A., J. Chem. Soc. Fara. Trans. 2, **75**,1620,(1979)

(references continued)

201. Ahmed K. M., and Henry B. R., J. Phys. Chem. **90**,1737,(1986).

202. Henry B. R., Gough K. M., and Sowa M. G., Int. Rev. Phys. Chem. **5**,133,(1986).

203. Susskind J., J. Chem. Phys. **53**,2492,(1970).

204. Schwoch D. and Rudolph H. D., J. Mol. Spec. **57**,47,(1975).

205. Sowa M. G., unpublished results.

206. Gough K. M., unpublished results.

207. Okuyama K., Mikami N., and Ito M., J. Phys. Chem. **89**,5617,(1985).

208. Breen P. J., Warren J. A., and Bernstein E. R., J. Chem. Phys. **87**,1917,(1987).

209. Ghosh P. N., J. Mol. Spec. **138**,505,(1989).

210. a.) Rudolph H. D., Dreizler H., Jaeschke A., and Wendling P., Z. Naturforschg. **22A**,940,(1967).

b.) Kreiner W. A., Rudolph H. D., Tan B. T., J. Mol. Spec. **48**,86,(1973).

211. Rudolph H. D. and Trinkaus A., Z. Naturforschg. **23A**,68,(1968).

212. Herberich G. E., Z. Naturforschg. **22A**,761,(1967).

213. Rudolph H. D. and Seiler H., Z. Naturforschg. **20A**,1682,(1965).

(references continued)

214. a.) Pang F. and Boggs J. E., J. Mol. Struct. **66**,281,(1980).

b.) Xie Y. and Boggs J. E., J. Comp. Chem. **7**,158,(1986).

215. Schaefer T. and Penner G. H., J. Mol. Struct. (Theochem) **138**,305,(1986).

216. Penner G. H., unpublished results.

217. Arnold W., Dreizler H., and Rudolph H. D., Z. Naturforschg. **23A**,301,(1967).

218. Moss D. B., Parmenter C. S. and Ewing G. E., J. Chem. Phys. **86**,51,(1987).

219. Carpenter J. E. and Weinhold F., J. Phys. Chem. **90**,6405,(1986).

220. a.) Stone B. M. and Parmenter C. S., J. Chem. Phys. **84**,4710,(1986).

b.) Longfellow R. J. and Parmenter C. S., J. Chem. Soc. Fara. Trans 2, **84**,1499,(1988).

c.) Longfellow R. J., Moss D. B., and Parmenter C. S., NATO ASI Series, vol. 200, "Stochasticity and Intramolecular Redistribution of Energy", ed. Lefebyre R. and Mukamel S., (D. Reidel, Dordrecht, 1987).